

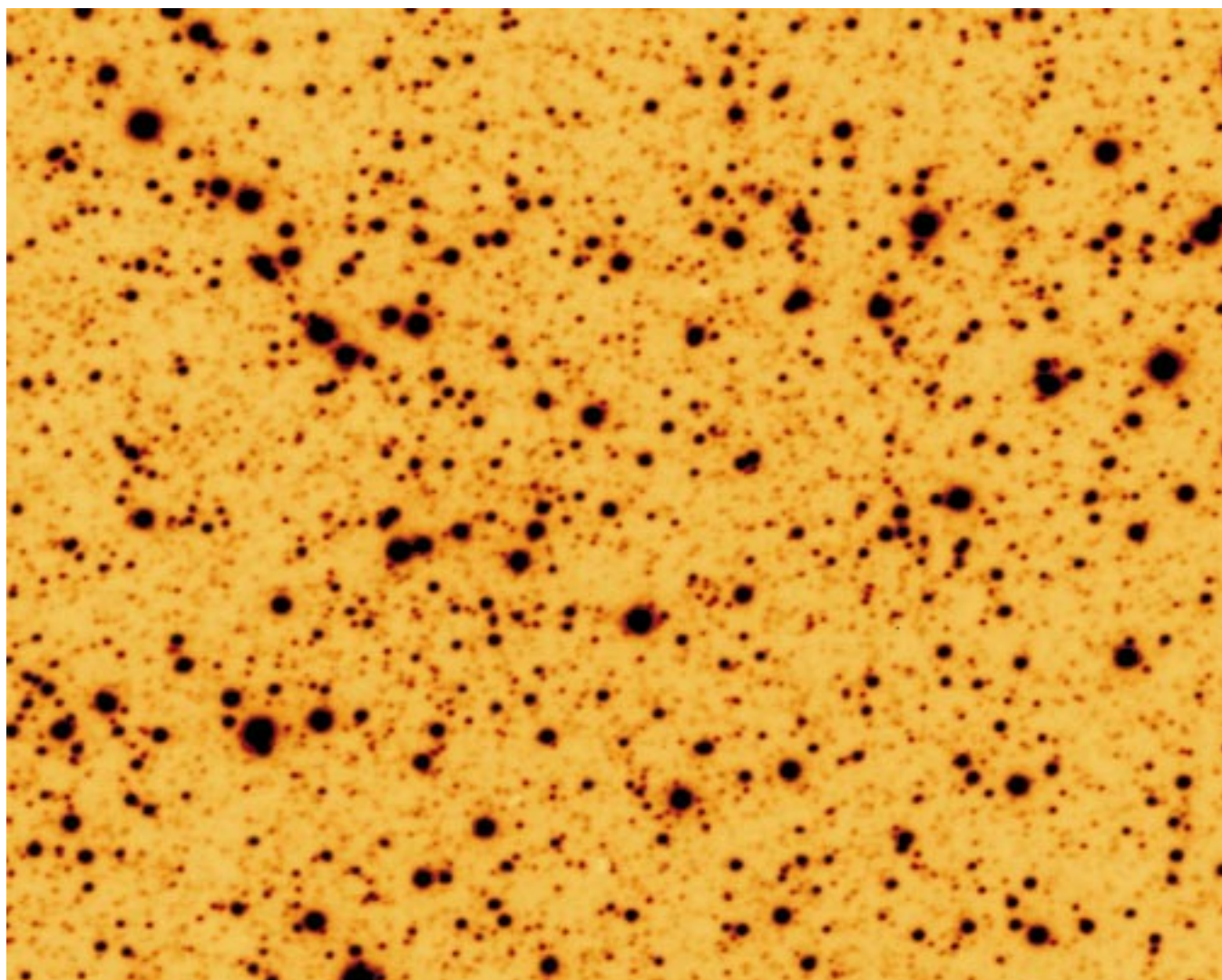
THE MESSENGER



EL MENSAJERO

No. 92 – June 1998

FIRST LIGHT



Omega Centauri, obtained with the VLT UT1 on May 16, 1998. (For more details, see text in box on page 3.)

First Light of the VLT Unit Telescope 1

R. GIACCONI, Director General of ESO

The VLT represents a major new step forward for world astronomy. The new concept of active control of a thin monolithic large mirror, embodied in the design, yields, even at this early stage, an angular resolution among the finest ever achieved in optical and infrared wavelengths from the ground. The full realisation of the VLT array (which will include four 8.2-metre and three 1.8-metre telescopes) will result in a combination of area and angular resolution which will permit us to achieve sensitivity comparable or superior to any on Earth. When the array is used in the interferometric mode, it will result in angular resolution superior to that yet achieved in space.

This formidable new observational capability will provide astronomers a new opportunity for the study of the Universe. In particular we will be able to probe the great questions of modern astrophysics:

- The beginning, evolution and future of the Universe we live in.
 - The formations in the most remote past of large structures, galaxies and stars and their life cycle.
 - The formation and evolution of planets and of the physical and chemical conditions for the development of life.
- In each of these fields, VLT will give astronomy new capabilities for greater in-

depth investigation and understanding, thus further enhancing the great prestige which astronomy is now enjoying in the world. The combination of high technology and deep scientific and philosophical questions is fascinating to young and old and to the general public, touching as it does on the sense of awe and wonder that accompanies our quest for the origins of the cosmos and our place in it.

For Europe this event marks the realisation for the first time in this century of a facility for ground-based optical and IR astronomy which equals or surpasses any available in the world.

Institutes of research and industries from all European member states have contributed to this effort which clearly exceeds what any European nation could achieve using its own resources. It would be impossible to recognise each contribution on this very large programme which has extended over more than a decade and represents literally more than ten thousand man years of effort.

The VLT programme has been executed within planned schedule and cost. Even at this very early stage of evaluation we can state with confidence that the technical performance of the first of the four identical 8.2-m telescopes meets or exceeds our expectations in all respects.

I should emphasise that while this moment is very significant, it is only a beginning. It marks the start of operations for a very powerful new observational facility which will be completed in 2003. The full scientific utilisation of VLT and VLTI will occur over a period of at least two decades. The new design of the telescopes, their truly exceptional realisation by industry and their excellent performance will present the astronomers with the challenge of taking full advantage of this new instrument and of inventing new ways to do their research and maximising its effectiveness. The enormous amount of data which will become available over this period will require archiving capabilities much greater than hitherto used in astronomy. Marvellous as this machine is, it will not hold its competitive edge forever, and ESO and the scientific and industrial community it represents are already at work to prepare new technology for the next round of observational facilities.

Finally I wish to recognise the united and extraordinary contributions of the ESO staff in Garching, La Silla, Paranal and Santiago. This great success of VLT of which we are all so proud is due in large measure to your competence, enthusiasm and dedication.

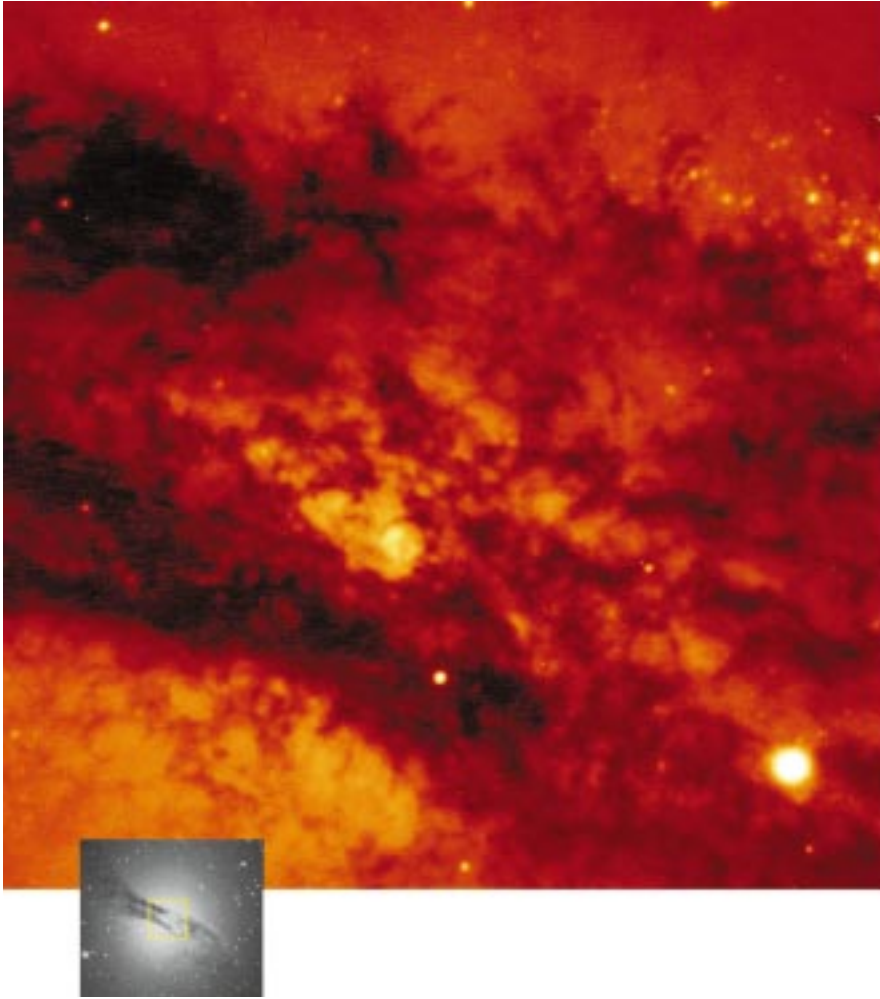


This colour image of a famous southern Planetary Nebula, the Butterfly (NGC 6302), was obtained by combining blue, yellow and red images obtained on May 22, 1998, with 10-minute exposures and an image quality better than 0.6 arcseconds.

Towards the end of their life, some low-mass stars expand to giant dimensions. They shed most of the hydrogen in their outer layers as a strong "stellar wind", before they contract towards a final compact stage as "white dwarfs". After this ejection process, the star remains thousands of times brighter and also much hotter than the Sun during a few thousand years. Its strong ultraviolet radiation has the effect of ionising the previously ejected gas, which then shines before it disperses into interstellar space. The resulting nebulae (traditionally referred to as Planetary Nebulae, because of their resemblance to a planet in a small telescope) often exhibit very complex morphologies.

The Butterfly Nebula belongs to the class of bipolar nebulae, as this picture clearly illustrates. A dark, dusty and disk-like structure – seen edge-on in this image – obscures the central star from our view. However, its strong radiation escapes perpendicular to the disk and heats and ionises the material deposited there by the stellar wind.

The origin of the dark disk may be due to the central star being a member of a double star system. This has been shown to be the case in some other bipolar nebulae in which, contrary to the Butterfly Nebula, there is a direct view towards the star.



Centaurus A is the closest active elliptical galaxy and one of the strongest radio sources in the sky. This image shows part of the dust lane that obscures the central regions of the galaxy. This complex structure is believed to be the result of the recent collision between the old elliptical galaxy and a dwarf, gas-rich galaxy. Intense star formation is taking place within the violently stirred gas during the merging event.

This image was taken with the Test Camera of the VLT UT1 telescope on May 22, 1998, during a short, 10-sec exposure through a red filter to demonstrate the large light collecting power of the 53-m² mirror of the VLT UT1. It shows a wealth of fine details. The image quality is about 0.49 arcsec.

The insert shows a complete view of Centaurus A taken with another telescope. The brightest stars are foreground objects located within our own galaxy, but clusters of recently formed stars are visible at the edge of the dust lane.

With powerful infrared detectors to be mounted on the VLT later this year, astronomers will soon be able to probe deep into the dust lane, infrared light being less absorbed by dust than red light.

The Final Steps Before “First Light”

The final, critical testing phase commenced with the installation of the 8.2-m primary (at that time still uncoated) Zerodur mirror and 1.1-m secondary Beryllium mirror during the second half of April. The optics were then gradually brought into position during carefully planned, successive adjustments.

Due to the full integration of an advanced, active control system into the VLT concept, this delicate process went amazingly fast, especially when compared to other ground-based telescopes. It included a number of short test expo-

tures in early May, first with the Guide Camera that is used to steer the telescope. Later, some exposures were made with the Test Camera mounted just below the main mirror at the Cassegrain Focus, in a central space inside the mirror cell. It will continue to be used during the upcoming Commissioning Phase, until the first major instruments (FORS and ISAAC) are attached to the UT1, later in 1998.

The 8.2-m mirror was successfully aluminised at the Paranal Mirror Coating facility on May 20 and was reat-

tached to the telescope tube the following day. Further test exposures were then made to check the proper functioning of the telescope mechanics, optics and electronics.

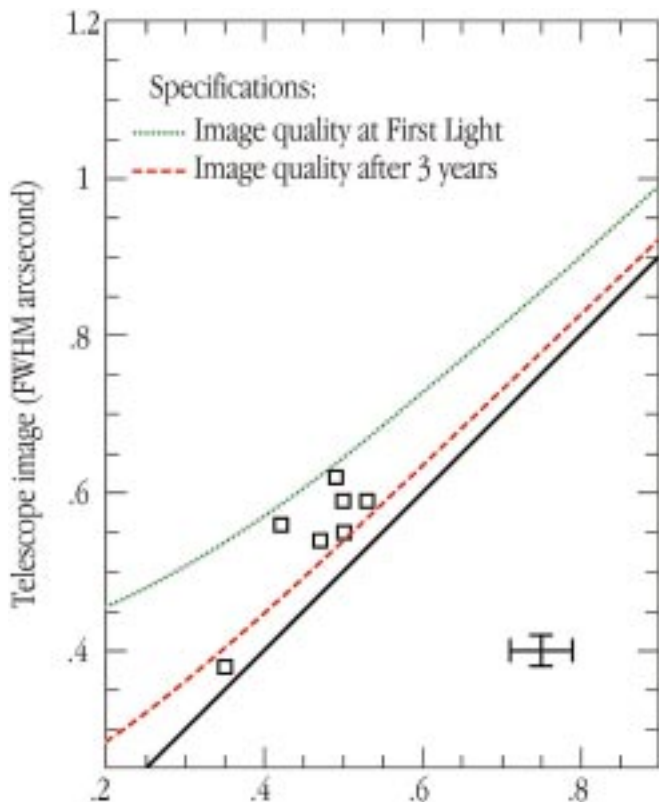
This has led up to the moment of First Light, i.e. the time when the telescope is considered able to produce the first, astronomically useful images. Despite an intervening spell of bad atmospheric conditions, this important event took place during the night of May 25–26, 1998, right on the established schedule.

The image shown on page 1 was obtained with the VLT UT1 on May 16, 1998, in red light (R band), i.e. while the mirror was still uncoated. It is a 10-minute exposure of the centre of Omega Centauri and it demonstrates that the telescope is able to track continuously with a very high precision and thus is able to take full advantage of the frequent, very good atmospheric conditions at Paranal. The images of the stars are very sharp (full-width-at-half-maximum (FWHM) = 0.43 arcsec) and are perfectly round, everywhere in the field. This indicates that the tracking was accurate to better than 0.001 arcsec/sec during this observation.

Omega Centauri is the most luminous globular cluster in our Galaxy. As the name indicates, it is located in the southern constellation Centaurus and is therefore observable only from the south.

At a distance of about 17,000 light-years, this cluster is barely visible to the naked eye as a very faint and small cloud. When Omega Centauri is observed through a telescope, even a small one, it looks like a huge swarm of numerous stars, bound together by their mutual gravitational attraction.

Most globular clusters in our Galaxy have masses of the order of 100,000 times that of the Sun. With a total mass equal to about 5 million solar masses, Omega Centauri is by far the most massive of its kind in our Galaxy.



In this diagram, both seeing (horizontal axis) and telescope image quality (vertical axis) are measured as the full-width-at-half-maximum (FWHM) of the light-intensity profile of a point-like source. The uncertainty of the measurements is indicated by the cross in the lower right corner.

Superb image quality is the prime requirement for the VLT. The VLT should take full advantage of the exceptionally good "seeing" conditions of the Paranal site, i.e. periods of time when there is a particularly stable atmosphere above the site, with a minimum of air turbulence. In this diagram, the measured image quality of the VLT UT1 astronomical images is plotted versus the "seeing", as measured by the Seeing Monitor, a small specially equipped telescope also located on top of the Paranal Mountain.

The dashed line shows the image quality requirement, as specified for the VLT at First Light. The dotted line shows the specification for the image quality, three years after First Light, when the VLT will be fully optimised. The fully drawn line represents the physical limit, when no further image distortion is added by the telescope to that introduced by the atmosphere.

The diagram demonstrates that First Light specifications have been fully achieved and, impressively, that the actual VLT UT1 performance is sometimes already within the more stringent specifications expected to be fulfilled only three years from now.

Various effects contribute to degrade the image quality of a telescope as compared to the local seeing, and must be kept to a minimum in order to achieve the best scientific results. These include imperfections in the telescope optical mirrors and in the telescope motion to compensate for Earth rotation during an exposure, as well as air turbulence generated by the telescope itself. The tight specifications shown in this figure translate into very stringent requirements concerning the quality of all optical surfaces, the active control of the 8.2-m mirror, the accuracy of the telescope motions, and, in the near future, the fast "tip-tilt" compensations provided by the secondary mirror, and finally the thermal control of the telescope and the entire enclosure.

The only way to achieve an image quality that is "better than that of the atmosphere" is by the use of Adaptive Optics devices that compensate for the atmospheric distortions. One such device will be operative on the VLT by the year 2000, then allowing astronomers to obtain images as sharp as about 0.1 arcsec.

VLT First Light and the Public

R.M. WEST, ESO

On the unique occasion of the "First Light" of VLT Unit Telescope 1 (UT1), ESO went to great lengths to satisfy the desire by the media and the public to learn more about Europe's new giant telescope. Already three months earlier, preparations were made to have related photos, texts and videos available before the event and to involve the astronomical communities in the member countries in the presentation of the First Light results.

Two slide sets were published on the Web and as photographic reproductions that illustrate VLT Milestones and the Paranal Observatory as it looks now. A comprehensive series of 41 viewgraphs about the VLT, its technology and scientific potential was published in April. They are useful for talks about the VLT and related subjects. All of this material is available on the Web at URL:

<http://www.eso.org/outreach/info-events/ut1f/>

A 200-page VLT White Book was compiled and published on the Web and in printed form just before the First Light event. It gives an overview of this complex project and its many subsystems.

In order to receive and process the first images from VLT UT1 in the short time available, a small group of ESO astro-

nomers got together at the ESO Headquarters to form the "First Light Image Processing Team". As soon as the images arrived from Paranal, they were flatfielded and cosmetically cleaned by the members of this group. In the late afternoon of May 26, it was decided which of these images should be included in the series of First Light photos that was released the following day. There were nine in all, including some that demonstrated the excellent optical and mechanical performance of the VLT UT1, others which were more "glossy", for instance a colour picture with fine details in a beautiful southern planetary nebula.

Through the good offices of ESO Council members, VLT First Light press conferences were organised in the eight ESO member countries on May 27 and also in Portugal and Chile on the same day. In the early morning of May 27, the members of the Image Processing Team travelled with the still hot press material from Garching to these meetings. Most of the meetings were opened by ministers or high-ranking officials from the Ministries of Education or Science. Introductory talks followed by the astronomer members of the ESO Council and other specialists knowledgeable of the VLT project. At the end, the "messengers"

from ESO presented the new images and gave a personal account of the hectic, but exciting work that had taken place during the previous days.

There is little doubt that these press conferences were highly successful in conveying information about the VLT and its potential for astronomical research in a very positive way. In any case, literally hundreds of newspaper articles, TV reports, etc. appeared in the following days in all of these countries and elsewhere.

The introduction of the VLT to the European public and, not least, the future users of this wonderful new facility, has had a good start.



In the VLT control room at the moment of "First Light".

Science Verification of the VLT Unit Telescope 1

B. LEIBUNDGUT, G. DE MARCHI and A. RENZINI, ESO

Introduction

The VLT first Unit Telescope (UT1) is now being commissioned, and ESO is committed to deliver to its community a fully tested and understood telescope by April 1, 1999. To this end, brief periods of Science Verification (SV) are now planned for the telescope and each of its instruments. SV data will become immediately public within the ESO community, and will offer the earliest opportunity of scientific return from the VLT and its newly installed instruments. Feedback from early users is expected to be an integral part of SV, with the understanding that the system is subject to the best possible check when one tries to squeeze as much science as possible out of it. It is expected that this feedback will help to improve and tune the systems before telescope and instruments are offered to the community.

During SV of UT1 the various components of the operations will for the first time work as a single machine, thus making sure the systems work from end to end. This encompasses the technical performance of the telescope, the operations of the data flow and a complete test of all the interfaces in the system. Science Verification should then demonstrate to the community the capabilities of the telescope and its instruments. For community astronomers, SV will deliver data allowing them to assess promptly the suitability of the VLT and its instruments for their own scientific programmes, thus submitting the VLT to a wider scrutiny.

Science Verification will consist of a set of *attractive* scientific observations, so as to involve in the process as many scientists as possible. There will be no restrictions for the data distribution within the ESO member countries. However, observations of the Hubble Deep Field South will be made immediately public world-wide, so as to parallel the release of the HST data.

The telescope SV is planned for August 17–31, which includes new moon (August 21), and will be conducted using the VLT Test Camera. A broad list of possible SV observations was discussed by the scientific management of ESO, and narrowed to a set of higher-priority and second-priority observations. The surviving list (see below) is still meant to oversubscribe the available time, thus allowing the final selection to be done on the spot, depending on the prevailing atmospheric conditions. The observations have

been chosen to represent typical imaging applications for an 8-m telescope. However, several technical restrictions (field of view, image scale and CCD characteristics) as well as astronomical constraints (accessible sky) will apply.

This article summarises the planned observations and describes their technical and operational implications. We start first with a summary of the technical aspects of the VLT Test Camera, the instrument with which the telescope is being commissioned and which will be used for SV of UT1. Additional constraints are presented in the next section followed by a brief overview of the calibrations. We end with a description of the scientific goals of the observations.

We invite all astronomers to visit the SV Web site (<http://www.eso.org/vltsv/>) for further information. All SV observation blocks will be available at this Web page, as well as the full text of the SV Plan and of the VLT Test Camera Calibration Plan.

Science Verification has been planned by a small team of astronomers at ESO acting under the overview of the VLT Programme Scientist. The team members are Martin Cullum, Roberto Gilmozzi, Bruno Leibundgut (Team Co-ordinator), Guido de Marchi, Francesco Paresce, Benoit Pirenne, Peter Quinn and Alvio Renzini (VLT Programme Scientist).

The same group, together with the PI of each instrument, will plan the SV for the instruments as well. Science Verification of FORS1 will take place in mid-January 1999, then followed by SV of ISAAC in mid-February, with each SV period consisting of seven nights. The plans for the SV of these instruments will be advertised in the next issues of *The Messenger* and on the SV Web site.

External Constraints

Telescope commissioning will deliver the Cassegrain focus for scientific observations in the middle of August. The SV phase will take place just before the focus will become available for the installation of FORS1. The schedule for the data flow commissioning foresees to provide a functional system at the same time so that SV can be done within the VLT operational paradigms. The data generation from the definition of the observation blocks, which are currently being prepared, to the archiving of the data in the VLT archive will be integral to SV.

The VLT Test Camera

The VLT Test Camera consists of a fully reflective re-imaging system which provides a clean pupil and prevents direct illumination of the detector. The telescope plate scale (1.894"/mm – Cassegrain focus) is maintained. With 24 μm pixels this translates into 0.0455"/pixel. With a thinned, anti-reflection coated Tektronix 2048² CCD, this yields a field of view of 93" on a side at the Cassegrain focus.

The VLT-TC will be equipped with a filter wheel with 7 positions. The filter size and optical parameters are the same as the ones of the SUSI2 camera at the NTT, and the filters can be exchanged between the two instruments. A standard Bessell filter set (UBVRI) has been ordered for the VLT-TC and it is foreseen to add a set of intermediate-band filters suitable for photometric measurements of redshifts. Narrow-band filters will be borrowed from the SUSI2 filter set, if required. Neutral density filters for bright objects are available as well.

TABLE 1: Expected signal for point source objects

magnitude	(S/N in 1 hour integration)							
	filters							
	B (seeing) ^a		V (seeing)		R (seeing)		I (seeing)	
	1.0	0.5	1.0	0.5	1.0	0.5	1.0	0.5
22	703	972	503	773	447	744	201	370
23	321	506	217	375	187	341	82	157
24	137	241	90	167	76	146	33	64
25	56	106	36	70	31	60	13	26
26	23	42	15	29	12	24	5.2	10
27	9.1	18	5.8	12	4.9	9.7	2.1	4.2
28	3.6	7.2	2.3	4.6	1.9	3.9	<1	1.7

^a Seeing in arcseconds FWHM

The shutter of the camera will provide exposure times as short as 0.2 seconds which, with the specified shutter timing, will provide a non-uniformity of 25% between centre and edge of the field. An illumination uniformity of better than 1% is achieved with exposures longer than 5 seconds.

The expected signal for a point source is given in Table 1. The figures have been calculated for an A0 spectrum assuming a dark sky (new moon), two reflections in the telescope, three reflections in the test camera, the Bessell (1990, PASP, 102, 1181) filter transmissions, the CCD efficiency and noise parameters, and two cases of image quality.

The VLT-TC is equipped with a high-quality coronagraphic capability including an occulting mask located at the UT focal plane to block out light in the core of a bright source and an apodising mask to suppress diffraction at the edges of the aperture and on the spiders. This capability is there in order to carry out precise quantitative measurements of the scattering wings of the UT PSF. The position and slope of these wings carry important information on the scale and power spectrum of the micro imperfections of the primary mirror and on the size and distribution of dust on the mirrors. These wings are the dominant contributors to the extended halos or aureoles around the seeing-dominated core of the PSF which limit the contrast of the VLT even with perfect adaptive optics compensation. This facility will be used to assess the effect of the PSF halo on the precision photometry of faint sources in the presence of brighter objects.

Data Flow Operations

The operations during SV can be carried out fully employing the VLT data-flow system (Silva and Quinn, *The Messenger* 90, 12; Quinn, *The Messenger*, 84, 30). This implies that, as far as possible, all observations will be done with observation blocks (OB). Observation blocks for each observation and the corresponding calibration OBs are prepared in advance. The OB database for SV is the basis for the mid-term and short-term schedules which will be prepared by the SV team for the period of interest and each night according to the atmospheric conditions. OBs for all foreseeable conditions will have to be prepared so that the SV period will be 'oversubscribed' by the available OBs to provide a sufficiently large selection pool of observations for any conditions.

The observations and the immediate quality assessment will be performed by the SV team. This includes all calibrations needed for a complete reduction of the data. Science Verification team members in Garching will carry out the data reduction using the data reduction pipeline.

Archiving of the data will be the responsibility of the VLT archive and the

SV team will not assume a role here. However, reduced data (e.g. object magnitudes) should be made available through the archive when released by the SV team in Garching.

Boundary Conditions

The sky coverage of the VLT at the end of August will be from RA of 14^h to 7^h. The declination range reaches from the Southern pole all the way to +40°. The accessible sky at the end of August is shown in Figure 1.

For scientifically interesting observations, we have to explore the unique features of the VLT-TC. As a simple imager, the VLT-TC has presumably among the highest throughput of any (imaging) instruments on an 8-m telescope. The reflective optics make the UV wavelength range down to the atmospheric cut-off accessible. The large oversampling of any seeing condition will make the accurate determination of point spread functions possible, which is a pre-requisite for PSF subtraction. For most extended objects and point sources which do not have to be largely oversampled, it will be advantageous to bin the CCD to reduce the effect of readout noise, although, for broad-band filter observations, the VLT-TC will work in the background (sky) limited regime most of the time.

Calibrations

The simplicity of the VLT Test Camera also means that the calibrations are restricted to only a few subsystems. The CCD calibrations will include bias subtraction and (sky and dome) flatfield division. Dark frames will be acquired to check for the dark current. A bad pixel map will be constructed and may be used for some of the observations. Also fringe frames in the case of narrow-band imaging may be required. Other checks for the camera include the CCD linearity and shutter calibrations. We do not anticipate that corrections for these will be necessary, but will acquire the necessary data for control.

Photometric calibration will be achieved through the observation of standard stars. Colour terms for the instrument throughput and second-order extinction coefficients should be established during SV. In the case of narrow-band imaging, we plan to observe spectrophotometric standards to calibrate the filter transmission.

The VLT Test Camera calibration plan gives a detailed description of the planned calibration observations and also describes templates and template parameters. The plan is available at the SV Web site.

Planned Observations

In the following sections the planned science observations are described. They

have been sorted into two priority groups. The first set describes the higher-priority observations which will be attempted first. The second group of observations are maintained as backup should the conditions be very favourable. We give here only a very brief account of these observations and refer interested astronomers to the SV Plan available at the SV Web site.

Criteria for the Selection of SV Observations

The following guidelines were adopted for the selection of the observations:

- (1) scientific attractiveness,
- (2) broad range of "topics" (from Solar-system objects to very high-redshift targets) to ensure involvement of a large fraction of the community,
- (3) projects which are generally photon starved,
- (4) low-surface brightness objects,
- (5) observations which require a large dynamic range,
- (6) faint ultra-violet objects,
- (7) time-resolved photometry of some very faint objects.

Even with this set of criteria a certain degree of arbitrariness is inevitable, when it comes to the selection of specific targets. We are sure everybody will understand.

Though the VLT image quality is expected to be outstanding among the ground-based telescopes, it makes no sense to attempt using the VLT test camera to compete on image quality with HST.

The observations described in the following section are targeted at representative astronomical objects, but it is not planned to observe complete samples of objects.

During the SV period of UT1 the Galactic plane is accessible for part of the nights, but also a fair fraction of the "extragalactic sky" can be observed (Fig. 1). Three of the four EIS fields and the planned Hubble Deep Field South are also accessible to the VLT during SV. The SV team will run the telescope with flexible scheduling mixing observations of different scientific goals depending on the actual conditions.

Higher-Priority Observations

Hubble Deep Field – South

The HDF-S will be optimally observable in late August, and certainly this field will attract a great deal of follow-up work both from ground and space in the next few years. The SV plan is to observe the STIS field containing the quasar at redshift 2.54 and the two NICMOS fields. Deep imaging of the NICMOS fields in *UBVRI* will complement the near-IR HST data. The quasar will be observed in a narrow-band which isolates objects emit-

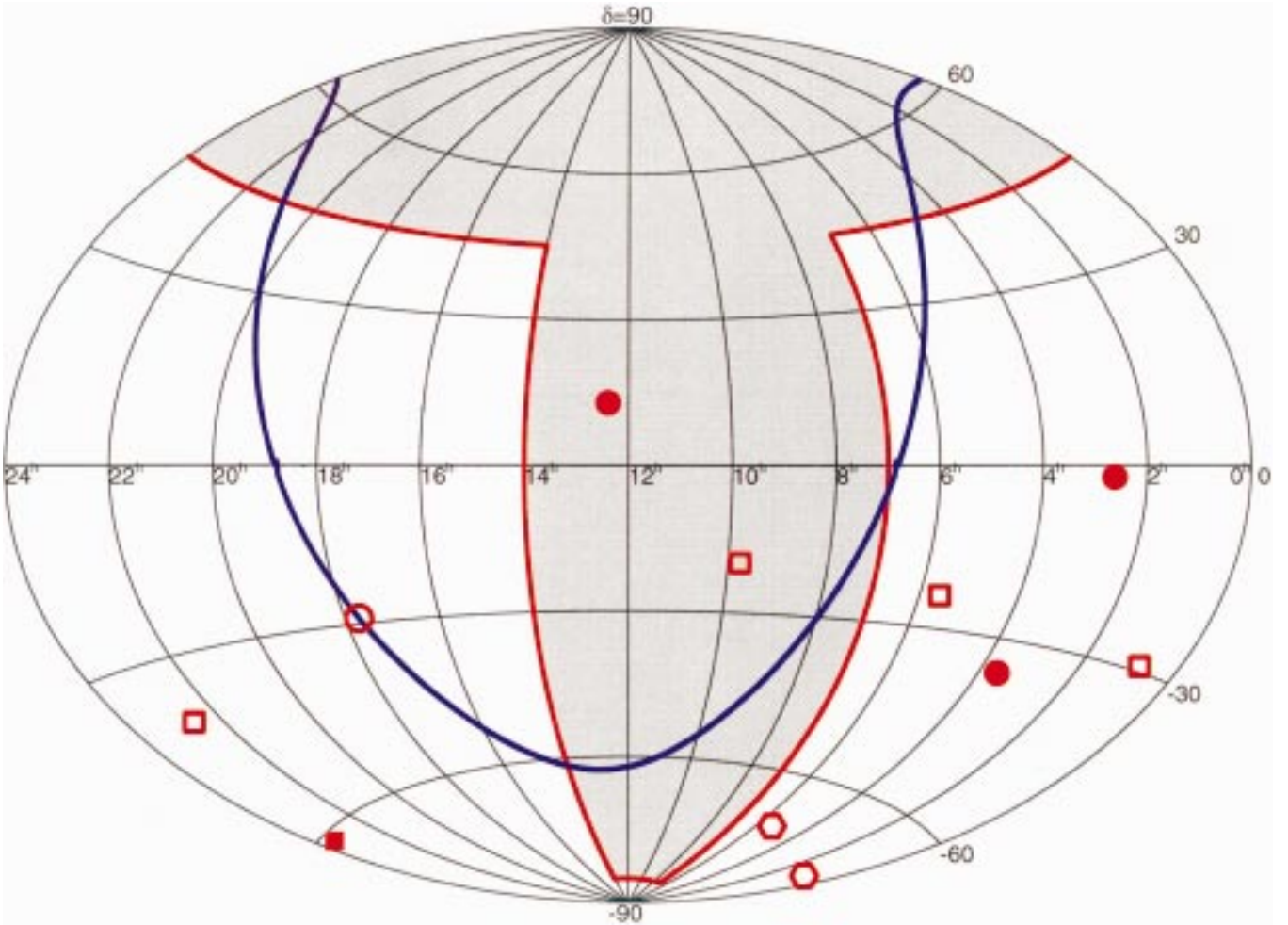


Figure 1: Accessible sky (white area) for SV of UT1 (end of August). The galactic plane is indicated by the thick line. The Galactic Centre(circle), the EIS fields (open squares), position of HDF-S (filled square), the LMC and SMC (hexagons), and the galaxy clusters Virgo, Fornax and Abell 370 (dots) are marked.

ting in Ly α at the QSO redshift to look for companion objects. This will also select candidate objects for spectroscopic redshift observations with FORS1. With somewhat lower priority, one of the WFPC2 fields may also be observed with the SUSI2 set of intermediate band filters.

Detection of the Gravitational Lens responsible for multiply-imaged QSOs

The photon collecting power of the VLT can detect very faint surface-brightness galaxies. The plate scale of the test camera should further provide very good point spread functions for the subtraction of the quasar images. The image quality of the VLT can be readily demonstrated with such observations. The luminosity profiles of the lensing galaxies are fundamental input parameters for the modelling of the lenses.

In order to confirm the presence of the lens, a sequence of co-added VLT Test Camera images, together with the application of powerful deconvolution algorithms, should push the detection limits to considerably fainter magnitudes. A promising object in this category is the optical Einstein ring.

High-z cluster candidates

Mass concentrations can be detected by the effects they have on the light travel through potential wells. An easy way to identify massive clusters of galaxies are the distorted images of background objects (arcs). The ESO Imaging Survey will provide a list of candidate clusters. X-ray selected candidate clusters will also be targeted. Detailed and systematic study (redshifts, structure, galaxy populations, gravitational shear maps, strongly lensed background galaxies at very high redshift, etc.) will certainly form a major set of early VLT projects. Observations in two colours (V and I) will detect and clearly define the elliptical galaxy sequence in the colour-magnitude diagram. The field of view of the VLT-TC is well matched to the expected size of high-redshift clusters ($\sim 30''$ at $z \approx 1$). In excellent seeing conditions it should be possible to obtain high S/N shear maps, and detect very high-redshift arcs, if present.

Gamma-Ray Bursters

The optical detection of Gamma-Ray Bursters (GRBs) has opened a new window onto these enigmatic objects. The spectral confirmation of the high-redshift

nature of some of these events has been demonstrated. Still, not all GRBs are detected in the optical and their association with distant galaxies has not been shown in every case. Only a small number (< 5) GRBs have been actually detected in the optical. Statistics of the gamma-ray and optical emission will build up very slowly. Deep imaging will provide stronger limits on the optical brightness distribution of the host galaxies of GRBs, if present. A problem with the hosts of GRBs has been their relative faintness. The three cases investigated so far show sub-luminous ($\leq L^*$) objects, which may rule out very massive stars as progenitors of GRBs. Imaging of sites of optically identified GRBs could provide more information on this issue. Should there be a GRB alert during SV with an error box not exceeding the field of view of the VLT-TC, we would certainly attempt an identification and observe its afterglow.

The imaging of a former GRB site is not a problem. Imaging of former sites of GRBs will also prepare the spectroscopic observations by FORS1.

SN 1987A

The shock from the supernova is predicted to reach the inner ring only in the

next decade. However, it is starting to ionise material left over by the fast, hot star wind. An HII region inside the ring, i.e. gas ionised by the progenitor Sk -69 201, has been stipulated to be responsible for the observed slow-down of the shock in the radio. X-ray emission is also associated with the shock interaction region. If there are substantial amounts of ionised gas inside the ring, it should be at very low surface brightness. It still has not been detected conclusively. Narrow-band imaging in H α and [O III] is the best chance to see this emission with the VLT. STIS has detected high-velocity Ly α from inside the ring. The ring itself has started to brighten in a single spot. So far it is undecided whether this brightening is due to changing ionisation or an early interaction of material which did not suffer any braking by shocks.

UV imaging of HST fields in globular clusters

One of the most intriguing, yet most interesting aspects of globular cluster dynamics is the fate of these systems after core collapse. While it is today demonstrated, on solid theoretical grounds, that they all must undergo this catastrophic phase on a timescale of order ~ 10 Gyr, it is still not at all clear how the stellar population in their cores would react to strong densities (up to $\sim 10^9 M_{\odot} \text{pc}^{-3}$) such as those expected to accompany the gravothermal instability. Coupled with the relatively low velocity dispersion of the stars in the core, such an extremely high density sets the ideal conditions for the formation of hard binaries, which will eventually heat the cluster core. Close binary systems and cataclysmic variables are, therefore, expected to play a dominant role in the post-collapse evolution of clusters, and should populate in large amounts the densest cores which are at higher risk of collapse.

Although only a few cataclysmic binary systems have so far been detected in globular clusters from the ground, a random and sporadic search for blue variable objects in globular cluster cores conducted with HST has already turned up quite a good number of interacting binaries. While no ground-based instrument can achieve the spatial resolution needed to peer deep into the cores of dense clusters, the collecting area of the VLT and the good near-UV sensitivity of the VLT-TC, coupled with the astrometric information of the available HST data, can serve this job by allowing us to locate all the variables in the cores and to obtain a good light curve of the objects having a period in the 2–10 hr range as might be expected from most interacting and eclipsing systems. We will then be able

to evaluate observationally the influence of these binaries on the dynamical evolution of the clusters. Images will be analysed with a restoration technique which makes use of high-resolution astrometric information to reach high-quality photometry of stellar objects in ground-based crowded fields.

Timing of Pulsars

The first pulsar detected in γ -rays, Geminga (PSR J0633+1746), is one of the most mysterious objects in the sky. Its parallax and proper motion have been measured and its luminosity has been obtained at various wavelengths. It carries all signatures of an isolated cooling neutron star. The period derivative measured in the γ -rays suggests an age of about 3.4×10^5 years, typical of a fairly settled object. Geminga has been observed as a faint optical source at $B \approx 26.5$. Recently, optical pulses have been reported from this object. Already five pulsars have data on optical pulses, all with photon-counting devices. The VLT-TC should be able to detect the optical pulses of some of these objects as well. The pulse measurement can be achieved by repeated integrations while moving the charge on the CCD. Since the pulse period is known very accurately from observations at other wavelengths, we can move the image on the CCD at this period and detect the pulse shape and any thermal, inter-pulse emission.

Lower-priority observations

Giant arcs in clusters

Through the amplification of the light by gravitational lenses, we are able to examine faint objects at larger distances in the Universe than allowed by other techniques. Observations of lensed galaxies can provide important new insights into their formation and chemical evolution as well as clarify when in time these processes took place. Broad-band observations of distorted galaxies have been used to infer the redshift distribution to $R = 27$. Since the asymmetry is best observed at the faint, outer isophotes, the VLT can significantly increase the S/N.

Quasar host and companion galaxies

The intense radiation emitted by QSOs must have a significant impact on their host galaxies. Very few host galaxies of quasars have been observed so far because of the strong contrast between the luminosity of the galaxy and that of the QSO. The morphologies of these objects span all known galaxy types including

disturbed systems. Since, however, no colour information is available to date, the current star-formation rate or its history remain still unexplored. Detecting host galaxies of quasars and determining their accurate colours through broad-band imaging can teach us about the influence of the central power house on the surrounding material.

The large brightness contrast between the bright nuclear region and the galaxy requires a large photon-collecting power and small pixel sizes so as not to saturate the point source, yet still reveal the comparatively faint surface brightness host.

Proper motion projects: Trans-Neptunian objects

The current inventory of the outer Solar System includes about 50 Trans-Neptunian objects (TNOs), whose orbit semi-major axis is in the 30–45 AU range, 7 Centaurs, orbiting between Saturn and Neptune, and many Short-Period and Long Period Comets (SP and LP respectively, a few hundred in total).

The dynamical studies and theoretical models of these populations link their formation to different regions of the Solar System: while the LP comets were formed in the Jupiter-Saturn region, then ejected by these planets to the outer Solar System, forming the Oort Cloud(s), the SP comet would have formed *in situ*, together with the TNOs, in 30–150 AU ecliptic region, forming the Kuiper Belt. The scattering of some of these comets and TNOs by the planets caused them to migrate on to larger orbits. The outward migration of Neptune caused its accompanying orbital resonance to sweep a broad region of the inner Kuiper belt, and explains the observed eccentricity distribution of the observed TNOs. The major problem is that these models need observational support: for most of the TNOs discovered, the only magnitude available is a crude estimate made from the discovery image, and only a few have colour measurements. About a dozen of short-period comets and a couple of the Centaurs have been measured.

With projected proper motions in the range of a few arcsec per hour and magnitudes around $V \approx 23$ –26 for a typical TNO, several short exposures will have to be collected for each object in order to minimise tracking problems. Candidates are available around the ecliptic, however, there is a concentration near 0^h and 12^h RA due to selection effects (low star density).

B. Leibundgut
bleibund@eso.org

Scientific Evaluation of VLT-UT1 Proposals

OBSERVING PERIOD 63 (APRIL 1 – OCTOBER 1, 1999)

The procedure for time allocation on the VLT and on the La Silla telescopes will basically follow the same principles, i.e.

- Observing proposals will have to be submitted every six months.
- The scientific evaluation of the VLT proposals and the proposals for the La Silla telescopes will be performed at the same time and by the same OPC and Panels.

For Observing Period 63, the submission of proposals and the related OPC activities will follow the time table given below:

August 1, 1998	Web release of the Call for Proposals for the Paranal and La Silla observatories. This release will include a new application form.
October 1, 1998	Deadline for the submission of VLT-UT1 and La Silla proposals
October 15, 1998	Distribution of the VLT-UT1 and La Silla proposals to members of the OPC Panels, and to the directors of the Paranal and La Silla observatories for technical feasibility assessment
November 2, 1998	Distribution of the technical feasibility reports to the members of the OPC Panels
November 25, 1998	Deadline for submission of reports by the members of the OPC Panels
Nov. 30 – Dec. 4, 1998	Meetings of the Panels and of the OPC

First VLT Call for Proposals

P. QUINN, J. BREYSACHER, D. SILVA

1. Introduction

On 1 August 1998, ESO will release the Period 63 call for proposals for all ESO telescopes. For the first time this will include the 8.2-m Unit Telescope 1 of the VLT. The deadline for proposals will be 1 October 1998 for all telescopes which represents an increase of one month in the preparation period from previous rounds. The OPC will meet in the first week of December 1998 for both UT1 and La Silla telescopes (see the box "Scientific Evaluation of VLT-UT1 Proposals" in this issue). Period 63 operations will commence on 1 April 1999. Proposals for Period 64 will be called for on 1 February 1999 and close 1 April 1999.

During Period 63, UT1 will offer instruments in both Service Mode and Visitor Mode. It is ESO's intent to ultimately offer Service Mode observations for all most frequently used modes of instruments on the VLT in order to permit the best utilisation of the unique properties of the Paranal site and to guarantee a minimum level of consistency to the archived data. As we accumulate experience on the most effective use of the instruments and develop adequate software tools, we plan to support service as well as visitor observing with automated calibration pipelines to initially remove instrument signatures and ultimately to provide physical quantities. Initially, such pipelines will exist only for the simplest modes of use of the instruments offered. Service observing can "of course" be carried out without the benefit of such standardisation in the same manner that

visitor observing is carried out. This mode of operation is much more manpower intensive and will be offered on a best-effort basis. ESO will work closely with the user community to develop service and visitor mode operations and resources that will maximise the scientific return of the VLT.

In Service Mode, successful principal investigators will specify observation programmes as a series of Observation Blocks (OBs) using Phase 2 Proposal Preparation (P2PP) software tools (see Silva and Quinn, December 1997, *The Messenger*). These OBs will be executed by ESO staff astronomers on UT1 to a schedule dictated by OPC ranking and prevailing conditions. In Visitor Mode, astronomers will again construct OBs but will journey to Paranal and be present when they are executed.

2. Instruments for UT1 in Period 63

ESO plans to offer FORS1 and ISAAC on UT1 beginning in April 1999. Detailed descriptions of these instruments can be accessed from the ESO Web

page <http://www.eso.org/instruments>.

All VLT instruments are commissioned in two phases. In the first phase, the instrument is mounted on the telescope for the first time and functional tests are made of all operational modes. This phase is followed by an assessment period where instrument performance is evaluated and observing templates are optimised. The second and final commissioning phase sees operational tests of all observing modes to be offered to the community. Each instrument then enters a Science Verification period in which test science programmes are executed under actual operations conditions to assess science performance and readiness for operations. At this time ESO is planning to carry out the commissioning schedule for FORS1 and ISAAC outlined in Table 1.

The final set of instrument modes and the measured instrument performance on UT1 offered to the ESO community on 1 April 1999 will depend on the results of the commissioning and science verification processes. Principal investigators may have to make modifications to observing programmes in early March

TABLE 1: FORS1 and ISAAC Commissioning Periods.

Instrument	Phase 1 Commissioning	Phase 2 Commissioning	Science Verification
FORS1	10/9/98 – 4/10/98	10/12/98 – 26/12/98	14/1/99 – 20/1/99
ISAAC	14/11/98 – 4/12/98	4/2/99 – 17/2/99	18/2/99 – 24/2/99

TABLE 2 : Modes for FORS1 in Period 63.

FORS1 Instrument Mode	Pipeline in Period 63
Direct Imaging	Yes
Multiobject Spectroscopy	No
Longslit Spectroscopy	Yes
Imaging Polarimetry	No
Spectropolarimetry	No

TABLE 3 : Modes for ISAAC in Period 63.

ISAAC Instrument Mode	Pipeline in Period 63
Short Wavelength Imaging	Yes
Long Wavelength Imaging (without chopping)	No
Short Wavelength Spectroscopy	Yes
Long Wavelength Spectroscopy (without chopping)	No

1999 based on the outcome of commissioning.

Tables 2 and 3 present the FORS1 and ISAAC instrument modes ESO plans to commission by 1 March 1999 and offer during Period 63.

3. Application Process for Period 63

Observing proposals for all ESO facilities on La Silla and Paranal will use a revised application form. Although revisions were necessary to provide VLT support, ESO took this opportunity to streamline the form in many areas and to provide the capability to include Postscript figures.

As usual, the La Silla Call for Proposals will only be available from the ESO Web site.

A separate VLT Call for Proposals will be published both on paper and on the Web. The VLT Call for Proposals will contain all the information necessary to complete and submit a VLT observing proposal, including a description of the detailed supplementary documentation available to proposers. Such detailed documentation includes the VLT White Book (a technical overview of the entire VLT facility) and the individual instrument

handbooks. The VLT Call for Proposals will also provide the information necessary for proposers to decide whether Visitor Mode or Service Mode is more appropriate for their project. Information about the FORS1 and ISAAC Exposure Time Calculators (ETCs) and how they can be used to support the proposal process will also be provided. Preliminary versions of the FORS1 and ISAAC ETCs are available via the ESO Web site at <http://www.eso.org/observing/etc>.

Astronomers preparing VLT observing proposals should be aware that if they are awarded VLT time, they will be asked to complete a Phase 2 proposal process. During the Phase 2 process, proposers will create detailed descriptions of their observing programme in the form of Observation Blocks (OBs). Visitor Mode PIs will be strongly encouraged to construct their OBs before traveling to Paranal but will not be required to finalise their OBs until after they have arrived there. Service Mode PIs, however, will be required to submit their OBs to ESO before their programme will be executed. More information about this process will be provided in the VLT Call for Proposals. Astronomers planning to propose for VLT time may also wish to read Silva & Quinn (*The Messenger*, December 1997) and Silva (this issue). A detailed guide to preparing OBs using Phase 2 tools will be published in the December 1998 *Messenger*.

Astronomers with further questions regarding the call for proposals for Period 63 are asked to contact the User Support Group at ESO (usg@eso.org).

P. Quinn
pquinn@eso.org

P. Quinn
pquinn@eso.org



In this evening view, obtained about half an hour after sunset, the UT1 telescope structure is seen through the dome slit. The assembly of UT2 is well on its way in the next dome, and the first parts of UT3 are in place in the third.

AMBER, the Near-Infrared/Red VLT/Instrument Focal Instrument

R.G. PETROV¹, F. MALBET², A. RICHICHI³, K.-H. HOFMANN⁴

¹Université de Nice – Sophia Antipolis, and Département Fresnel, Observatoire de la Côte d'Azur, France (OCA)

²Laboratoire d'Astrophysique, Observatoire de Grenoble, France (LAOG)

³Osservatorio Astrofisico di Arcetri, Italy (OAA)

⁴Max-Planck-Institut für Radioastronomie, Germany (MPIfR)

Abstract

The near-infrared/red focal instrument of the VLT, called AMBER, will operate between 1 and 2.5 μm in a first phase (2001–2003) with two UTs. This instrument has been designed for three beams to be able to perform images through phase closure techniques. The wavelength coverage will be extended in a second phase down to 0.6 μm at the time the ATs become operational. The magnitude limit of AMBER is expected to reach $K = 20$ when a bright reference star is available and $K = 14$ otherwise. The main scientific objectives are the investigation at very high angular resolution of disks and jets around young stellar objects and AGN dust tori with a spectral resolution up to 10,000.

1. Introduction

The interferometric mode of the VLT (VLT/Instrument) has always been present in the VLT project. In the last *Messenger* issue (No. 91, March 1998), the ESO Director General, Riccardo Giacconi, has presented the role of ESO in European Astronomy by stressing the important and unique scientific contribution expected from the VLT/Instrument. The VLT/Instrument implementation plan has been reviewed in 1995–1996 by ISAC, the Interferometry Science Advisory Committee, who gave its recommendation to the ESO community in *The Messenger* No. 83 (March 1996). The committee recommended early operations of the VLT/Instrument as well as a phased development that would focus in the infrared wavelength range (1–20 μm). A new plan has then been proposed by the ESO VLT/Instrument team with an updated timetable: operations with two 8-m unit telescopes (UTs) before the

end of 2000, with two 1.8-m auxiliary telescopes (ATs) before the end of 2002 and the full complement of 4 UTs and 3 ATs starting in 2003. In 1997, three instruments were proposed:

- AMBER, Astronomical Multi BEam combineR: a near infrared/red instrument (0.6–2.5 μm). At this time, AMBER included adaptive optics.

- MIDI, MID-infrared Interferometric instrument: a thermal infrared instrument (10–20 μm).

- PRIMA, Phase Referencing Imaging and Micro-arcsecond Astrometry: an instrument based on the simultaneous operation of two fields.

On 14 April 1998, the VLT/Instrument Steering Committee recommended that ESO take the lead to deliver a dual field and stabilised beams (adaptive optics and fringe tracking), in order to boost the performance of AMBER and MIDI, as early as in 2001, much earlier than expected in the first version of the instrumentation plan.

AMBER intends to combine the main advantages of the interferometric instruments for which Europe has acquired experience: the FLUOR instrument [1, 2] and the GIST interferometer [6].

This paper presents a preliminary report on AMBER, where we detail the science drivers, the concept, the expected performance and the overall project organisation. The work presented here is the result of two preliminary working groups [4, 5] in addition to the AMBER present group [7].

2. Science Objectives

Of course, a major role in the science operation of AMBER will be played by the limiting magnitude that the system will permit (see Section 4). With such sensi-

tivities, there is a wealth of scientific issues that AMBER will allow us to tackle. Within the project, it has been decided that, at least at an initial phase, the instrument should be dedicated to relatively few topics. An investigation based on criteria of feasibility on one side, and strong interest in the scientific community on the other side, has resulted in a few selected areas which are listed, with a list of typical parameters, in Table 1.

It is important to note that AMBER will allow us in principle to cover a wide range of scientific objectives including:

- the search of hot exoplanets
- the formation and evolution of stars
- extragalactic studies

which will be our first scientific targets.

A detailed description of the scientific rationale cannot be given in full here, but the reader is referred for instance to the proceedings of the workshops organised by ESO (*Science with the VLT*, Walsh and Danziger eds.; and *Science with the VLT Interferometer*, Paresce ed.).

3. Preliminary Optical Layout

Figure 1 shows a possible optical layout of AMBER which is mainly intended to illustrate the functions of the different modules of the instrument. Three parts must be distinguished. Firstly, each beam is processed independently (1–4 in the figure); then they are combined (5–8); and finally a spectrograph and a detector (9–13) analyse the combination focus. The figure represents a layout for three telescopes.

The incoming beams have their wavefronts corrected by low-mode adaptive optics modules provided by ESO for the UTs and by the AMBER consortium for visible wavelengths. The expected Strehl

TABLE 1: Scientific characteristics for AMBER

Target	Visibility Accuracy	Minimum K magnitude	Wavelength coverage	Spectral resolution	Polarisation useful	3 beams useful	Wide-field useful
Exozodi / Hot exoplanets	10^{-4}	5	K	50	N	N	Y / N
Star-forming regions	10^{-2}	7	JHK -lines	1000	Y	Y	Y
AGN dust tori	10^{-2}	11	K	50	Y	Y	Y
Circumstellar matter	10^{-2}	4	JHK -lines	1000	Y	Y	Y
Binaries	10^{-2}	4	K	50	N	N	Y
Stellar structure	10^{-4}	1	lines	10000	N	Y	N

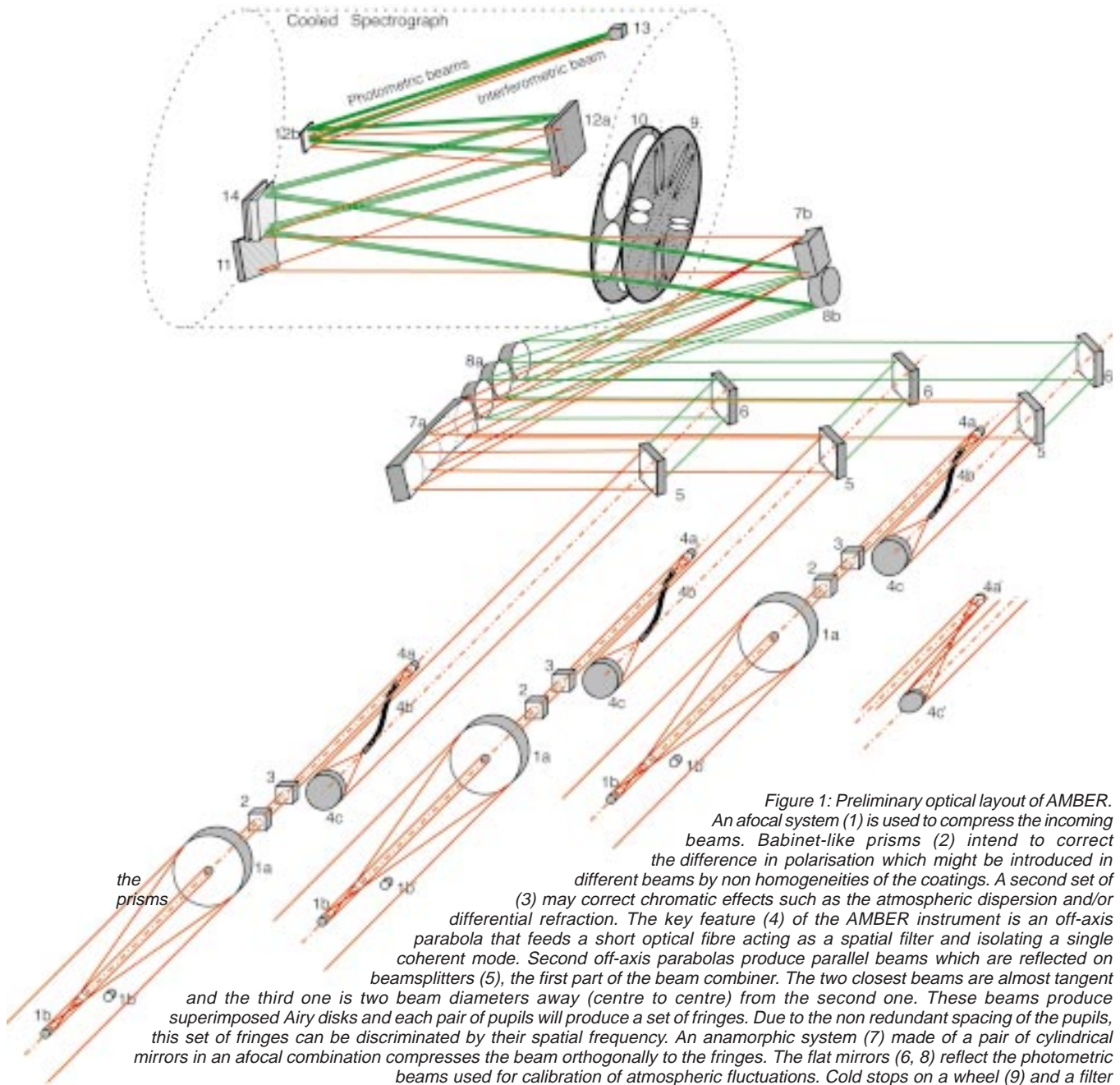


Figure 1: Preliminary optical layout of AMBER. An afocal system (1) is used to compress the incoming beams. Babinet-like prisms (2) intend to correct the difference in polarisation which might be introduced in different beams by non homogeneities of the coatings. A second set of (3) may correct chromatic effects such as the atmospheric dispersion and/or differential refraction. The key feature (4) of the AMBER instrument is an off-axis parabola that feeds a short optical fibre acting as a spatial filter and isolating a single coherent mode. Second off-axis parabolas produce parallel beams which are reflected on beamsplitters (5), the first part of the beam combiner. The two closest beams are almost tangent and the third one is two beam diameters away (centre to centre) from the second one. These beams produce superimposed Airy disks and each pair of pupils will produce a set of fringes. Due to the non redundant spacing of the pupils, this set of fringes can be discriminated by their spatial frequency. An anamorphic system (7) made of a pair of cylindrical mirrors in an afocal combination compresses the beam orthogonally to the fringes. The flat mirrors (6, 8) reflect the photometric beams used for calibration of atmospheric fluctuations. Cold stops on a wheel (9) and a filter wheel (10) are located at a pupil position. The light is then dispersed by a grating (11). A compact spectrograph design requires two chamber mirrors (12). The detector (13) will probably be 1024×1024 HAWAII Rockwell array. With three telescopes, the fringes are analysed within a strip of $12 \times n$ pixels, where n is the number of spectral channels ($n > 1024$). The photometric beams are slightly dispersed by a fixed prism (14) to take into account the chromatic variations of the Strehl ratio and the spatial filter efficiency. For some objects, we plan to use the $2''$ non-vignetted field available in the VLTI laboratory. This is achieved by replacing the spatial filter unit by an afocal system without spatial filter (4a', 4c') which maintains the direction of the output beam but divides its diameter by two. The figure roughly respects the proportion between the elements. The size of the spectrograph is 45 cm \times 30 cm.

ratio should reach 0.5 for the Unit Telescopes in the K band and should remain as high as 0.25 for reference stars of magnitude $V \approx 15$. The optical path differences between the beams are compensated by an ESO fringe tracker. Thanks to the dual field, wavefront correction and fringe stabilisation can be performed on a star up to 25 arcseconds away from the scientific target.

The compressed pupil after the cylindrical optics has the same shape whatever the number of telescopes. We plan to use the same spectrograph and detector in all cases. Therefore, increasing the number of telescopes from two to three, and then to four, requires only the addition of one incoming beam with the corresponding optics and the modification of the anamorphic system without changing anything in the already existing beams.

The effect of the spatial filter is to reduce the wavefront perturbations to a flux variation in the fibre [3]. If these photometric fluctuations are measured with a good precision, and if the fringe exposure times are short enough, then the fringe visibility can be measured with no experimental bias as has been demonstrated by the FLUOR experiment. The spatial filter and the photometric calibration are therefore necessary to measure visibili-

ties with extremely high accuracy (our ambitious target is 10^{-4}) on relatively bright sources (up to $K \approx 9$). With the spatial filter, the instrument has a field limited by the size of the Airy disk of the individual telescopes.

4. Expected Performances

At this stage of the project, this parameter is still subject to several uncertain-

TABLE 2: Expected limiting magnitude for two UTs (left) and two ATs (right). See text for details.

	Two UTs					Two ATs			
Fringe accuracy Self-reference	$\lambda/4$ 14		$\lambda/40$ 9.7		Fringe accuracy Self-reference	$\lambda/4$ 11.3		$\lambda/40$ 7	
Spectral resolution Off-axis reference	Broad-band 20.7	100 17.7	1000 15.2	10000 12.7	Spectral resolution Off-axis reference	Broad-band 18	100 15	1000 12.5	10000 10

ties linked to exact specifications of optics throughput, detector and electronics characteristics, as well as fringe tracker and adaptive optics performance. At present (see Table 2), we estimate that AMBER coupled to the VLT UT telescopes should allow us to reach, when a bright star reference is available, $K \lesssim 20$ in broad band and $K \lesssim 15$ at a resolution of 1000. When the interferometer uses the object as a reference, the limiting magnitude is rather $K \lesssim 14$. At the 1.8-m AT telescopes these limits drop by about 2.7 mag.

The upper half of Table 2 gives the limiting magnitudes of AMBER when the instrument detects fringes on the scientific source (self-reference mode). These numbers would also be the limits for the fringe sensor (for example the ESO/OCA Prototype Fringe Sensor Unit equipped with PICNIC detector with 18 electrons read out noise, Rabbia et al., 1996). In this mode, AMBER can detect fringes with $\lambda/4$ accuracy on stars up to $K = 14$ with 25-ms exposure time. For stars brighter than $K = 9.7$, the fringes can be detected at $\lambda/40$ accuracy with 4-ms exposure time. In this self-referencing mode, the limiting magnitudes are valid for all spectral resolutions.

The dual field allows for off-axis reference stars. The limiting magnitude for these references are the same as the ones quoted above. The lower half of Table 2 gives the limiting magnitudes on the science object in order to reach a 1% visibility accuracy within 4 hours of observation sliced into 100-second individual exposures.

These numbers are given for poorly resolved objects producing maximum fringe contrast in the fringe sensing spectral band. A 0.1 object visibility would lead to a 2.5 mag penalty.

5. Organisation

5.1 Institutes involved

The AMBER consortium is composed of four institutes:

- Laboratoire d'Astrophysique, Observatoire de Grenoble (LAOG, France).
- Observatoire de la Côte d'Azur (OCA, France)
- Osservatorio Astrofisico di Arcetri in Firenze (OAA, Italy)
- Max-Planck-Institut für Radioastronomie in Bonn (MPIfR, Germany).

Other institutes provide expert scien-

tists or engineers but do not build or integrate hardware. They are:

- Institut de Recherche en Communications Optiques et Microondes in Limoges (IRCOM, France)
- Université de Nice – Sophia Antipolis (France)
- Office National d'Études et de Recherches Aérospatiales in Paris (ONERA, France),
- Centre de Recherche Astronomique de Lyon (CRAL, France).

5.2 Project structure

The AMBER project includes a principal investigator (PI: R. Petrov OCA), a project scientist (PS: F. Malbet LAOG), a chairman of the science group (SGC: A. Richichi OAA), a project manager (PM: P. Kern LAOG), a system engineer (SE: S. Ménardi OCA) and a co-investigator (Col: K.-H. Hofmann MPIfR). AMBER has been divided in a set of working groups, each one in charge of one AMBER subsystem.

In addition to the ESO ISAC (Interferometry Science Advisory Committee), there is a science group for each VLTI instrument with the task of identifying and prioritising the key targets in order to maximise the scientific return of the instrument, especially during early operations. In the case of AMBER, the science group (SGR) includes scientists working on star formation, galaxies, AGN, exoplanets, low-mass stars, AGB stars, Be stars and circumstellar medium. The project scientist (PS) is in charge of translating the scientific needs in terms of instrument specifications. He is helped by an interferometry group (IGR), for interferometry offers a large range of observing modes and procedures, whose priorities must be analysed and specified by specialists.

The subsystem working groups of the AMBER instrument are:

- Optomechanics
- Cooled spectrograph
- Detector and associated electronics
- Instrument control (VLTI interface included)
- Observations support (observation preparation, data reduction)
- Testing, integrating equipment and performance tests.

5.3 Budget

Many elements still have to be defined in the present system definition

phase. Therefore, the final budget cannot be completely defined before the Preliminary Design Review (PDR) in November 1998. The estimated final budget for the hardware of the infrared part of AMBER for two beams (phase 1) is 4 MF $\pm 10\%$. Extension to three beams and to visible wavelengths (phase 2) require additionally 4 MF $\pm 30\%$ including the adaptive optics modules for two ATs (1 MF each).

The preliminary and still approximate general timetable combines the planning for each subsystem and integrates them in a general planning with the following important dates:

- July 1998: Full definition of the project (Final Concept Review). Problems have been identified and a concept has been selected.
- November 1998: Preliminary Design Review. Problems have been solved, detailed system analysis is finished. All interfaces are analysed. Precise timetable is known.
- April 1999: Final Design Review. All orders can be issued.
- July 2000: Manufacturing and Integration Review. All subsystems have been integrated and tested and it is possible to start the global integration and tests.
- December 2000: Shipment to Paranal where, after 3 months of laboratory and siderostat tests on site, we expect to start observations.
- April 2001: Observations with the UTs.

Note:

The AMBER documentation is available on the following Web site:

<http://www-laog.obs.ujf-grenoble.fr/amber>

References

- [1] Coudé du Foresto V., Ridgway S. 1991, FLUOR: a Stellar Interferometer Using Single-Mode Infrared Fibers. In: Beckers J., Merkle F. (eds.) Proc. ESO Conf., *High-resolution imaging by interferometry II*. ESO, Garching, 731.
- [2] Coudé du Foresto V., Perrin G., Mariotti J.-M., Lacasse M., Traub W. 1996, The FLUOR/IOTA Fiber Stellar Interferometer. In: Kern P., Malbet F. (eds) Proc. AstroFib'96, *Integrated Optics for Astronomical Interferometry*. Bastianelli-Guirmand, Grenoble, p. 115.
- [3] Coudé du Foresto V. 1996, Fringe Benefits: the Spatial Filtering Advantages of Single-

Mode Fibers. In: Kern P., Malbet F. (eds) Proc. AstroFib'96, *Integrated Optics for Astronomical Interferometry*. Bastianelli-Guirimand, Grenoble, p. 27.

- [4] Malbet F., Coudé du Foresto V., Mékarnia D., Petrov R., Reynaud F., Tallon M. 1997a, *Étude préliminaire de l'instrument proche-infrarouge / rouge du VLTI et de GI2T*, available on the AMBER Web (AMB-REP-001).
- [5] Malbet F., Perrin G., Petrov R., Richichi A., Schöller M. 1997b, *AMBER Report 2 – The*

imaging and spectroscopic VLTI focal instrument, available on the AMBER Web (AMB-REP-002).

- [6] Mourard D., Tallon-Bosc I., Blazit A., Bonneau D., Merlin G., Morand F., Vakili F., Labeyrie A. 1994, *A&AS* **283**, 705.
- [7] Petrov R., Malbet F., Antonelli P., Feautrier Ph., Gennari S., Kern P., Lisi F., Monin J.-L., Mouillet D., Puget P., Richichi A., Rousset G. 1998, *AMBER, The near infrared / red VLTI focal instrument*, Report for the Steering Committee meeting, 30 January 1998.

Available on the AMBER Web (AMB-REP-003).

- [8] Rabbia Y., Ménardi S., Reynaud F., Delage L. 1996, The ESO-VLTI Fringe Sensor. In: Kern P., Malbet F. (eds) Proc. AstroFib'96, *Integrated Optics for Astronomical Interferometry*. Bastianelli-Guirimand, Grenoble, p. 175.

F. Malbet
Fabien.Malbet@obs.ujf-grenoble.fr



NEWS FROM THE NTT

G. MATHYS, ESO

The NTT Upgrade Project has come to an end at the end of March. Over the past 4 years, the readers of this column have been able to follow the progress of this project through its three distinct phases: the stabilisation of the operations of the NTT, the installation at the NTT of the VLT control system, and the use of this refurbished facility for scientific observations within the framework of the VLT operational model (see *The Messenger* Nos. 75 to 91). The upgrade project has fulfilled its objectives of strengthening the NTT as a world leading 4-metre-class telescope and of using it as a testbench for the technical and operational concepts and solutions adopted for the VLT, prior to the entry of its first unit telescope into operations. With consideration for the latter objective, the NTT Upgrade Project has been conducted under the overall responsibility of the ESO VLT Division (but with important resources of other divisions, in particular the La Silla Division). Now that the project is completed, quite naturally, NTT operation has come back since the beginning of Period 61 under the responsibility of the La Silla Division, like all the other ESO telescopes on La Silla.

The end of the NTT Upgrade Project also marks the end of the present series of dedicated articles presenting "News from the NTT", or more specifically, news from the upgrade project: this note is the last one of this series. From the next issue of *The Messenger* on, in line with the above-mentioned reassignment of the responsibilities, information about the NTT will be reintegrated in "The La Silla News Page". The author of these lines will, as a matter of fact, have left the NTT to move to the Paranal Observatory and to participate in the preparation of the operations of UT1. He will be replaced, in his function of NTT Team Leader, by Olivier Hainaut,

who has recently joined the NTT Team (see below).

The end of the Upgrade Project

The NTT News published in the last issue of *The Messenger* had been written between the installation and the commissioning of SUSI2. The latter was completed at the end of February, in spite of adverse weather conditions, and a brief report was given in a dedicated article by S. D'Odorico in the previous issue of *The Messenger*.

Bad weather also severely hampered the SOFI commissioning period, in March. In spite of the limited amount of astronomical observations that could be carried out during the latter, its outcome was very positive, with the successful implementation of a number of new features:

- an ATM connection between the Local Control Unit (LCU) of the detector and the instrument control and acquisition workstation (*wsofi*). The use of such a connection in a real-time operational environment is a première at ESO. Until now, at the NTT as well as at the other telescopes on La Silla, data read out from the detectors were transferred to the acquisition computers through an Ethernet link. For its installation at the NTT in December, SOFI also was initially configured in this way. However, with the most recent increases of instrument performance in terms of detector array size and readout speed, Ethernet becomes a bottleneck for the achievable rate of data acquisition (both for the IR and for the visible: SUSI2 also suffers from this). In order to overcome this limitation, the option retained by ESO for new instruments (and existing instrument upgrades) is the replacement of Ethernet by ATM. SOFI is the first instrument to benefit from this new tech-

nology. The success of its implementation is a major step for the future of the ESO observatories, as it paves the way for other instruments on La Silla (in particular, the Wide Field Imager and SUSI2) and on Paranal.

- a new version of the Phase 2 Proposal Preparation (P2PP) tool, which supports the preparation of Observation Blocks for SOFI (in addition to EMMI and SUSI2, which were already supported before).

- an on-line reduction pipeline for imaging, through which, in particular, large sets of dithered images can be automatically combined in a very effective manner, taking away a large fraction of the burden typically affecting IR observers. SOFI is the first instrument to come on line which has been designed from the start for use within an end-to-end data flow context: thanks to this, it has been possible to develop for it powerful and effective automatic reduction tools which are far superior to those that could up to now be offered for conceptually older-fashioned instruments such as EMMI.

On the other hand, the end of the Upgrade Project has also marked the end (or, at least, the temporary suspension) of the Service Observing experiment at the NTT. The outcome of the latter and the lessons that can be drawn from it are reported in a separate dedicated article in this issue of *The Messenger*. Here, it should just be pointed out that, in spite of a number of shortcomings and weaknesses in what was primarily a learning period for both ESO and the astronomical community, Service Observing at the NTT has been quite favourably perceived by ESO users, to the extent that ESO has been urged by various of its advisory committees to consider the possibility to keep offering this option at the NTT (and possibly to develop it at other La Silla telescopes)

in the future. The requirements and implications of this service are currently being studied by ESO.

Current NTT Status

In the last issue of *The Messenger*, I reported the emergence of a few new technical problems as a result of the installation in January of the latest version of the NTT common software at the NTT. The two new problems with the highest rate of occurrence in the weeks following the software upgrade, and with the most damageable impact on operations (or, in other words, those responsible for the largest amount of technical downtime), were the spontaneous reboots of LCUs and the random failures of technical CCDs. The origin of both was found to be related to inaccuracies in the time distribution protocol. While the technical CCD control software was successfully modified to handle properly such inaccuracies and avoid further failures, the exact mechanism by which the time inaccuracies trigger the LCU reboots has not been identified yet. As a provisional workaround, LCUs are now running on their internal clock rather than on a centrally distributed time. Although the internal LCU time is considerably less accurate, so that the currently adopted option is not conceptually satisfactory, it does not have any significant negative impact on the operation of the telescope and of the instruments, and it effectively solves the annoying problem of the LCU self-reboots. Therefore, it is quite acceptable until a "cleaner", more permanent solution has been worked out and is implemented. With it, and with the above-mentioned modified technical CCD software, the re-

liability of the NTT control system has now come back to the excellent level achieved in the last months of 1997.

From the point of view of the visiting astronomers, the end of the NTT Upgrade Project and the return of the telescope fully within the La Silla operational context should, in practice, be a very smooth transition, since classical observing at the NTT will continue to follow the scheme set up during the last year. After the completion of the major technical works of the December 1997 – March 1998 period, time and resources have been, and will in coming months be, available to refine and to consolidate a stable operational model, in which emphasis will be laid especially on an improved service to observers. In particular, we hope to be able to provide NTT users with a few new auxiliary tools, which should allow them to have a better interaction with the system and with their data. One such product that has been put into service on the astronomer's workstation is the File Handling Tool, which provides the observer with a number of features allowing him, for instance, to examine the headers of his FITS files, to have a quick look at his data, or to take advantage of various options for easy saving of his data to tape.

Staff Movements

End of March, Domingo Gojak, an electronic engineer who was in the NTT Team since the beginning of the Upgrade Project, was transferred to the team in charge of the 3.6-m telescope to support the upgrade of the latter. Domingo had been one of the key players in the success of the technical up-

grade of the NTT, and he will undoubtedly play an equally important role in the upgrade of the other La Silla major telescope. I have enjoyed to work in the same team as Domingo during more than 4 years and I wish him all the best in his new assignment.

At about the same time, Olivier Hainaut, a former fellow from the Medium-size Telescope Team, passed to the NTT Team as a new senior staff astronomer. Olivier, a very experienced observer specialised in the study of small bodies of the solar system, has been designated as the future Leader of the NTT Team, a responsibility that he will take over from the author of these lines in July, after a period of overlap which will allow him to integrate himself in the team and to become familiar with his future task.

Two new fellows have also joined the NTT Team, at the end of April and the beginning of May: Vanessa Doublier, a former student at ESO in Garching, and Leonardo Vanzi, who comes from Arcetri (Italy). Both have experience in IR observations, and they will accordingly, at least in part, be assigned to the support of SOFI.

It is a pleasure to welcome these newcomers, with whom I am looking forward to collaborating in the last months of my involvement with the NTT and to whom I shall be pleased to hand over the responsibility of this telescope, trusting that they will maintain it as a world leading 4-metre-class telescope for the greatest benefit of the ESO astronomical community.

G. Mathys
gmathys@eso.org

Tuning of the NTT Alignment

Ph. GITTON and L. NOETHE, ESO

1. Introduction

Since the end of the NTT upgrade project it has been known that the alignment of the secondary mirror (M2) was only marginally within specification. When the atmospheric seeing was greater than one arcsecond, the misalignment had no noticeable effect on the image quality. But, under better seeing conditions, it was a limiting factor for the image quality. Therefore, it was decided to tune the position of the M2 unit. We used the NTT wave front sensors, which are part of the Active Optics system, in a novel way to measure the required realignment of M2.

2. Effects of a Telescope Misalignment on the Image Quality

2.1 The NTT optics

The NTT is an aplanatic telescope of the Ritchey-Chretien type. Aplanatic means that the telescope, if it is properly tuned and aligned, is free of spherical aberration and coma in the field. A proper alignment requires that the distance between the primary mirror and the secondary mirror is correct and that the optical axes of the two mirrors coincide. The by far most important aberration remaining in the field is then astigmatism, which is zero at the centre of the field and in-

creases quadratically with the field angle. The aberration is therefore rotationally symmetric with respect to the centre of the field.

In reality, any telescope is to some extent misaligned. Such a misalignment will introduce additional optical aberrations, first of all the so-called decentring coma. At the NTT, a wave-front sensor is used to measure the aberrations affecting the telescope. The detected coma is corrected by tilting M2 around its centre of curvature.

Since coma is not field dependent, the telescope will then, despite the misalignment, be free of coma over the whole field. But this coma correction is not sufficient for a complete alignment, since the axes of the two mirrors are not yet necessarily coincident. In this optical configuration, the axes of M1 and M2 will actually intersect at the coma-free point (CFP), forming an angle α (Fig. 1). The name

CFP stems from the fact that a rotation of M2 around this point will not change the coma of the telescope. In the NTT, the coma-free point is 1676 mm above the vertex of M2 (which has a radius of curvature of 4417 mm).

The residual misalignment of the two axes will destroy the rotational symmetry of the field astigmatism. This can approximately be described as a shift of the rotationally symmetric pattern of astigmatism away from the centre of the field. The measured astigmatism may then be smaller than in the aligned configuration at some position at the edge of the field, but it will be significantly larger at the opposite side. This will lead, at least in some areas of the field and under good seeing conditions, to a noticeable image degradation compared with the aligned configuration.

2.2 Image quality problems reported at the NTT

Strong asymmetric variations of the image quality under very good seeing conditions were reported for the detector in the red arm of the EMMI instrument where the diameter of the field of view is close to 10 arcmin. The pattern of image degradation was actually fixed with respect to the telescope (and therefore apparently rotated on the scientific de-

tector as the instruments were mounted at the Nasmyth foci). The problem was therefore due to the telescope optics and not to the instrument itself. Any dynamic cause (telescope tracking, vibration, ...) could also be ruled out as the effect on the images was not uniform across the field. This led us to question again the alignment of the M2 mirror. Indeed it had been reported during the Big Bang that the alignment of this element was only marginally within specification (see "News from the NTT" by J. Spyromilio in *The Messenger* No. 87). Most convincing was the fact that such a misalignment would introduce similar effects as the ones measured with EMMI.

2.3 Consequences for the image quality

2.3.1 PSF across the chip

As mentioned earlier, the PSF is quite inhomogeneous across the field which makes any attempt of deconvolution very difficult. This was clearly a strong limitation for astronomers looking for high resolution.

2.3.2 High PSF sensitivity to focus errors

Even in the presence of astigmatism, the images are round when the telescope is at best focus. However, even with a small amount of defocus, image elongations will appear. For a given defocus, the ellipticity will grow with the amount of astigmatism. This means that at the side of the field with the large

astigmatism the image elongations will be stronger than in an aligned telescope.

2.3.3 Focus variation measured by the wave-front sensor

The NTT wave-front sensor measures six modes of aberrations (defocus, decentering coma, spherical aberration, astigmatism, triangular coma and quadratic astigmatism). The measurement of defocus is also affected by the misalignment of M2. Indeed the field curvature is corrected under the assumption that the incoming optical beam is centred on the axis of the adapter. This is not true in the case of a misaligned M2 and, therefore, the amount of defocus was not correctly calculated. Therefore, a specific focus sequence had to be executed (either a thorough focus sequence or the use of the focus wedge).

2.3.4 Inaccurate calculation of the on-axis astigmatism

In order not to interfere with the observations, the measurements performed by the wave-front sensor are normally done off axis although the astigmatism to be corrected is the one affecting the centre of the field. To get the corresponding value of astigmatism at the centre, one has to subtract the field contribution from the value measured off axis. A model assuming a rotationally symmetric field astigmatism therefore gave inaccurate results for the on-axis astigmatism.

2.3.5 Out of specification condition for the field lens

The field lens is located between the f/5.3 EMMI red camera and the CCD detector. Its purpose is to compensate the field curvature such that the focal plane is flat over the whole field at the level of the detector. With a misaligned

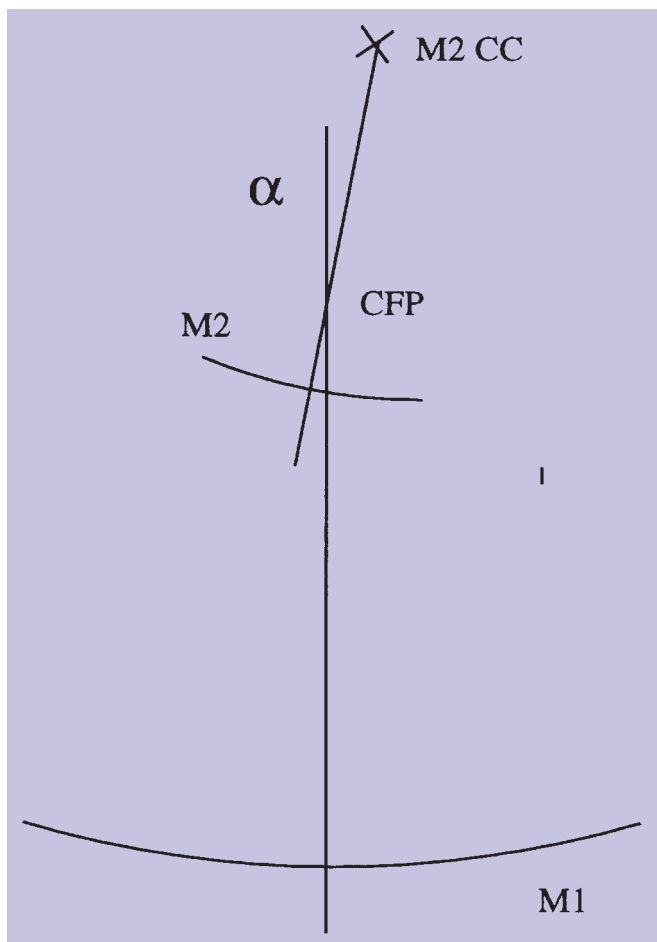


Figure 1: Telescope configuration after removal of coma.

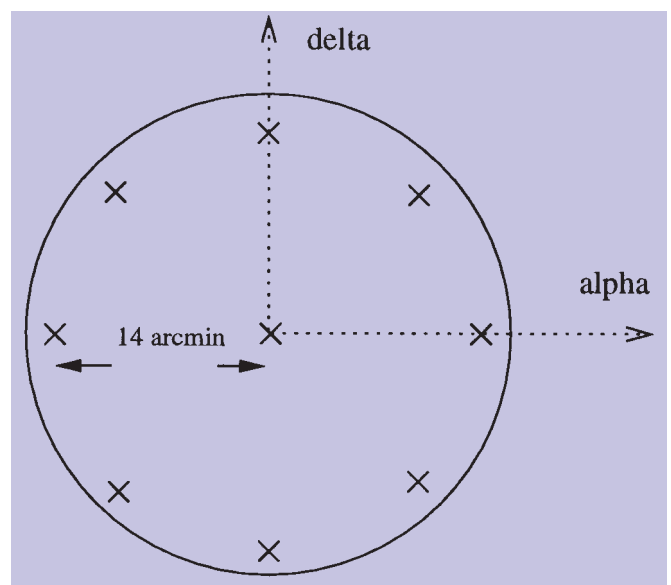


Figure 2: Measurement points for astigmatism mapping.

M2 the field lens did not give the desired result.

3. Wave-Front Sensor as an Alignment Tool

A method presented by B. McLeod [1] uses the measured field astigmatism to calculate the angle by which M2 has to be rotated around the CFP. The original method deduces first the field astigmatism and then the telescope misalignment from the ellipticities and elongation angles of images in the field. In the case of the NTT, this can be greatly simplified by using directly the output data of the wave-front sensor.

3.1 Theoretical basis

In his article, B. McLeod gives an expression relating the astigmatism components (Z_4, Z_5) to the field angle (θ_x, θ_y) for a secondary mirror tilted by an angle (α_x, α_y) around the CFP.

$$Z_4 = A_x + B_0(\theta_x^2 - \theta_y^2) + B_1(\theta_x\alpha_x - \theta_y\alpha_y) + B_2(\alpha_x^2 - \alpha_y^2) \quad (1)$$

$$Z_5 = A_y + 2B_0\theta_x\theta_y + B_1(\theta_x\alpha_y + \theta_y\alpha_x) + 2B_2(\alpha_x\alpha_y) \quad (2)$$

The (A_x, A_y) terms correspond to the residual astigmatism introduced by the M1 support on the primary mirror. The coefficients B_0 , B_1 and B_2 are constants depending on the geometry of the telescope. Using the optical parameters of the NTT we get:

$$\begin{aligned} B_0 &= -24.3679 \mu\text{m/degree}^2 \\ B_1 &= 30.0719 \mu\text{m/degree}^2 \\ B_2 &= 0.1768 \mu\text{m/degree}^2 \end{aligned}$$

3.2 The measurement procedure

In our case, the wave-front sensor allows a direct measurement of the astigmatism vector (Z_4, Z_5) at any position in the field just by moving the guide probe. As shown by formulae (1) and (2), the difference between an aligned and misaligned telescope is larger at the edge of the field due to the linear terms in θ_x and θ_y . In these equations, there are only 4 unknowns ($\alpha_x, \alpha_y, A_x, A_y$). Theoretically, two astigmatism measurements should be sufficient to deduce the misalignment parameters. Nevertheless, we preferred to perform 9 measurements distributed over the field as shown in Figure 2.

The results of the field astigmatism mapping have then been fitted using a least squares algorithm. The computation is done completely automatically using as input the log file produced by the Active Optics system. Here are the steps performed successively by the programme:

- retrieve guide probe positions and astigmatism measurements (Z_4, Z_5) from AO log file

TABLE 1: Initial misalignment parameters

Nasmyth focus	date	σ_{fit} (nm)	α_x (deg)	α_y (deg)
A	18/01/98	366	0.052	0.074
B	18/01/98	173	0.089	0.087

TABLE 2: Initial astigmatism parameters

	EMMI	EMMI	NTT	NTT
Case considered	c_{ast}	d_{80}	c_{ast}	d_{80}
Perfectly aligned M2	286 nm	0.121"	1520 nm	0.641"
Misaligned M2	632 nm	0.266"	2230 nm	0.940"

- convert guide probe positions to field offsets (θ_x, θ_y) in telescope reference frame
- Compute M2 misalignment (α_x, α_y) via a least squares fit.

3.3 Misalignment data

The mapping of the astigmatism was done at both foci. The results are presented in Table 1. σ_{fit} is the residual r.m.s. after the least squares fit. There is a reasonable agreement between the two foci. The averaged misalignment angle is 0.090 degrees. Using equation (1), one can calculate the resulting highest value c_{ast} of the coefficient of astigmatism and the corresponding diameter d_{80} containing 80% of the geometrical energy both at the edge of the detector in the EMMI red arm and at the edge of the field of the NTT (15 arcmin). The value of d_{80} can directly be compared with the *FWHM* values for the atmospheric seeing. The values for c_{ast} and d_{80} are shown and compared with the corresponding values for a perfectly aligned telescope in Table 2.

3.4 Method for the correction of the misalignment

The active optics system allows to correct the astigmatism affecting the telescope by deforming the primary mirror. Such a correction of astigmatism is uniform over the whole field while the deviation of the astigmatism from an aligned

telescope is field dependent. The NTT active optics system is therefore not capable of restoring the optimum rotationally symmetric pattern of the field astigmatism.

Therefore, the only possibility to correct the effects of the misalignment was a realignment of M2, that is a rotation around the CFP. At the NTT, the computer-controlled lateral motions of the secondary mirror are limited to rotations around the centre of curvature of M2. Therefore, the rotation around the coma free point had to be achieved by a combined rotation around the centre of curvature and a tilt of M2 around its pole. The second action could most easily be performed by a rotation of the whole support structure of M2, that is by moving the spiders at the connection points to the top ring.

4. Realignment and Results

The realignment has been performed in February just before the installation of SUSI2 with the help of Francis Franza and Stephane Guisard. Two opposite spider arms were moved in opposite direction at the top ring by 1.3 mm.

New astigmatism mappings have been performed just after the realignment. They gave very good results as shown in Table 3. Overall, the misalignment of the M2 is now 0.018 deg which is 5 times smaller than the previous value. Table 4 shows for this new configuration the astigmatism values at the edge

TABLE 3: Final alignment parameters

Nasmyth focus	date	(σ_{fit} (nm))	α_x (deg)	α_y (deg)
A	12/02/98	157	0.002	0.016
B	12/02/98	77	-0.003	0.021

TABLE 4: Final astigmatism parameters

Case considered	EMMI	EMMI	NTT	NTT
	c_{ast}	d_{80}	c_{ast}	d_{80}
Perfectly aligned M2	286 nm	0.121"	1520 nm	0.641"
Realigned M2	350 nm	0.148"	1666 nm	0.702"

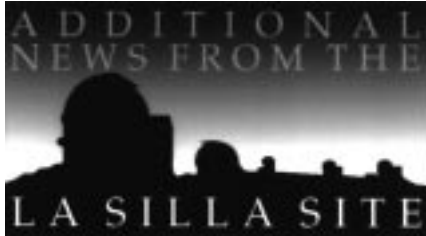
of the detector in the EMMI red arm and at the edge of the field of the NTT. The small differences both in the coefficients and the d_{80} values at the edge of the EMMI detector between the corrected and a perfectly aligned NTT will be virtu-

ally undetectable. Therefore, for all practical purposes, the NTT can now be regarded as a perfectly aligned telescope. The improved optical quality of the NTT has been confirmed by subsequent observers.

Reference

[1] Collimation of Fast Wide-Field Telescopes, McLeod, B.A., 1996, *PASP* **108**, 217–219.

pgitton@eso.org



The La Silla News Page

The editors of the La Silla News Page would like to welcome readers of the tenth edition of a page devoted to reporting on technical updates and observational achievements at La Silla. We would like this page to inform the astronomical community of changes made to telescopes, instruments, operations, and of instrumental performances that cannot be reported conveniently elsewhere. Contributions and inquiries to this page from the community are most welcome.

(R. Gredel, C. Lidman)

CES Very Long Camera Installed

M. KÜRSTER, ESO, Chile

After a general overhaul of the Coudé Echelle Spectrometer (CES), its new Very Long Camera was successfully installed between April 9 and 20. It consists of a new f/12.5 camera mirror that was mounted in the frame of the old scanner mirror and an x-y table on new pillars which hold a new 45° folding mirror and the CCD mount. The new Very Long Camera was jointly built by Uppsala Astronomical Observatory (optics) and the University of Liège (mechanics). It replaces the previous Long

Camera (f/4.7) which was decommissioned.

During a first series of test measurements with the thorium-argon lamp, resolving powers of $R = 235,000$ were obtained at different wavelengths. At this resolving power the sampling was determined to be ≈ 2.45 pixels/FWHM.

The Very Long Camera will be commissioned during May 14–20 together with the new fibre link to the Cassegrain focus of the 3.6-m telescope and image slicers built by ESO Garching

(optics) and ESO La Silla (mechanics). A sliding carriage with housings for up to four different image slicers has already been installed. The slit unit was also integrated on this sledge. The weeks before the commissioning will see the installation of the fibre in the Cassegrain adapter, and the installation of the fibre exit unit in the CES pre-slit area. The latter unit will be movable (with very accurate repositioning capabilities) to permit the continued use of the CAT telescope with the CES.

Improving Image Quality at the Danish 1.54-m Telescope

J. BREWER, ESO, La Silla

J. ANDERSEN, Copenhagen University Observatory, Denmark

The image quality achieved at a telescope depends on many factors, not the least of which is the thermal environment of the dome, telescope, and mirror. During the daytime, the dome, telescope and mirror heat up; at night this heat is released, causing air turbulence which degrades the seeing by causing the starlight to be diffracted along different paths. As part of the seeing improvement campaign at the major La Silla telescopes, it has been decided to address these problems also at the Danish 1.54-m telescope,

which was once known for its excellent images (e.g. *The Messenger* No. 17, p. 14, 1979).

After a lengthy period of measurements and analysis by Danish and ESO staff (in particular M.I. Andersen and A. Gilliotte), it was concluded that both charge diffusion effects in the (thinned Loral 2K) CCD and thermal problems near the mirror and in the dome and building were responsible for the currently observed image degradation. Considering that the contract between ESO and

Copenhagen University on the operation of the telescope had been extended for a ten-year period from 1996, a substantial investment in reducing daytime heating of the dome, telescope and mirror was found justified.

There are two ways to address this problem. One solution is to estimate the nighttime temperature and to maintain the dome, telescope and mirror at this temperature during the daytime by use of a cooling system. The other solution is to increase the natural ventilation in the



Figure 1: View of the open ports from the inside of the dome.

evening and during the night, while at the same time reducing the radiative heat flux from the concrete surfaces of the dome interior. Both approaches have advantages and disadvantages, and they are not mutually exclusive: An already partly cool dome reaches equilibrium faster when ventilated, and good ventilation in the evening and during the night reduces demands on the cooling system. A main advantage of the natural ventilation approach is, however, that it is simple to implement, requires little maintenance, and has no significant operational cost (unlike a large refrigeration plant).

After commissioning a number of cost/benefit engineering studies, it was decided by Copenhagen University Observatory (CUO) to implement a natural ventilation solution by raising the entire dome by 70 cm and installing side ports in the space between the dome and the building. A similar system is already in use at the Nordic Optical Telescope on La Palma, Spain, and will be used at the new Swiss telescope at La Silla. It was agreed with ESO that this would be supplemented by an effort to improve the thermal insulation and the performance of the existing ventilation and cooling systems in the building (which, unlike the telescope itself and the dome, is ESO property).

The mechanical design and prefabrication of the dome ports was undertaken by the Danish engineering company Richard Thomsen A/S. The ports were shipped to Chile and installed at the telescope during the period 4 April – 1 May 1998 by Anders Larsen and Kjeld Olsen of Richard Thomsen A/S in collaboration with CUO staff members Morten Jensen,

Hans Henrik Larsen, Niels Michaelsen and Preben Nørregaard.

Figure 1 is a view of the open ports seen from the inside of the dome. The ports are split into 8 sectors of 4 ports each, and it is possible to open or close any of the sectors separately. This will allow the system to be used in strong wind conditions when wind-borne dust is of concern and the dustladen wind must be kept from entering the telescope building. The system is mechanically simple and should require minimal maintenance. For simplicity, it is planned initially to apply the standard La Silla wind limits for domes also to the ports; i.e., all ports may remain open if the wind speed is less than 14 m/s, while ports in the wind direction should be closed when the wind speed is above 14 m/s. At wind speeds greater than 20 m/s, all ports (and, of course, the dome itself), must remain closed.

The side ports are opened and closed from a large control box located on the west wall next to the telescope. Having the control box on the dome floor will ensure that observers will not use the system blindly. The side ports can only be fully open or closed; it is not possible to open the ports partially.

The next stage of the project is to improve the internal insulation of the dome to reduce the heat flow from the concrete floors and walls of the building. The insulation work will be carried out by the La Silla Infrastructure Group in the next few months after a final design has been agreed upon and the materials purchased. Meanwhile, the ventilation system in the dome will be refurbished so as to primarily draw warm air away from the

telescope, especially from the control room under the observing floor. Ways will also be investigated to use any additional capacity of the cooling plant above that needed to cool the TCS rack to reduce the daytime temperature in the dome.

In addition, with a much improved thermal monitoring system at several locations in the telescope and dome, and with improved access to the mirror, it is intended to gradually bring the mirror cooling system into operation when safe ways to avoid accidental condensation of moisture have been worked out. In parallel, the design and operation of the mirror ventilation system will be improved, drawing on the very encouraging experience from the ESO 3.6-m telescope. The final step in the process would be to replace the CCD with one that does not suffer from the degradation in resolution seen with the Loral chips, but a suitable chip with the desired combination of high spatial resolution, availability and affordable price has not yet been identified.

Additional work which has been done during this extended technical period includes:

- Clean and bake the CCD dewar and its molecular sieve (CUO).
- Move the CCD preamplifiers to the outside of the dewar (CUO).
- Re-aluminise and realign M1 (LS Optics Team).
- Refurbish the drive and install limit switches for the DFOSC rotator (CUO).
- Install new, more powerful fans with air filters for mirror ventilation (CUO).
- Drill holes in the mirror cell to improve the air flow of the mirror cooling system (CUO).
- Remove many obsolete cables and re-route many of the loose cables hanging from the telescope (CUO and 2p2 Team).
- Remove instruments that have been definitively retired from active service at the telescope (two-channel photometer, polarimeter, CORAVEL).
- Upgrade the version of VXworks for the TCS VME (2p2 Team).
- Upgrade the workstations to HP/UX 10.20 (LS Software group).
- Install 2 9-GB disks on the data-acquisition WS (LS Software group).

We trust that these major efforts by many staff members of CUO and of ESO will give this favourite workhorse of many ESO and Danish observers another long period of productive service, even in a world of stiffening competition. The substantial investment in the dome upgrade has been provided by the Danish Natural Science Research Council through its Infrastructure Centre for Ground-Based Astronomy, located at CUO.



The NTT Service Observing Programme: Period 60 Summary and Lessons Learned

D. SILVA (dsilva@eso.org), Data Management and Operations Division

This is the second in a regular series of articles about VLT Data Flow Operations (DFO). In this article, the NTT service observing programme, a VLT DFO prototype, is discussed.

1. Introduction

Between February 1997 and March 1998, ESO ran a service observing programme at the NTT. The primary goal of this programme was to develop and test prototype operations tools and concepts for the planned VLT service observing programme. The NTT programme has been halted for now and service observing is not scheduled for Periods 61 or 62. However, the Observing Programmes Committee and the Users Committee have recommended that NTT service observing resume during Period 63, provided ESO can devote resources to this programme without hindering the development or implementation of VLT science operations. ESO is also studying what is necessary to provide limited service observing support for use of the Wide Field Imager at the 2.2-m starting in Period 63.

Before continuing service observing at the NTT or implementing it at other ESO facilities, it is appropriate to ask: what have we learned? In this article, the concepts and history of the NTT service observing programme are described. Then some lessons learned and how they will affect VLT planning are discussed.

2. Why Service Observing?

When assessing the success of a prototype programme, it is important to keep in mind the original high level goals. Service observing (as previously discussed by Silva & Quinn, 1997) has three main goals:

2.1 Maximise science efficiency

Service observing attempts to maximise science efficiency in two ways. First, at any given moment, the highest OPC ranked programme with Principal Investigator (PI) specified observing conditions

requirements which match the current observing conditions is given highest priority. In this way, the most scientifically meritorious programmes are executed first and under the PI defined optimal observing conditions. Remember, however, that no matter how highly a programme is ranked by the OPC, if a PI requests rare conditions, such as exceptionally good seeing, their programme may never be executed if those conditions do not arise.

A second goal is to acquire scientifically useful datasets, as defined by the programme Principal Investigator (PI). For example, in a multi-cluster sample, it may be more useful to have a complete dataset for one cluster than randomly incomplete datasets for all clusters. Over the course of some time interval, these goals should assure that the highest ranked proposals are completed first as long as they do not require rare observing conditions.

A third goal is to facilitate the scheduling of a broader range of science programmes, such as synoptic and Target of Opportunity programmes as well as programmes that require co-ordination between several different facilities. Such programmes are difficult to support in a standard operations model.

2.2 Maximise operational efficiency

Service observing tries to maximise operational efficiency in two ways. First, whenever possible, scientifically appropriate, and consistent with OPC recommendations, observations that require common calibration data are executed as a group so that the calibration data can be shared between several different programmes. Second, experienced staff observers are used to execute observations. Since they are more familiar with the facility, these observers should be more efficient relative to visiting astrono-

mers who only use the facility once or twice a year. Furthermore, most visiting astronomers, no matter how experienced, are less efficient on their first night. For the two- or three-day observing runs typical at heavily used facilities like the NTT, this first night inefficiency can have a significant impact on the overall productivity of the observing run. Staff astronomers, given their familiarity with the facility, can usually minimise this problem.

2.3 Maximise ability to re-use data

An important goal for the VLT and other ESO facilities like the NTT is to maximise the ability of future researchers to re-use data to address different science problems. It is easy to capture all acquired data and store them, but these data will be worthless without suitable calibration data and proper records. Anecdotal evidence as well as a review of the NTT data archive suggests that many visiting astronomers do not perform a calibration and operations plan rigorous enough to produce uniform datasets for future use. During service observing, however, the observatory has total control and can assure that proper calibration data are acquired and sufficient records kept. This process is facilitated by the implementation of calibration plans for each instrument by the scientist responsible for that instrument.

3. Why the NTT?

As part of the NTT Big Bang process, ESO installed a VLT Data Flow System (DFS) prototype. The DFS is a set of software tools and procedures to manage VLT science programmes from the initial proposal to future archival research (Quinn, 1997). These tools were designed with the needs of both service observing and visiting astronomer programmes in mind.



Figure 1: Period 60 NTT Service Observing task flow.

But do these tools work? Do they facilitate or hinder service observing? Do they make general observatory operations more efficient or less efficient? These are issues that ESO wanted to address and resolve before VLT operations began.

Furthermore, VLT science operations are not simply a matter of implementing the right software and hardware. The proper procedures must also be developed and documented. Some of the most important procedures involve providing adequate user support, which involves not only answering user queries and providing adequate general documentation, but also providing the right level of real-time information about observatory operations. Again, ESO saw that it was better to develop these procedures as early as possible, so that VLT science operations would be as efficient as possible right from the start.

4. Periods 58 and 59: Learning the Hard Way

NTT service observing began at the NTT during February 1997. During the second half of Period 58 and the first half of Period 59 (February – June 1997), service observing was executed by the NTT Team on a “shared risk” basis as Big Bang activity and weather permitted. Despite heroic efforts by the NTT Team (led at the time by Jason Spyromilio), operations were plagued by a number of technical problems, as well as a particularly strong El Niño weather pattern, reducing the amount of useful data acquired to a minimum. To make matters worse, users were required to come to Garching to prepare Observation Blocks (OBs)¹, assist-

ed by the DMD User Support Group (led by the author), using prototype software. Several frustrated users who invested many hours in preparing OBs never received any data. Due to poor planning and bad records (e.g. faulty FITS headers), data quality control and distribution by the USG fell behind. Although this period had been advertised as “shared risk” and “best effort”, most users were unhappy. Nevertheless, some interesting science programmes were successfully supported, such as the SUSI Deep Field project (D’Odorico, 1997) and follow-up spectroscopy of Galactic bulge microlensing events (Lennon et al., 1997).

The second half of Period 59 (July – September 1997) (often called NTT2 or Period 59.2) was supposed to be a return to full NTT operations. On the mountain, technical operations proceeded much more smoothly, thanks again to the hard work of the NTT Team (led then by Gautier Mathys). Unfortunately, observing conditions continued to be poor, especially the seeing, due to the strong El Niño effect. In Garching, although the OB creation and scheduling process went much better, USG data quality control and distribution activity continued to be very inefficient. Much of the Period 59.2 data was not distributed to the proper end users until December 1997, i.e. 3–6 months after the data were acquired. Simply put, the USG did not have sufficient personnel during Period 59.2 to accomplish its assigned tasks in a timely manner.

These were painful months for everyone, users and ESO staff members alike.

¹Observation Blocks (OBs) describe how simple datasets are acquired and record the status of those datasets. OBs are simple – they consist of just one telescope pointing and the acquisition of a single dataset. They are the smallest items that can be created, scheduled, and executed by the Data Flow System.

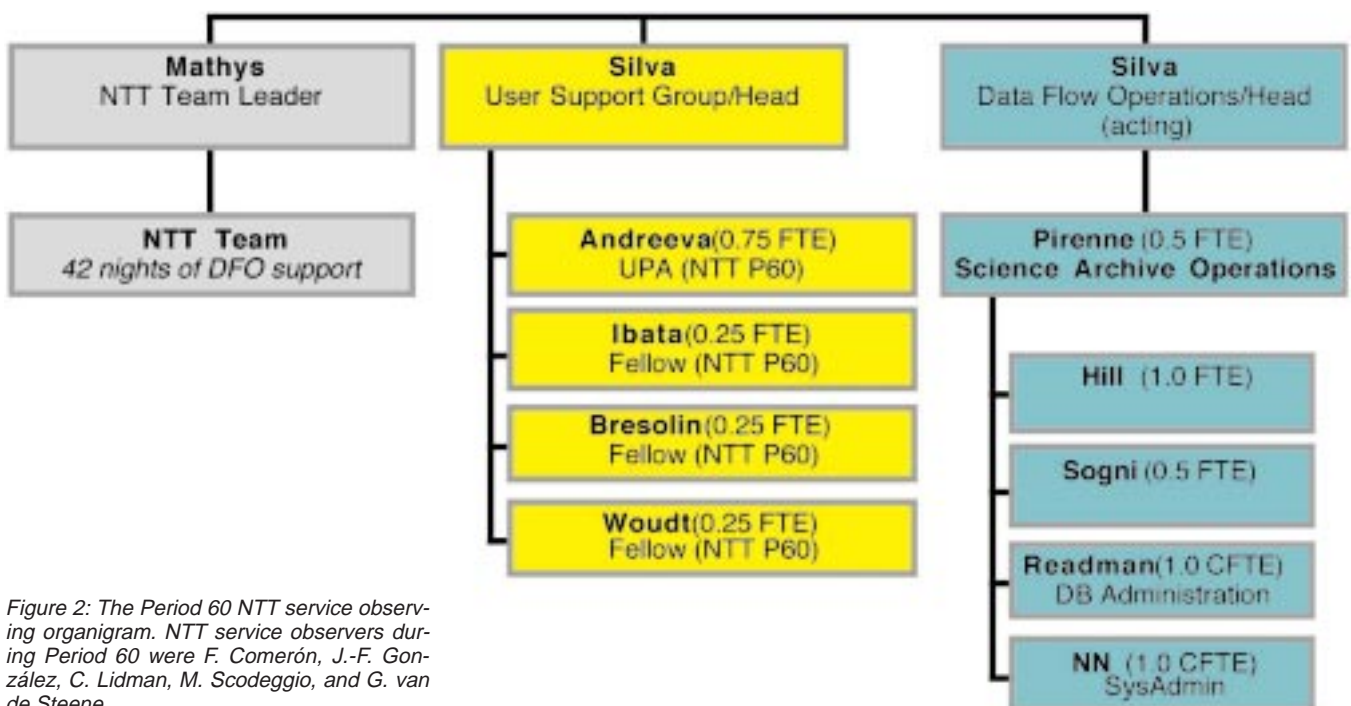


Figure 2: The Period 60 NTT service observing organigram. NTT service observers during Period 60 were F. Comerón, J.-F. González, C. Lidman, M. Scodiggio, and G. van de Steene.

5. Period 60: A New Beginning

In many ways, Period 60 represented a new beginning for the NTT service observing programme. With improved software tools, adequate staffing, and improved weather conditions, ESO was able to provide much better service to our users.

5.1 The Tasks

Figure 1 illustrates the NTT service observing tasks during Period 60.

Observation Blocks (OBs) were created by PIs assigned NTT service observing time using the Phase 2 Proposal Preparation (P2PP) tool. Most Period 60 users were able to create their OBs at their home institutions without significant assistance from the USG. Only one user had to come to Garching and the USG did create OBs for two programmes. After creation, OBs were submitted directly across the Internet to ESO by the P2PP tool for scheduling.

Scheduling was a two-part process. For any given service observing run, the USG created a Medium-Term Schedule (MTS) which contained a list of all executable OBs for the given Local Sidereal Time range, lunar phase, and available instrumentation. The MTS also contained information about relative OPC priorities, user specified observation condition requirements, and required instrument configurations. Typically, the MTS was created less than 36 hours before the start of a service observing run. The second phase of scheduling, creating the Short-Term Schedule (STS), was done by the NTT Team at the telescope. In real-time, the NTT service observer would select an OB from the MTS pool with the highest OPC priority which could be executed under the current observing conditions. For most of Period 60, this was done manually, although during early February 1998, a prototype STS creation software tool was tested.

NTT mountain operations was the responsibility of the NTT Team. Tasks included science OB selection and execution, calibration plan execution, real-time data quality checking, and a variety of record-keeping tasks.

Once acquired, data were transferred back to Garching, usually immediately via FTP transfer. The next day, all data were reviewed and classified manually using a standardised data quality control process. Frames were graded:

- A – all user specifications met
- B – all user specifications met within 25%
- C – all user specifications violated by 25% or more

If an OB (or some part of an OB) failed to pass data quality control, attempts were made to re-execute it later.

Once a logical dataset was collected for any given programme (e.g. all observations in a given filter, all observations

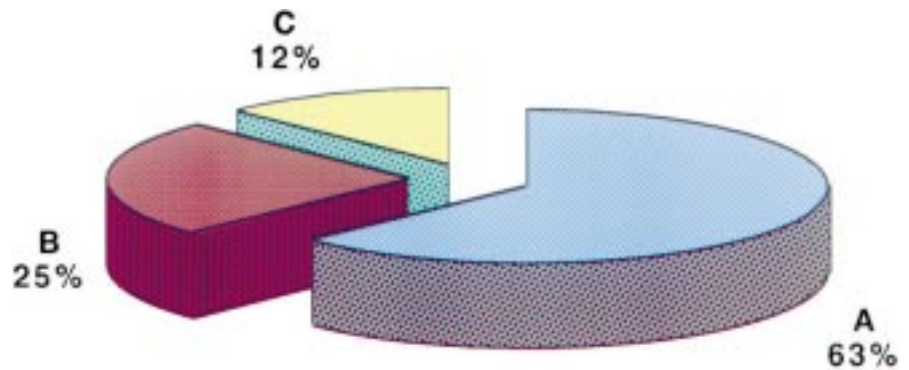


Figure 3: Period 60 OB Grade Distribution. Total number of science OBs executed: 495. See text for grade definition.

of a given cluster), a CD-ROM was prepared containing all the science data plus the relevant calibration data. Users were sent all data taken for their programme, no matter what the quality control grade. In practice, Period 60 data were distributed three times: in December 1997 when SUSI was decommissioned (all SUSI PIs were issued whatever data were available for their programmes), in February 1998, when a number of EMMI programmes were completed, and in April 1998 (i.e. the end of Period 60), at which point all remaining data were distributed. In short, within one month of the completion of Period 60, all data had been distributed, a vast improvement over the Period 58 and 59 problems.

Finally, user information was regularly updated on our Web site, which is still available at <http://www.eso.org/dmd/usg>. Information posted included nightly activity summaries and updates on the progress of individual programmes.

5.2 The Team

Although many improved tools and procedures were used during Period 60, the most significant improvement was allocating the right number of people. The Period 60 team is shown in Figure 2. Keeping in mind that the DMD Science Archive Operations team was supporting NTT and HST/ECF archive activities as well as VLT archive operations start-up

work, the Period 60 NTT service observing programme personnel cost was 2.0–2.5 Full Time Equivalents (FTEs), including all USG, NTT Team, and Science Archive Operations activities.

5.3 The Results

During Period 60, we tried to quantify as many operations processes as possible so we can analyse where we had been successful and where we needed to improve. Here, three examples of the information available are discussed.

In Figure 3, the distribution of OB grades based on the post-observation quality control check is shown. Most Grade B OBs were observed under slightly worse seeing than specified, typically because the seeing deteriorated during an exposure or because these were the best OBs available during a period of marginal seeing. Grade C OBs represent more serious failures: poor tracking near the zenith or sudden change in sky transparency are typical causes. Fortunately, we were able to repeat most Grade C OBs. The generally high success rate was due to the fact that OBs which spanned a large range of observing conditions were almost always available. Rarely did we have problems with not having enough OBs for a given night.

Our records also allow us to accurately account for the time we used on the NTT. Figure 4 shows the fractional breakdown.

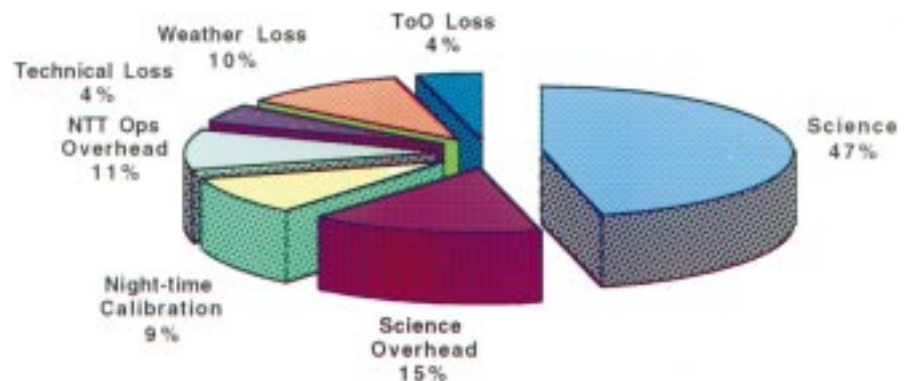


Figure 4: Period 60 Service Observing Programme NTT Time Usage. Science time = integration time only. Science Overhead = slews, CCD read-down, instrument set-up. NTT Ops Overhead = focus and active optics updates. ToO Loss = time used on service observing nights for Target of Opportunity observations (including all overheads).

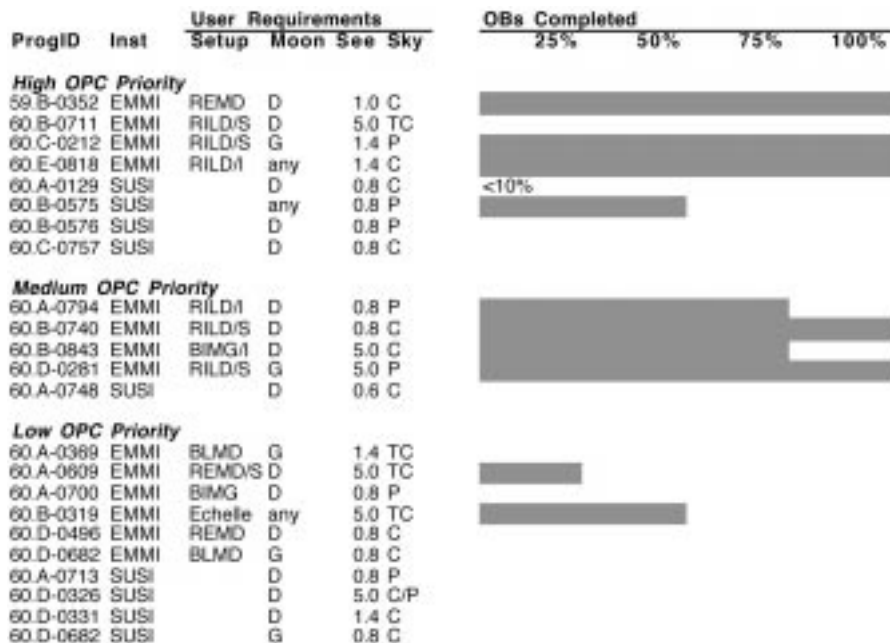


Figure 5: Period 60 Observing Programme Final Status Summary. For Moon (for “moon phase”), D = dark, G = gray. Under See (for “seeing”), these are upper limits on acceptable PSF FWHM in arcseconds. Under Sky (for “sky transparency”), P = photometric, C = clear, and TC = thin cirrus.

Several interesting things are revealed. First, the weather down time was only 10% because during service observing runs there is almost always an OPC approved programme available to take advantage of worse than median seeing or reduced sky transparency. Second, the 15% science overhead, is mostly EMMI CCD readout time, will be more than cut in half when EMMI is upgraded to FIERA controllers. Finally, the NTT operations overheads during Period 60 were mostly caused by inefficient telescope focus and active optics update procedures. However, these procedures have recently been made more efficient – hopefully, Period 61 users have already benefited from this! Finally, it is remarkable (at least to the author) that the NTT is only suffering 4% technical downtime so soon after the Big Bang.

A common question asked is “how many programmes did you complete?” This issue is addressed by Figure 5. Again, this figure has several interesting features. First, no SUSI programme was completed because: (1) many SUSI programmes required excellent seeing; (2) the actual seeing was seldom sub-arcsecond during the first half of Period 60; and (3) SUSI was decommissioned during the first week of December, halting SUSI operations. Second, programmes with less stringent user requirements were more successful. Finally, convincing the OPC to assign a high grade is very helpful! Given this latter point, we did not request OBs from all programmes in the low OPC priority group unless there was a high probability that we could execute some part of their programme. Our projections were not always accurate (i.e. some PIs submitted OBs which we nev-

er executed) but we spared some users unnecessary work.²

6. Lessons Learned

NTT service observing has been halted until at least Period 63 and ESO is now preparing for the VLT service observing programme. What have we learned from the NTT experience?

6.1 Queue Management

It is important that service observing queues span a sensible range of observing conditions. For example, if on average only 10% of the available time is expected to have seeing less than 0.5 arcseconds, 30% of the available time should not be allocated to programmes that require such good seeing. Or, if good bright-time instrumentation is unavailable, do not assign many bright-time programmes to the service observing queue. Similarly, it may be more desirable to have a much larger relative fraction of dark-time than bright-time assigned to service observing if suitable bright-time programmes are unavailable. Be prepared for abnormal conditions by over-subscribing service observing – not by numbers of targets or hours, but by observing conditions. For example, since the NTT usually delivers good image quality, the ESO OPC tends to allocate a large fraction of time to programmes that require sub-arcsecond seeing. Unfortu-

²Regrettably, no data were acquired for 60.B-0711, despite having a high grade and less restrictive requirements, because the PI did not submit any OBs. But, of course, other programmes benefited from this decision.

nately, it was not anticipated that 1997 would be a strong El Niño year and the OPC continued to allocate time to good seeing programmes. As a result, the 1997 NTT service queues contained too many sub-arcsecond seeing programmes and not enough programmes that could tolerate worse than arcsecond seeing.

6.2 User Information Management

Users with programmes in the service observing queue typically want to know the following things: why is their programme not being executed right now; if not now, when is their programme going to be executed; what OBs have been executed to date, and when are they going to receive their data. At the end of a schedule period, if their programme was not initiated or completed, they want to know why. If they had been at the telescope, they would know the answers to these questions (e.g. it was cloudy, there was an instrument failure). In service observing, the answers can be more complicated (e.g. the conditions were never right, your programme did not have a high enough OPC scientific ranking) and sometimes the final answers are not available until the entire scheduling period is completed.

The NTT experience demonstrates that service observing user anxiety can be greatly reduced by publishing the OPC recommended scientifically ranked queue at the beginning of the period and nightly summaries of service observing activity during the period, including programmes serviced, observing conditions, usable time vs. lost time, and updated summaries of individual programme progress. In combination, this information allows individual users to understand for themselves why scheduling decisions have been made about their programme. The basic information desired is actually quite simple and is easily published via the Web (see <http://www.eso.org/dmd/usg/>). In addition, the VLT Data Flow System will provide tools for users to retrieve information about individual OBs as their programme progresses.

6.3 OB Management

Philosophically, Observation Blocks are supposed to be indivisible objects. Users are instructed to keep OBs as simple as possible – no more than one instrument configuration per OB and a total execution time of no more than one (1) hour, preferably as short as possible. Nevertheless, it is very tempting for users to make OBs more complicated. This may seem more natural to users because during traditional observing runs users are familiar with the need to interrupt and re-arrange their programme in real-time to match observing conditions. Users expect that service observers will do the same. However, service observers are not restricted to executing any particular

programme during the night. They have the freedom to pick observations to meet conditions from a variety of programmes. To make this process efficient, service observers want OBs to be as simple and as short as possible to maximise scheduling flexibility.

Two example OBs illustrate this point: consider OBs which request N imaging integrations through M filters of the same target or N 3600-second spectroscopic integrations of the same target. During service observing operations, such complex OBs are difficult to schedule efficiently. Furthermore, the schedule problem is exacerbated when part of a complex OB produces bad data and the observation must be re-scheduled. Since the DFS is only supposed to re-schedule complete OBs, not parts of OBs, re-scheduling complex OBs reduces the overall productivity of the queue.

Such inefficiencies can be avoided in two ways. First, users must be educated to make OBs which are easy to schedule, so they must be told how OBs are scheduled and given OB construction guidelines. In the examples above, the simplest and easiest to manage choices would have been $M \times N$ imaging OBs and N spectroscopic OBs. Second, the tools for OB construction must be able to make OBs efficiently so the user is willing to make many simple OBs as opposed to a few complex OBs.

6.4 Data Management

One of the most important experiences from the NTT is the need to review and distribute service observing data as quickly as possible. Timely data review, preferably the next day after a service night, is critical for uncovering data problems (e.g. deficient calibration data, instrument performance anomalies) early enough that many subsequent nights of data are not corrupted. Timely review maximises schedule flexibility by providing information about which OBs need to be re-scheduled and which programmes need to be serviced (or can stop being serviced because enough OBs have been completed). Finally, timely review also allows more rapid data distribution. One VLT goal is to have 90% of the data distributed within one month of the observation execution, with the biggest anticipated bottleneck being the transfer of data from Paranal to Garching on digital media. Improved tools to make data quality control activities more efficient, more informative, and more uniform, are planned for UT1.

Efficient data management also relies on correct and complete FITS headers. During the first half of 1997, the NTT headers had a number of problems which exacerbated our data distribution problems. It is obviously critical to stabilise FITS headers early and then rigorously maintain them.

6.5 Operations Management

A requirement for the success of VLT science operations is the need to co-ordinate science operations across transcontinental distances. The NTT service observing programme demonstrated that the DFS will be able to handle the technical co-ordination issues. During 1997, it was possible: for OBs made by users at their home institutions to be submitted electronically to Garching and then automatically forwarded to La Silla; for Medium-Term Schedules to be generated in Garching and transferred electronically to La Silla; for operational problems to be resolved via e-mail; and for acquired data to be automatically transferred from La Silla back to Garching for ingestion into the science archive.

However, the NTT programme also illustrated that not all relevant information is or can be encoded in the OBs, logs, and FITS files transferred between Chile and Germany, that real-time decisions must sometimes be made when the time zone difference and/or workshift inversion make real-time communication between the two groups difficult to co-ordinate; that it is usually easier for the local team to anticipate and solve local problems than the remote team; and that deviations from standard procedures or the original plan must be globally communicated and explained.

Applying these lessons to VLT science operations implies a high degree of personal operational awareness and responsibility from the members of the operations teams to assure success, especially by the on-duty service observer. One of the biggest challenges of service observing is assuring that the service observer has enough information to make good real-time scheduling decisions. Service observers cannot just blindly follow a schedule made remotely – they must be trained and empowered to make the right real-time decisions to use the VLT in a scientifically effective and operationally efficient manner.

Clearly stated, globally communicated lines of responsibility and authority are also important for a distributed operations model. Early operations efficiency at the NTT was reduced because the tasks and responsibilities of the various sub-teams were not sufficiently defined. By Period 60, this issue had been resolved but it is unacceptable for this to happen again at the VLT. During 1998, ESO will be working on defining carefully the VLT science operations roles and responsibilities, as well as the VLT operations command structure.

Finally, task load must be matched to available resources. ESO did not adequately support NTT service observing during Period 59 and the result was deficient user services, particularly in the area of data distribution. We believe the VLT science operations task and available resources are properly matched.

6.6 Operations Tracking

Every oversight committee in the world interested in telescope operations wants to have detailed statistics about service observing programmes, especially in these early days as this technique is developed at ground-based observatories. It is not that they are skeptical, they are just being cautious. Common requests are: total integration time vs. total available time, programme completion status vs. TAC/OPC ranking, programme completion status vs. actual observing conditions, and relative fractions of operational overheads, calibration observations, technical downtime, weather-related downtime, and science observations. Other combinations are possible.

It is far better to anticipate these reporting requirements early and build up the statistical databases progressively during operations than to try to recover this information from observing logs, e-mail, OBs, etc. after the fact. Although not an explicit design requirement, as a by-product of operations, the Data Flow System generates all the relevant raw information. Tools for automatically generating the anticipated reports are planned.

7. Conclusions

We conclude with the obvious question: did we achieve our original high-level goals at the NTT as stated at the beginning of this article? In the area of science efficiency, as Figure 5 illustrates, we did concentrate on more highly ranked programmes and we were successful at completing programmes we executed. We were also operationally efficient (see Figures 3 and 4) – we were able to minimise weather down-time, most of the time we only had to execute an OB once to acquire data acceptable to the user, and we did share calibration data between programmes (although only for imaging programmes). Finally, because we did have a standard calibration plan and we did execute it faithfully, the data delivered to the archive should be quantitatively useful to archival researchers once the data become public.

However, other questions are important as well. Was service observing more or less efficient than standard visiting astronomer observing? Are the PIs who received data satisfied with their data and has it made them more productive? Does service observing increase or decrease the science impact of the NTT? ESO will try to answer the first question by analysing records from visiting astronomer runs. The second question will be addressed later this year via a survey of PIs assigned service observing time. The final question will only be answered over time as we see what and how many papers derived from service observing programmes are published in the scientific literature.

In the end, ESO made mistakes during the Period 58–60 NTT service observing programme, but we also learned many valuable lessons. VLT science operations will benefit significantly from this initial prototype programme.

In the next article of this series, the OB creation process will be discussed.

8. Acknowledgements

The NTT service observing programme was a team effort. During this programme, the NTT Team was led by Jason Spyromilio and Gautier Mathys, both of whom contributed enormous amounts of their time and energy into this

programme. Significant service observing support and operations feedback was provided by the following NTT Team members: Fernando Comerón, Jean-François Gonzalez, Chris Lidman, Pierre Martin, Marco Scodeggio, and Griet van de Steene. In Garching, NTT Data Flow Operations support came from the following DMD User Support Group members: Carlo Boarotto, A. Maurizio Chavan, Gino Giannone, Steve Roche; Petia Andreeva, Fabio Bresolin, Rodrigo Ibata, and Patrick Woudt. Data Flow Operations support also came from the DMD Science Archive Operations Team: Benoit Pirrenne, Susan Hill, and Fabio Sogni. As always, Bruno Leibundgut struggled valiantly to keep us on the True Path. Spe-

cial thanks to Stephanie Cote, and especially, Albert Zijlstra who contributed so much during the grim, early days.

Extra special thanks to all the astronomers who were awarded NTT Service Mode time during P58–P60. Hopefully, all your hard work has paid off in useful NTT data now and better VLT science operations in the future.

References

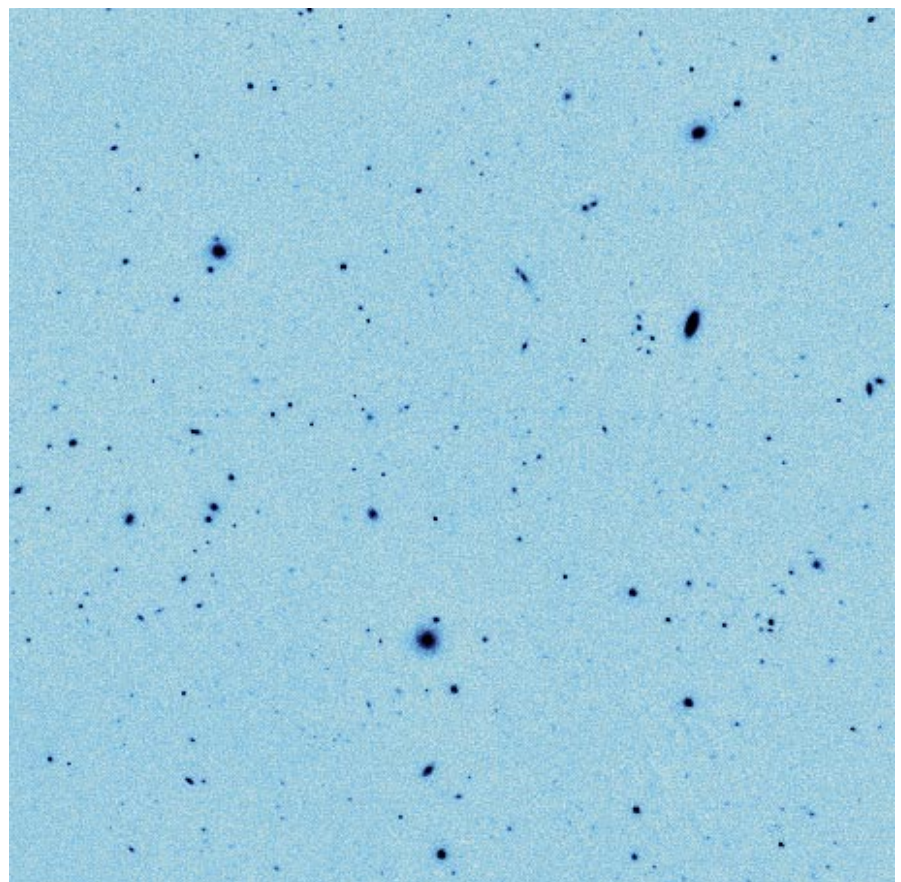
- D'Odorico, S. 1997, *The Messenger*, **90**, 1.
Lennon, D.J., Mao, S., Reetz, J., Gehren, T., Yan, L., and Renzini, A. 1997, *The Messenger*, **90**, 30.
Quinn, P. 1997, *The Messenger*, **84**, 30.
Silva, D. and Quinn, P. 1997, *The Messenger*, **90**, 12.

SOFI Infrared Images of the 'NTT Deep Field'

Deep infrared J (1.25 μm) and Ks (2.16 μm) band images of a 5×5 arcmin field centred on $12^{\text{h}} 05^{\text{m}} 26^{\text{s}}$; $-07^{\circ} 43' 27''$ (J2000) obtained during the commissioning of SOFI (Moorwood, Cuby and Lidman, 1998, *The Messenger*, 91, 9) at the NTT in March 1998 will be made available via the Web (under Science Activities on ESO's Homepage) in early June. The Ks image is shown here in Figure 1. This field contains the smaller region observed with SUSI (D'Odorico, 1997, *The Messenger*, 90, 1) for which visible images are already available on the Web. The infrared images have been constructed from jittered observations totalling 4.3 hours in J and 10.4 hours in Ks and have an average point source FWHM of about 0.75 arcsec. Limiting magnitudes (3σ within a 1.5 arcsec diameter aperture) are J = 24.66 and Ks = 22.87. Full details of the observations and data reduction will be put on the Web together with instructions for retrieving the images.

A. MOORWOOD

Figure 1: Ks (2.16 μm) image of the NTT Deep Field. The field is $\sim 5 \times 5$ arcmin, seeing is ~ 0.75 arcsec and the 3σ limiting magnitude in a 1.5 arcsec diameter aperture is 22.87 (data reduced by P. Saracco).



Upgraded NTT Provides Insights Into the Cosmic Big Bang

P. BONIFACIO and P. MOLARO, Osservatorio Astronomico di Trieste, Italy

The EMMI spectrograph with the upgraded NTT has been used to detect for the first time the Li I subordinate doublet at $\lambda\lambda$ 6104 Å (the doublet has three components: $2^2P_{1/2} - 3^2D_{3/2}$, $2^2P_{3/2} - 3^2D_{5/2}$, $2^2P_{3/2} - 3^2D_{3/2}$, at wavelengths 6103.538 Å, 6103.649 Å, 6103.664 Å respectively) in the prototype population II star HD 140283. The Li abundance from this line is consistent with that previously obtained from the widely used resonance line, thus giving confidence in the use of Li in the framework of standard nucleosynthesis (Bonifacio and Molaro, 1998).

On August 10 and 11, 1997, we were conducting an observing programme at La Silla, Chile, aimed at very precise measures of the Li I resonance line at $\lambda\lambda$ 6707 Å in a sample of halo dwarfs. On each night we observed HD 140283 for 40 and 20 minutes, respectively, as a calibration star since this is a very bright ($V = 7.24$) and metal poor ($[Fe/H] \approx -2.7$) star. The telescope was the ESO NTT and the spectrograph was EMMI equipped with the R4 (i.e. $\tan \theta = 4$) echelle grating ESO #14 (D'Odorico and Fontana, 1994). The seeing in those nights was sub-arc-second and we used a projected slit width of 0.8", obtaining a resolution of $\lambda/\Delta\lambda \approx 61000$, as measured from the Th-Ar lamp emission lines. As cross-disperser we employed grism # 6 which achieves a wide-order separation allowing to keep a slit height of 15" projected on the sky. Such a high slit is essential for a good sky subtraction. After full reduction with the MIDAS echelle package the coadded spectrum had a signal-to-noise of ≈ 360 .

On such high resolution, high S/N spectra we searched for the Li I $2^2P - 3^2D$, 6104 Å transition. This transition is the strongest subordinate line of Li I but is much fainter than the resonance line. So far this line has been detected only in young T Tauri stars (Hartigan et al., 1989) and Li-rich giants (Wallerstein and Sneden, 1982), where Li is about 1 dex more abundant than in Population II stars owing to the Galactic Li production. As can be seen in Figure 1, the Li I feature is clearly detected in the spectrum of HD 140283 at 6103.6 Å, redwards of the Ca I 6102.723 Å line, in the photospheric rest frame. The equivalent width is 1.8 ± 0.3 mÅ and the detection is at 6σ of confidence level.

This detection is clearly a credit to the high-resolution capabilities of the NTT,

and its improved efficiency allowed us to perform the observations in a reasonable amount of time; however, what is its astrophysical significance? Lithium, together with D and ^3He , is one of the few elements produced by nuclear reactions in the first minutes after the big bang (Wagoner, Fowler and Hoyle, 1967). The observations of these elements and their extrapolation to the primordial values are about consistent with the predictions of the primordial nucleosynthesis providing, together with the relic radiation and the expansion of the Universe, a robust support to the standard big-bang theory (nothing to do with NTT here). Since the yields of light elements depend on the single parameter $\eta = n_b/n_\gamma$, the baryon to photon ratio, the determination of the primordial Li abundance, as well as the other primordial elements, allows us to fix the value of η , and therefore of Ω_b . The possibility to determine the primordial abundance of Li relies on the discovery made by Spite & Spite (1982) that metal-poor halo dwarfs showed the same Li abundance regardless their metallicity or effective temperature: the so-called *Spite plateau*. This was interpreted as evidence that the Li observed in these stars was of primordial origin. Recently, additional support to the primordial nature of Li in halo dwarfs has come from the observations of Li in metal-poor stars of the thick disk (Molaro, Bonifacio and Pasquini,

1997). This population is chemically and kinematically distinct from the halo, but has the same Li abundance as the halo. Minniti et al. (1997) claimed detection of Li, at the plateau level, in a metal-rich, but old star, belonging to the Galactic Bulge. Finally, Li at the plateau level has also been detected in a star which was possibly born in an external galaxy and then accreted by the Milky Way (Molaro, 1997).

So far the Li abundance has always been obtained only from the analysis of the Li I $\lambda\lambda$ 6707 Å resonance doublet. This is not a very comfortable situation. Quite seriously, our ability to determine the Li abundance using simple plane-parallel homogeneous atmospheres, has been challenged by Kurucz (1995). The analysis of several lines, which sample different depths in the stellar atmosphere is crucial to test the correctness of the modelling. The one-dimensional, homogeneous, static models which are currently employed may arise concern because they ignore the fine structure and hydrodynamic phenomena such as granulation which are seen on the Sun. The detection of the Li I $\lambda\lambda$ 6104 Å transition in the spectrum of the metal-poor star HD140283 opens up for the first time the possibility of testing the applicability of our simple models to the determination of Li abundances. We have verified that both the subordinate

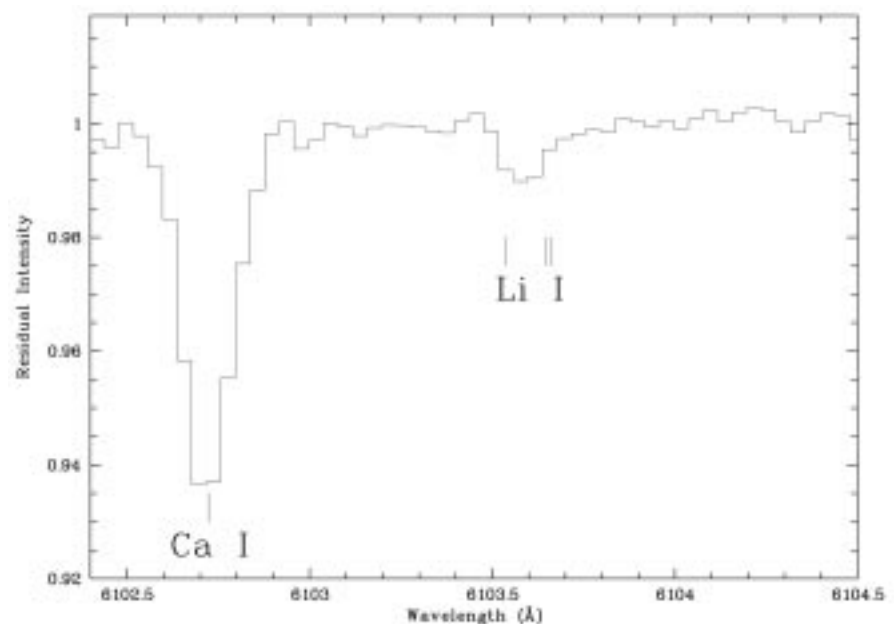


Figure 1: The observed Li I $2^2P - 3^2D$ transition.

and the resonance line are consistent with the computations made using a one-dimensional, homogeneous model atmosphere, thus increasing our confidence that this model represents a satisfactory average of the complex fine structure expected in metal-poor stars (Bonifacio and Molaro, 1998). The VLT and the high-resolution capabilities of the UVES spectrograph will allow to measure the Li 6104 Å Li I subordinate doublet in other much fainter population II stars, thus permitting to verify the consistency between the resonance and subordinate Li I lines on a statistically significant sample, thus achieving a more accurate measurement of the primordial Li abundance and ultimately of Ω_b .

In addition to the problems with the Li abundance determination, one must be careful about two other possible effects which are important in this context: Li production by galactic sources and Li depletion in the stars. Consider Li production first: we know that the meteoritic value is $(\text{Li}/\text{H}) = (2.04 \pm 0.19) \times 10^{-9}$, i.e. over one order of magnitude larger than that observed in the Pop II stars. Several mechanisms may contribute to raise the Li abundance from the Pop II value to the meteoritic value like spallation by cosmic rays in the ISM, production in AGB stars (Cameron-Fowler mechanism) or neutrino-induced nucleosynthesis in supernova explosions. There are several uncertainties in the various contributions, but it seems that there are no problems for a Galactic Li production of the order of 90% of the Li presently observed (Matteucci D'Antona and Timmes, 1995). Consider Li depletion next: Li is a very fragile element and can be destroyed if convection takes it down to temperatures of about 2.6×10^6 K where the $\text{Li}(p,\alpha)\text{He}$ reaction is effective. This is what probably happened in the sun where the Li abundance in the solar photosphere is two orders of magnitude less than the meteoritic val-

ue, and in solar metallicity field stars which show a scatter in the Li abundance of three orders of magnitude. For Pop II stars the situation is remarkably different. The Spite plateau shows no evidence for scatter in Li abundance (Bonifacio and Molaro, 1997). The surface convection zone of a metal-poor star is much shallower and more superficial than that of a solar-metallicity star of the same effective temperature probably preventing Li destruction. Standard models predict no Li depletion for metal-poor stars. Depletion is predicted by non-standard models which take into account rotational mixing or diffusion (Pinsonneault, Deliyannis and Demarque, 1992, Vauclair and Charbonnel, 1995). However, these models predict a downturn of the hot side of the Li plateau and considerable dispersion, which are not seen in the observations. This suggests that diffusion or rotational mixing do not affect significantly the Li observed at the stellar surface of metal-poor dwarfs.

Overall, the case for a primordial lithium at the value observed in the Population II stars, with no production by galactic sources or destruction inside the stars, is rather robust. The primordial yields for Li are not a monotonic function of η , due to the different contribution of the Li forming reactions at different η regimes. They show a minimum, i.e. the *Li valley*. This implies that in general a value for Li will provide two solutions for η . Only knowledge of the primordial abundance of the other light elements allows to rule out one of the two roots. The more recent value is $(\text{Li}/\text{H}) = 1.73 \pm 0.05_{\text{stat}} \pm 0.2_{\text{sys}} \times 10^{-10}$ (Bonifacio and Molaro, 1997), which gives two different values for η : $\eta = 1.7 \times 10^{-10}$, which is in agreement with the high deuterium ($D/H = 2.0 \times 10^{-4}$ Webb et al., 1997) and the low primordial helium ($Y = 0.228$ Pagel et al., 1992) and $\eta = 4.0 \times 10^{-10}$ which is in much closer agreement with the low deuterium ($D/H = 3.4 \times 10^{-5}$

Burles and Tytler, 1998) and relatively high primordial helium ($Y = 0.243$ Izotov et al., 1997). Thus a perfect concordance on the η value derived from the observations of the primordial elements has still to be found.

References

- Bonifacio P. & Molaro P., 1997, *MNRAS*, **285**, 847.
 Bonifacio P. & Molaro P., 1998, *ApJL*, in press.
 Burles S., & Tytler D., 1998, in *Primordial Nuclei and their Galactic Evolution*. ISSI workshop, Kluwer, Dordrecht, preprint astro-ph/9712265.
 D'Odorico S. & Fontana A., 1994, *The Messenger*, **76**, 16.
 Hartigan P., Hartmann, L., Kenyon S., Hewett, R. & Stauffer J., 1989 *ApJS*, **70**, 899.
 Izotov Y., I., Thuan T., X., Lipovetsky: 1997, *ApJS* **108**, 1.
 Kurucz, R.L., 1995, *ApJ*, **452**, 102.
 Matteucci F., D'Antona F., and Timmes, F. X. 1995 *A&A* **303**, 460.
 Minniti D., Vandehei T., Cook K. H., Griest K., & Alcock C., 1997, submitted to *ApJ*, astro-ph/9712047.
 Molaro P., 1997, in D. Valls-Gabaud, M.A. Hendry, P. Molaro, and K. Chamcham, eds., ASP Conference Series, Vol. 126, 1997, p. 103–120.
 Molaro P., Bonifacio P., & Pasquini L., 1997, *MNRAS*, **292**, L1.
 Pagel B.E.J., Simonson E. A., Terlevich R., J & Edmunds M. G. 1992, *MNRAS*, **255**, 325.
 Pinsonneault M.H., Deliyannis C.P., & Demarque P., 1992, *ApJs*, **78**, 179.
 Spite, F. & Spite, M., 1982, *A&A* **115**, 357.
 Vauclair S., & Charbonnel C., 1995, *A&A*, **295**, 715.
 Wagoner R.A., Fowler A., & Hoyle F., 1967, *ApJ*, **148**, 3.
 Wallerstein G., & Sneden C., 1982, *ApJ* **255**, 577.
 Webb J.K., Carswell R.F., Lanzetta K.M., Ferlet R., Lemoine M., Vidal-Madjar A., & Bowen D. V., 1997, *Nat*, **388**, 250.

P. Bonifacio
 bonifaci@oat.ts.astro.it

Ground-Based Detection of the Isolated Neutron Star RXJ185635-3754 at V = 25.7 Mag with the Upgraded NTT

R. NEUHÄUSER¹, H.-C. THOMAS², F.M. WALTER³

¹MPI Extraterrestrische Physik, Garching, Germany, rne@mpe.mpg.de

²MPI Astrophysik, Garching, Germany

³Department of Physics and Astronomy, SUNY, Stony Brook, USA

We report the first ground-based detection of the isolated, non-pulsating neutron star RXJ185635-3754 at V = 25.7 mag, obtained with the upgraded NTT in August 1997. This object has been detected first as ROSAT source and was subsequently identified as neutron star with the HST. It is located foreground to a dark cloud, i.e. at a distance of less than 130 pc. With future VLT observations, we may be able to measure its parallax.

The unidentified ROSAT X-ray source RXJ185635-3754 has been claimed to be an isolated (i.e. not in a binary

system) old neutron star (NS), because (1) it shows constant X-ray emission both on short time-scales (no pulses)

as well as on long time-scales, having been detected by the Einstein Observatory Slew Survey, the ROSAT All-Sky

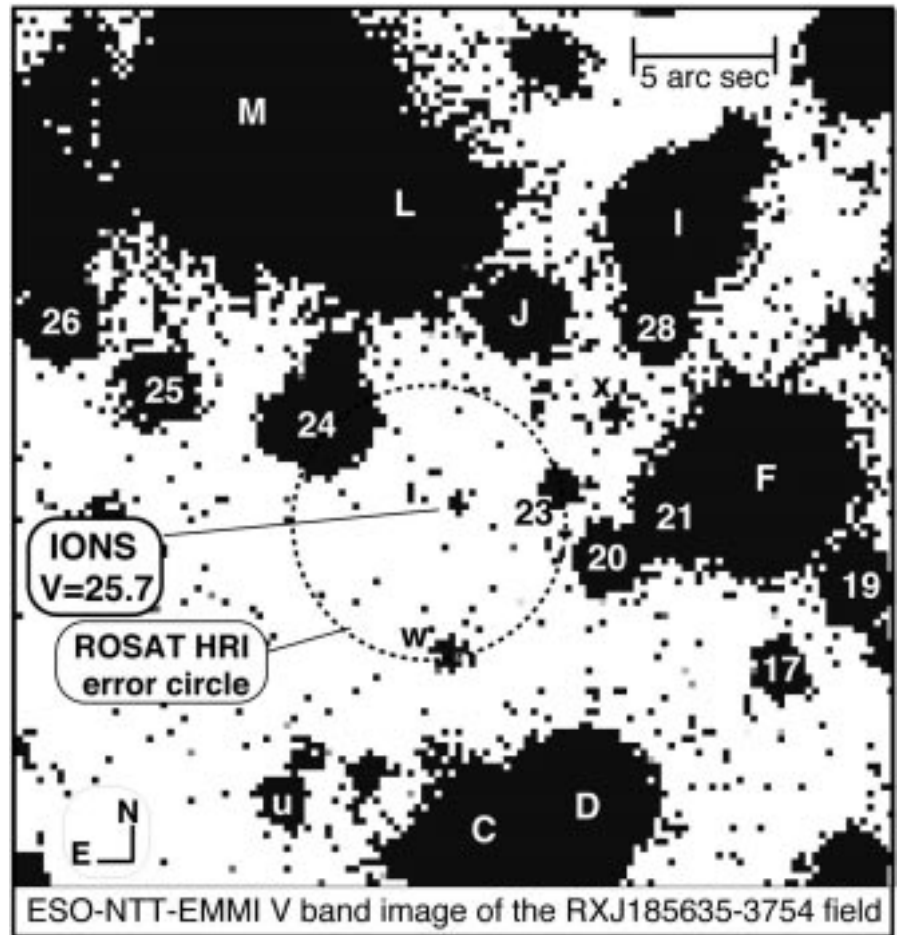
Survey, and in ROSAT PSPC and HRI pointed observations with very similar fluxes; (2) it is a very bright (3.7 ROSAT PSPC cts/sec) source with a very soft ($kT = 57$ eV blackbody) spectrum, as expected for an old NS; (3) no optical counterpart could be found down to $V \approx 23$ mag; and (4) the source appears to be projected towards the R CrA dark cloud located in Corona Australis at ≈ 130 pc, and the column density from the PSPC pointing places the source foreground to this cloud (Walter et al., 1996).

By re-evaluating the boresight correction of the ROSAT HRI observation, and identifying another source in the same HRI field of view with a coronally active T Tauri star by using the B&C spectrograph at the ESO 1.52-m telescope, we have revised the X-ray position and its error circle (Neuhäuser et al., 1997). Then, a very faint star was detected in this new error circle with the HST WFPC2 with 25.6 mag at $F_{606} \approx V$ and 24.4 mag at $F_{303} \approx U$ (Walter & Matthews, 1997). Hence, this star is very blue, suggestive of the hot surface expected in a NS.

This object is the first example of the long-sought isolated, non-pulsating NS, of which there should be $\sim 10^8$ to 10^9 in the Galaxy, based on pulsar birth-rates and the metallicity in the interstellar medium. Its X-ray emission is due to either accretion from the ambient interstellar material (old NS) or a cooling surface (middle-aged NS). Since Bondi-Hoyle accretion scales with v^{-3} , measurement of its velocity v will enable us to distinguish between these alternatives. Also, since it is an isolated (i.e. single) object, we can really study the surface and atmosphere of a NS.

ESO had allocated the grey night of 1997 August 9/10 at the NTT for the detection of the optical counterpart (programme 59.D-0580, PI Neuhäuser), i.e. shortly after the start of normal operation following the NTT "big bang" upgrade. The night was photometric, but the seeing conditions (varying between 1.1 and 1.4 arc seconds during exposures in V) required us to use EMMI instead of SUSI. We used the EMMI red CCD #36, first with the ESO V-band filter #606, then with the ESO R-band filter #608. We also observed Landolt standard star fields throughout the night.

We took several images to reduce the risk of cosmic-ray contamination and placed the expected target position onto slightly different areas on the chip in each exposure to avoid problems with bad pixels. After bias and flat-field correction, we added the images using standard MIDAS procedures to construct the final V-band image with a total exposure time of 150 minutes. This image is shown in the figure (background field stars are labelled as in Neuhäuser et



al., 1997, IONS indicates the location of the detected Isolated Old NS). The NS is clearly detected with a S/N of 18 inside the ROSAT error circle. The magnitude is $V = 25.70 \pm 0.22$ mag measured with the MIDAS command magnitude/circle (and $V \approx 25.72$ mag with the MIDAS Romafot package).

In addition, we have obtained images at the Cron-Cousins R-band with a total exposure of two hours towards the end of the night at air masses between 1.20 and 1.28 and seeing between 1.5 and 1.9 arc second. We could not detect the object down to $R \approx 24.5$ mag. The broad-band spectrum (X-ray and optical data from ROSAT, HST, and NTT) shows that the optical fluxes lie above the extrapolated pure blackbody and can best be fit with a Silicon-ash model atmosphere; in the Si-ash model, the NS surface composition is made up of 68% Fe-group elements, 11% Si, and 10% S, which is expected if a significant fraction of the mass was accreted by material falling back after the core collapse. More observations are planned for the near future to obtain the spectral energy distribution in the optical. ESO has allocated for us one dark night in July 1998 for more observations of this NS with the NTT-SUSI2 (PI Neuhäuser), where we plan to measure the fluxes in B and R, and to obtain a

new detection in V for measuring the proper motion.

Observations with FORS1 at the VLT UT1 can provide an optical spectrum. Measuring its parallax should be feasible on a time-scale of up to a few years, since the object is located foreground to the CrA dark cloud, i.e. at < 130 pc. Together with its X-ray flux and emitting area, we can then determine the radius of this NS. Forthcoming X-ray observations with AXAF and XMM can provide us with its surface gravity, so that we can, for the first time, obtain the mass of an isolated NS. This will constrain the equation of state of degenerate matter.

Acknowledgement

We are very grateful to the whole NTT team and in particular would like to thank Griet Van der Steene for her great help during our NTT run.

References

- Neuhäuser R., Thomas H.-C., Danner R., Peschke S., Walter F.M., 1997, *Astron. & Astrophys.*, **318**, L43–L46.
- Walter F.M., Wolk S.J., Neuhäuser R., 1996, *Nature*, **379**, 233–235.
- Walter F.M. & Matthews L.D., 1997, *Nature*, **389**, 358.

RX J0911.4+0551: A Complex Quadruply Imaged Gravitationally Lensed QSO

I. BURUD¹, F. COURBIN^{1,2}, C. LIDMAN³, G. MEYLAN⁴, P. MAGAIN^{1,*}, A.O. JAUNSEN^{5,6},
J. HJORTH^{6,7}, R. ØSTENSEN^{1,8}, M.I. ANDERSEN⁹, J.W. CLASEN⁹, R. STABELL^{5,6}, S. REFSDAL^{5,6,10}

¹*Institut d'Astrophysique, Université de Liège, Belgium*

²*URA 173 CNRS-DAEC, Observatoire de Paris, Meudon, France*

³*European Southern Observatory, Santiago, Chile;* ⁴*European Southern Observatory, Garching, Germany*

⁵*Institute of Theoretical Astrophysics, University of Oslo, Norway*

⁶*Centre for Advanced Study, Oslo, Norway;* ⁷*NORDITA, Copenhagen, Denmark*

⁸*Department of Physics, University of Tromsø, Norway*

⁹*Nordic Optical Telescope, St. Cruz de La Palma, Canary Islands, Spain*

* *Maître de Recherches au Fonds National Belge de la Recherche Scientifique*

1. Introduction

Deriving cosmological parameters has long been the motivation for the development of many observational tests. These parameters, including the troublesome Hubble parameter, H_0 , can be derived from different methods, e.g., monitoring of Cepheids in nearby galaxies, the use of the Tully-Fisher relation or, at higher redshifts, the photometric monitoring of supernovae. Another method to determine H_0 , independently of these classical methods, is to measure the time delay between the gravitationally lensed images of QSOs. However, a good knowledge of the geometry of the lensed system is mandatory in order to make use of this information. Unfortunately, this is rarely the case, in many lensed QSOs the main deflecting mass is not even detected.

This was the background for a deep IR imaging project started at ESO in 1996 with the 2.2-m telescope, with the primary aim of detecting possible high-redshift galaxy clusters in the vicinity of known multiply imaged QSOs, as well as the main lensing galaxy. Observing in the IR optimises the contrast between low- z field galaxies and higher z cluster members, since the latter have their 4000-Å break, typical for galaxy spectra, redshifted into the IR for $z \geq 0.8-1$. Therefore, near-IR observations make easier the discrimination between field galaxies and high-redshift cluster members.

Near-IR (1 to 2.5 microns) observations have the further advantage that the relative brightness between the lensed QSO and any lensing galaxy decreases, making the galaxy easier to detect. The disadvantage is that the sky is considerably brighter in the IR than in the optical, and one is forced to take many short-exposure images to avoid detector saturation. Nevertheless, the image deconvolution technique developed by Magain, Courbin & Sohy (1997, 1998; hereafter MCS) allows one to take advantage of the numerous dithered frames obtained and to combine them into a single deep sharp image.

Successful results have already been obtained from this project, e.g., the detection of the deflector in the gravitational lens HE 1104-1805 (Courbin, Lidman & Magain, 1998), also confirmed by Remy, Claeskens, Surdej et al. (1998).

In this paper we report the detection of four QSO images in the recently discovered lensed QSO RX J0911.4+0551. With a maximum angular separation of $3.1''$, it is the quadruply imaged QSO with the widest-known angular separation.

RX J0911.4+0551, was selected as an AGN candidate from the ROSAT All-Sky Survey (RASS) (Bade et al., 1995, Hagen et al., 1995), and was recently classified by Bade et al. (1997; hereafter B97) as a new multiply imaged QSO. The lensed source is a radio quiet QSO at $z = 2.8$. Since RASS detections of distant radio quiet QSOs are rare, B97 pointed out that the observed X-ray flux might originate from a galaxy cluster at $z \geq 0.5$ within the ROSAT error box.

We present here our first observations of RX J0911.4+0551 at the 2.2-m ESO/MPI IRAC 2b in K-band which made us suspect that the QSO might be quadruple. This was confirmed on our optical data from the 2.56-m Nordic Optical Telescope (NOT, La Palma, Canary Islands, Spain), and on the NTT/SOFI data of the object (Moorwood, Cuby & Lidman, 1998). Careful deconvolution of the data allows us to clearly resolve the object into four QSO components and a lensing galaxy. In addition, a candidate galaxy cluster has been detected in the vicinity of the four QSO images. We estimate its redshift from photometric analysis of its members.

2. Observations and Deconvolution

As a part of our near-IR imaging project of gravitational lenses, RX J0911.4+0551 was first observed in the K-band with IRAC 2b mounted on the ESO/MPI 2.2-m telescope on November 12, 1997. The data were processed as explained in Courbin, Lidman & Magain (1998), and they were deconvolved us-

ing the MCS algorithm. During the deconvolution process, the sampling of the images was improved, i.e., the adopted pixel size in the deconvolved image is half the pixel size of the original frames. The deconvolution procedure decomposes the images into a number of Gaussian point sources plus a deconvolved numerical background, and the quality of the results is checked from the residual maps, as explained in Courbin et al. (1998a,b). In spite of the poor seeing conditions ($1.3''$), preliminary deconvolution of the data made it possible to strongly suspect the quadruple nature of the object (see Fig. 1). From the observed image with a seeing of $\sim 1.3''$ only two separated components are resolved, one of them being elongated, suggesting that it is a blend of two or more images. The deconvolution programme was run once with three sources and then with four point sources (shown in the middle and bottom panel respectively in Figure 1). The residual maps, in units of the standard deviation in each pixel, indicate that the solution with four point sources gives a better χ^2 -fit to the data. Note also that even on these poor seeing data the deconvolution algorithm allowed us to suspect not only a quadruply imaged QSO, but also the presence of a lensing galaxy.

Much better optical observations were obtained at the NOT. Three 300s exposures through the I filter, with a seeing of $\sim 0.8''$ were obtained with ALFOSC under photometric conditions on November 16, 1997. Under nonphotometric, but excellent seeing conditions ($\sim 0.5-0.6''$), three 300s I -band exposures, three 300s V -band and five 600s U -band exposures were taken with HIRAC on the night of December 3, 1997.

These high-resolution data resolved the object into four components and clearly confirmed our preliminary IR-results from the ESO/MPI 2.2-m telescope.

RX J0911.4+0551 was also the first gravitational lens to be observed with the new wide-field near-IR instrument SOFI, mounted on the ESO 3.5-m NTT (Moor-

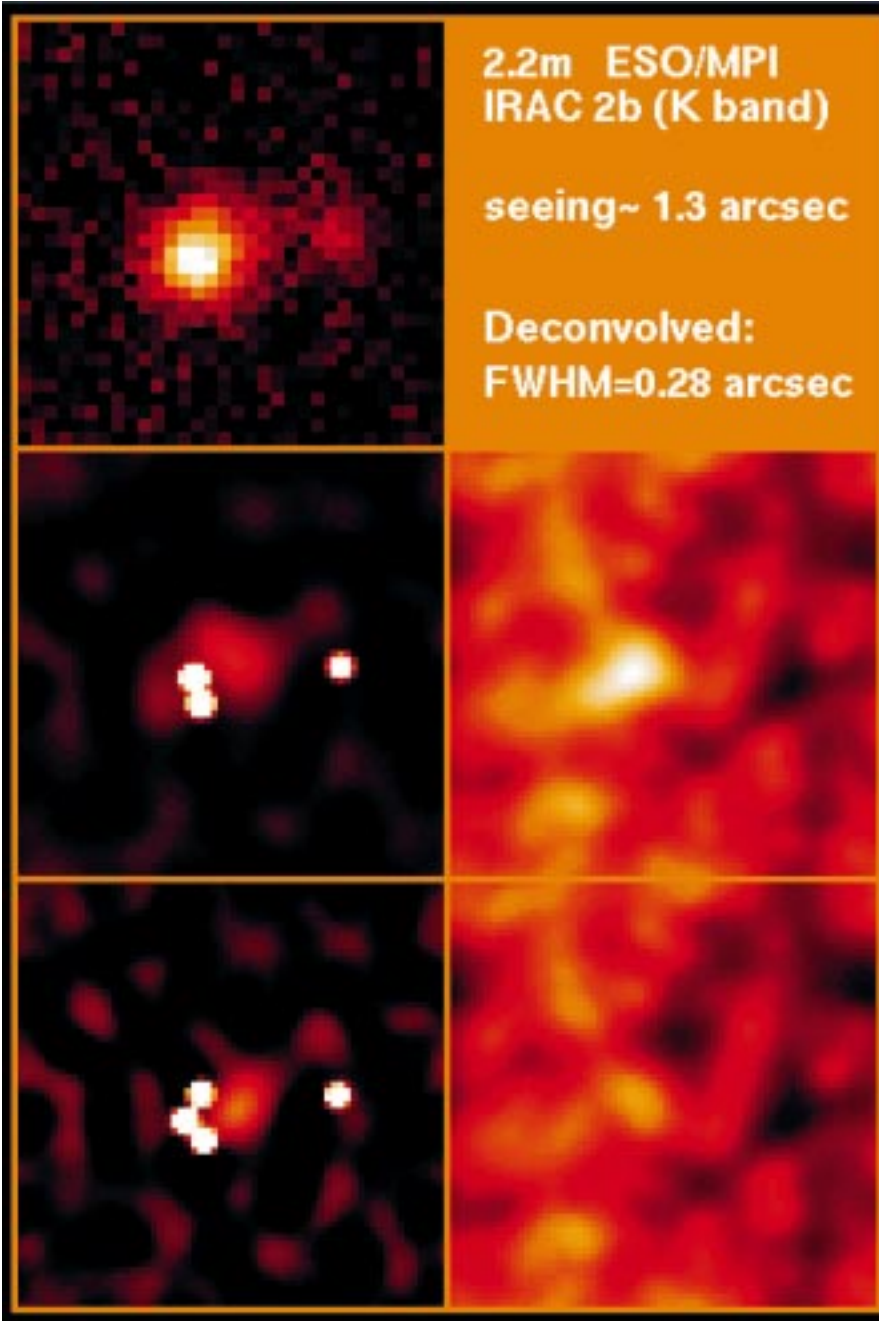


Figure 1: [Top:] Observed image from 2.2-m ESO/MPI IRAC 2b; [Middle:] Result from deconvolution with three point sources to the left and residual map to the right. The centre of the residual map has typical values of the order of $2\sigma_{\text{sky}}$ per pixel. [Bottom:] Same as above but with four point sources. All the values in the residual map are now close to σ_{sky} , showing that 4 point sources are needed to fit the data. The field is $9''$ on a side, North is to the top and East is to the left in all the frames. This figure is to be compared with Figure 2. Note how well the lensing galaxy shows up in the deconvolution.

the final resolution improving with the S/N. The deconvolution of NOT and SOFI frames are shown in Figure 2. Not only the quadruple configuration of the QSO is revealed but also the main lensing galaxy, as already suspected from our preliminary observations from the 2.2-m telescope, clearly confirming the lensing nature of this object.

3. Photometry

The flux ratios and positions of each QSO component relative to the brightest one (A1) as derived from the simultaneous deconvolutions are listed in Table 1. The position of the galaxy, also displayed in Table 1, was determined from the first-order moment of the light-distribution in the deconvolved numerical background. The galaxy is elongated in the I -band. In the near IR, it looks like an edge-on spiral, composed of a bright sharp nucleus plus a diffuse elongated disk. However, we can not exclude that the observed elongation is due to an unresolved blend of two or more intervening objects. Deeper observations will be required to perform precise surface photometry of the lens(es) and to draw a definite conclusion about its (their) morphology. The position angle of the major axis of the lensing galaxy is almost the same in the I , J and K bands: $\text{PA} \approx 140^\circ \pm 5$.

In order to detect any intervening galaxy cluster which might be involved in the overall lensing potential and contributing to the X-ray emission observed by ROSAT, we performed I , J and K band photometry on all the galaxies in a $2.5'$ field around the lensed QSO. Aperture photometry was carried out using the SExtractor package (Bertin & Arnouts, 1996).

wood, Cuby & Lidman, 1998). Excellent K and J images were taken on December 15, 1997, and January 19, 1998 respectively. The 1024×1024 Rockwell detector was used with a pixel scale of $0.144''$. These data were processed as the ones from the 2.2-m, but in a much

more efficient way since the array used with SOFI is cosmetically superior to the array used with IRAC 2b.

All these images were also deconvolved and the final resolution adopted in each band was chosen according to the signal-to-noise (S/N) ratio of the data,

Table 1: Flux ratios and astrometric properties relative to component A1. Positions are defined positive to the North and West of A1. All measurements are given along with their 1σ errors.

	A1	A2	A3	B	G
F_K	1.000 ± 0.001	0.965 ± 0.013	0.544 ± 0.025	0.458 ± 0.004	—
F_J	1.000 ± 0.002	0.885 ± 0.003	0.496 ± 0.005	0.412 ± 0.005	—
F_I	1.000 ± 0.017	0.680 ± 0.013	0.398 ± 0.002	0.420 ± 0.003	—
F_V	1.000 ± 0.007	0.587 ± 0.009	0.334 ± 0.004	0.413 ± 0.006	—
F_U	1.000 ± 0.003	0.590 ± 0.013	0.285 ± 0.007	0.393 ± 0.004	—
$x('')$	0.000	-0.259 ± 0.007	$+0.013 \pm 0.008$	$+2.935 \pm 0.002$	$+0.709 \pm 0.026$
$y('')$	0.000	$+0.402 \pm 0.006$	$+0.946 \pm 0.008$	$+0.785 \pm 0.003$	$+0.507 \pm 0.046$

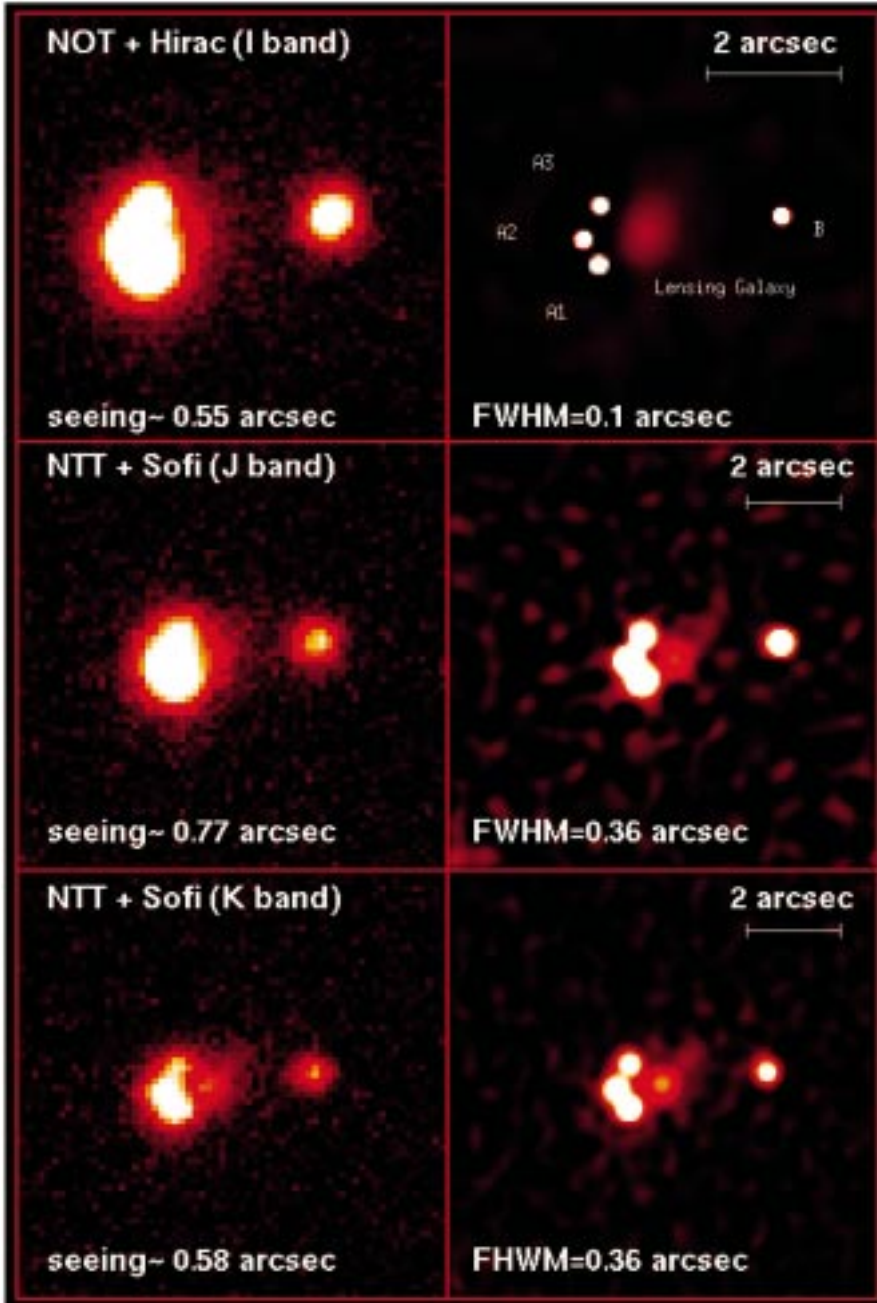


Figure 2: High-resolution images of RX J0911.4+0551 are displayed in the left panels together with their deconvolved versions with improved resolution and sampling in the right panels. In each band, the individual data frames are deconvolved simultaneously. [Top:] Stack of 3 NOT+HIRAC I-band image. The total exposure time is 900s. [Middle:] Stack of 9 NTT+SOFI J-band frames. The total exposure time is 1080s. [Bottom:] Stack of 19 NTT+SOFI K-band with a total exposure time of 2400s. For all three bands the object is clearly resolved into four QSO images plus the elongated lensing galaxy. The fields of the optical and near IR data are respectively 7" and 9" on a side. North is to the top and East is to the left in all the frames.

The faintest objects were selected to have at least 5 adjacent pixels above $1.2\sigma_{sky}$, leading to the limiting magnitudes 23.8, 21.6 and 20.0 mag/arcsec² in the I, J and K bands respectively. The faintest extended object measured in the different bands have a magnitude of 23.0, 22.0 and 20.3 (I, J and K).

A composite colour image was also constructed from the frames taken through the 3 filters, in order to directly visualise any group of galaxies with similar colours, and therefore likely to be at the same redshift. The colour composite is presented in Figure 3. The marked cir-

cle indicates a candidate galaxy cluster centred on a double elliptical, with the same colour as the main lensing galaxy. In addition, a group of even redder galaxies is seen a few arcseconds to the left and to the right of the marked cross.

4. Discussion

Thanks to our first observations from the 2.2-m telescope and the MCS deconvolution algorithm, RX J0911.4+0551 was resolved into a quadruply imaged QSO, and a lensing galaxy. Furthermore, these preliminary results were confirmed by

high-resolution optical data and new near-IR data from SOFI, thus clearly confirming the lensed nature of the system. The image deconvolution provides precise photometry and astrometry for this system.

Reddening in components A2 and A3 relative to A1 is observed from our U, V and I frames that were taken within three hours on the same night. The absence of reddening in component B and the difference in reddening between components A2 and A3 suggest extinction by the deflecting galaxy. Note that although the SOFI data were obtained from 15 days to 6 weeks after the optical images, they appear to be consistent with the optical fluxes measured for the QSO images, i.e. flux ratios increase continuously with wavelength, from U to K, indicating extinction by the lensing galaxy.

The observed orientation of the galaxy, together with the asymmetric image configuration, makes it difficult to model the lensing potential without including external shear from a nearby mass. If the lensing effect was only due to a symmetric galaxy, whose mass distribution is roughly aligned with the light, we should have observed a symmetric configuration of the QSO images about the axis through A2 and B.

A good galaxy cluster candidate has been detected in the vicinity of RX J0911.4+0551 from field photometry in the I, J and K bands. Comparison of our colours and magnitudes with that of a blank field (e.g., Moustakas et al., 1997) shows that the galaxies around RX J0911.4+0551 are redder than field-galaxies at an equivalent apparent magnitude. Furthermore, several of the galaxies are grouped in the region around a double elliptical at a distance of $\sim 38''$ and a position angle of $\sim 204^\circ$ relative to A1 (see the circle in Fig. 3).

There is considerable evidence for at least one galaxy cluster in the field. The redshift of our best cluster candidate (the one circled in Fig. 3) can be estimated from the I and K band photometry. We have compared the K-band magnitudes of the brightest cluster galaxies with the empirical K magnitude vs. redshift relation found by (Aragon-Salamanca et al. 1998). We find that our cluster candidate, with a brightest K magnitude of ~ 17.0 should have a redshift of $z \sim 0.7$. A similar comparison has been done in the I-band without taking into account galaxy morphology. We compare the mean I magnitude of the cluster members with the mean magnitude found by Koo et al. (1996) for galaxies with known redshifts in the Hubble Deep Field and obtain a cluster redshift between 0.6 and 0.9. Finally, comparison of the I-K colour of the cluster members with data and models from Kodama et al. (1998) confirm the redshift estimate of 0.6–0.8.

Some 10" away from the lens, a group of even redder objects can be seen (close to the cross in Fig. 3). These galaxies

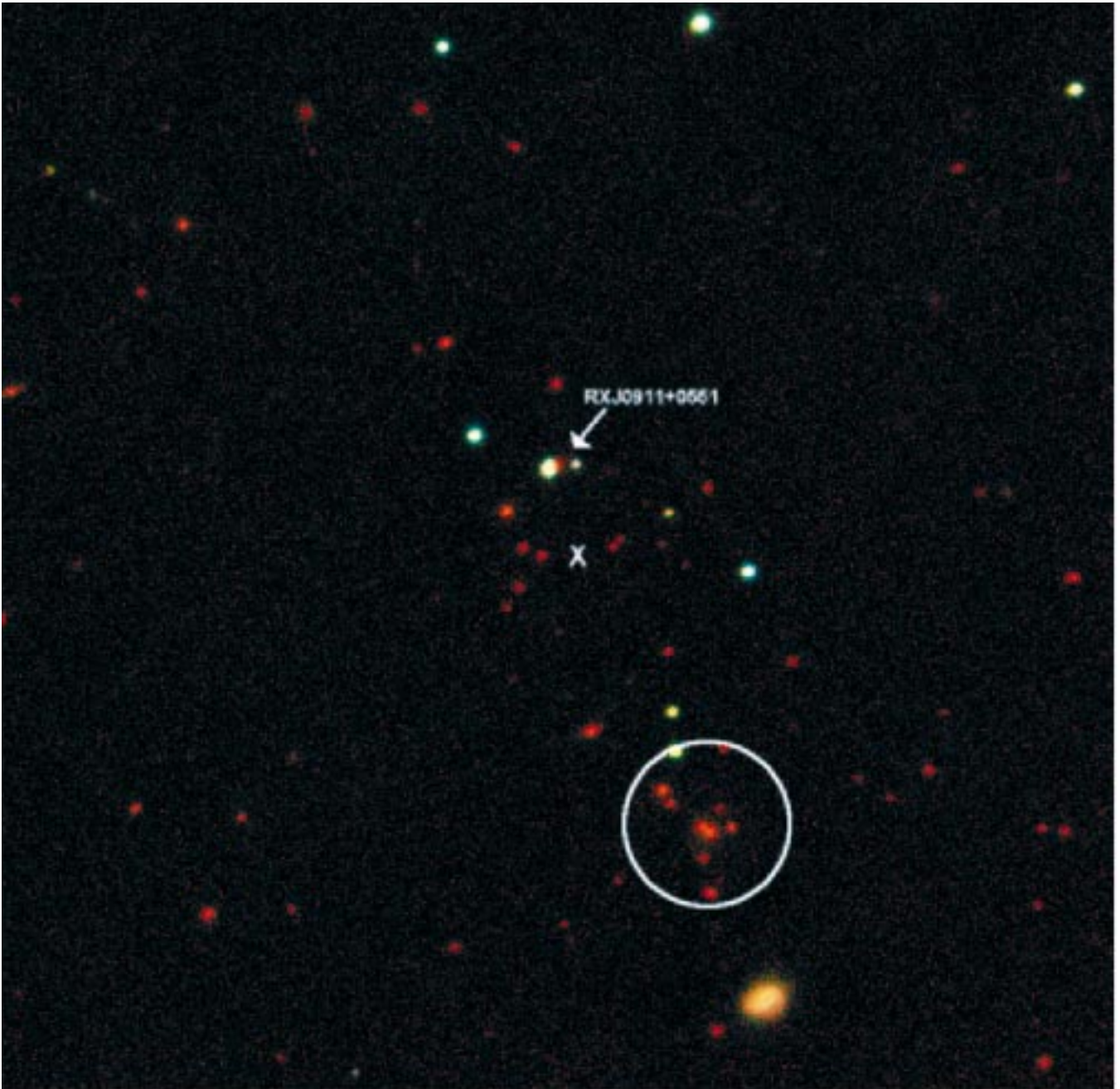


Figure 3: Composite image of a 2' field around RX J0911.4+0551. The frame has been obtained by combining the ALFOSC I and the SOFI J and K-band data. North is up and East is to the left. Note the group of red galaxies with similar colours, about 38" SW of the quadruple lens (circle) and the group of redder galaxies 10" SW of the lens (cross).

might be a part of a second galaxy group at a higher redshift.

The colour of the main lensing galaxy is very similar to that of the cluster members, suggesting that it might be a member of the cluster. However, internal reddening and inclination effects, in case it is a spiral galaxy, might bias the colour interpretation. Given the brightness of the nucleus of the lens in *K*, we cannot rule out the possibility of a fifth central image of the source, as predicted from lens theory. Near-IR spectroscopy is needed to get a redshift determination of the lens and show whether it is blended or not with a fifth image of the source.

RX J0911.4+0551 is a new quadruply imaged QSO with an unusual image configuration. The lens configuration is com-

plex, composed of one main lensing galaxy plus a plausible galaxy cluster at redshift between 0.6 and 0.8 and another possible group at $z > 0.7$. Multi-Object Spectroscopy is needed in order to confirm our cluster candidate(s) and derive its (their) redshift and velocity dispersion. In addition, weak lensing (shear) analysis of background galaxies will be useful to map the overall lensing potential involved in this complex system.

References

- Aragón-Salamanca, A., Baugh, C.M., Kauffmann, G., 1998, preprint astro-ph/9801277.
- Bade, N., Fink, H.H., Engels, D., et al., 1995, *A&AS*, **110**, 469.
- Bade, N., Siebert, J., Lopez, S., et al., 1997, *A&A*, **317**, L13.
- Bertin, E., Arnouts, S., 1996, *A&AS*, **117**, 393.
- Courbin, F., Lidman, C., Magain, P., 1998a, *A&A*, **330**, 57.
- Courbin, F., Lidman, C., Frye, B., 1998b, *ApJL*, in press (astro-ph/9802156).
- Hagen, H.-J., Groote, D., Engels, D., Reimers, D., 1995, *A&AS*, **111**, 195.
- Kodama, T., Arimoto, N., Barger, A.J., et al., 1998, preprint astro-ph/9802245.
- Koo, D.C., Vogt, N.P., Phillips, A.C., et al., 1996, *ApJ*, **469**, 535.
- Magain, P., Courbin, F., Sohy, S., 1998, *ApJ*, **494**, 452.
- Magain, P., Courbin, F., Sohy, S., 1997, *The Messenger*, **88**, 28.
- Moorwood, A., Cuby, J.G., Lidman, C., 1998, *The Messenger*, **91**, 9.
- Moustakas, L.A., Davis, M., Graham, J.R., et al., 1997, *ApJ*, **475**, 445.
- Remy, M., Claeskens, J.F., Surdej, S., et al., 1998, *New Astronomy*, in press.

Astrometry of Comet 46P/Wirtanen at ESO: Preparation of ESA's ROSETTA Mission

J. SANNER, M. GEFFERT (Sternwarte der Universität Bonn, Germany)

H. BÖHNHARDT (European Southern Observatory, Santiago de Chile)

A. FIEDLER (Universitätssternwarte München, Germany)

1. A New European Spacecraft to a Comet

1.1 The ROSETTA mission

Comets play an important role in the studies of the solar system and its origin, because they are believed to contain matter in a primordial form. After the success of the GIOTTO flyby at comet 1P/Halley in 1986, ESA plans to send a second spacecraft named "ROSETTA" to another comet, 46P/Wirtanen, for a more thorough investigation of a cometary nucleus and its physico-chemical nature. After its launch in 2003 and two asteroid flybys during the cruise phase to the prime target, ROSETTA will rendez-vous

with 46P/Wirtanen in 2011 and will orbit the comet in a distance of 10 to 50 km until at least its subsequent perihelion passage in 2013. During this orbiting phase it will perform *in situ* experiments of the coma, remote sensing of the nucleus and, most important, it will also place a lander called "RoLand" with several scientific experiments on the nucleus of the comet. The main scientific objectives of the mission are (see also [16]): global characterisation of the nucleus and its dynamic properties, chemical composition, physical properties and interrelation of volatiles and refractories in the nucleus.

ROSETTA shall help answering the questions of the origin of comets, the re-

lationship between cometary and interstellar material and its implications with regard to the origin of the Solar System.

The probe is named after the Rosetta stone which covers one text in three ancient scripts (hieroglyphs, demotic and Greek). After its discovery in 1799 it was possible to decipher the Egyptian hieroglyphs in 1822. Now the stone is on display in the British Museum in London, UK [13].

1.2 The target comet: 46P/Wirtanen

The comet was discovered on January 17, 1948, at Lick Observatory, USA, by Carl A. Wirtanen. With an orbital period of about 5 years, it belongs to the so-called Jupiter family comets, the orbits of which are subject to repeated close encounters with the planet Jupiter (then altering the orbit parameters severely). The most recent perihelion passage of 46P/Wirtanen took place on March 14, 1997. The parameters of the current orbit of the comet from [7] (see also [14]) are summarized in Table 1.

During its current revolution, the comet was recovered in 1995 – with a magnitude of about 24.5 in a very crowded star field close to the centre of the Milky Way – at ESO La Silla [1, 2]. The comet was found to have the smallest nucleus known so far, i.e. about 600–700 m in radius (measured first by [2] and confirmed later by HST observations [5]). Recent work based on some of our data reveals a light curve which hints at a rotation period of almost 7 hours [3].

The small size of 46P/Wirtanen makes the mission more difficult: A larger mass would be helpful in keeping the spacecraft in orbit around the nucleus and dropping the lander onto the surface.

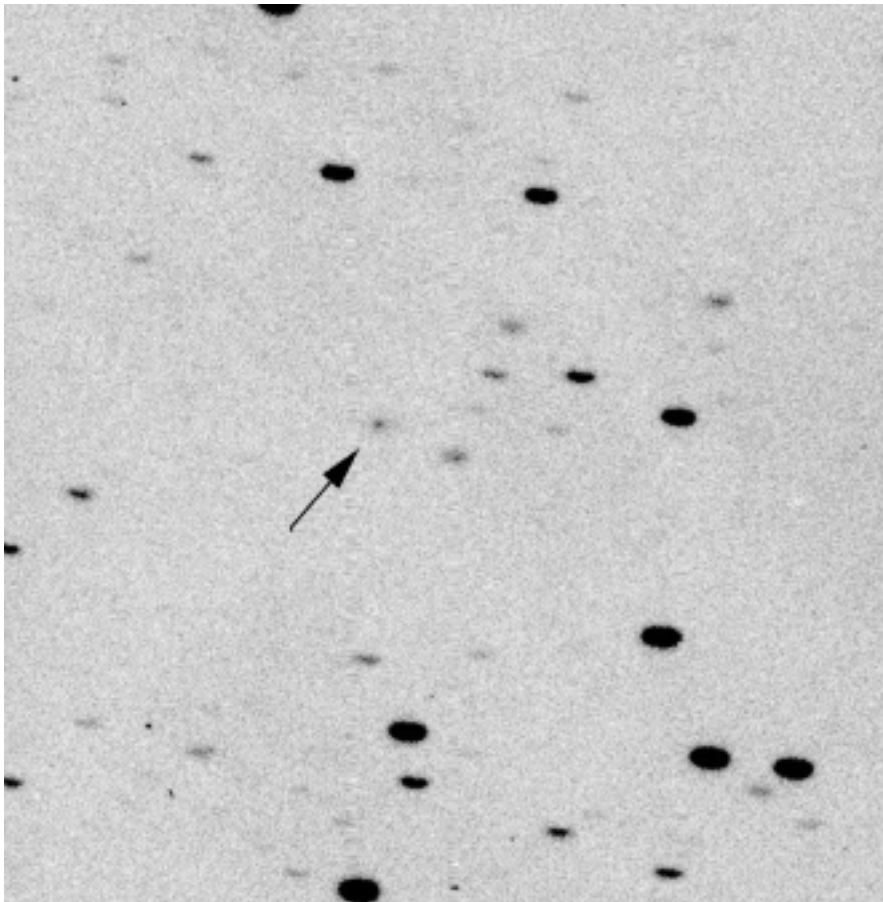


Figure 1: A 600 sec R filter image of comet 46P/Wirtanen taken on April 25, 1996, at the Danish 1.5-m telescope. North is up and east to the left. The image shows a field of view of 3.3'. Wirtanen is marked with an arrow. Note the elongated stellar images due to guiding with respect to the comet.

TABLE 1: Orbital elements of comet Wirtanen. The coordinates are given with respect to equinox 2000.0.

Date of perihelion	1997 03 14.14299
Distance at perihelion	1.0637469 AU
Perihelion Argument	356.34322°
Ascending Node	82.20387°
Inclination	11.72255°
Eccentricity	0.6567490
Orbital Period	5.46 years

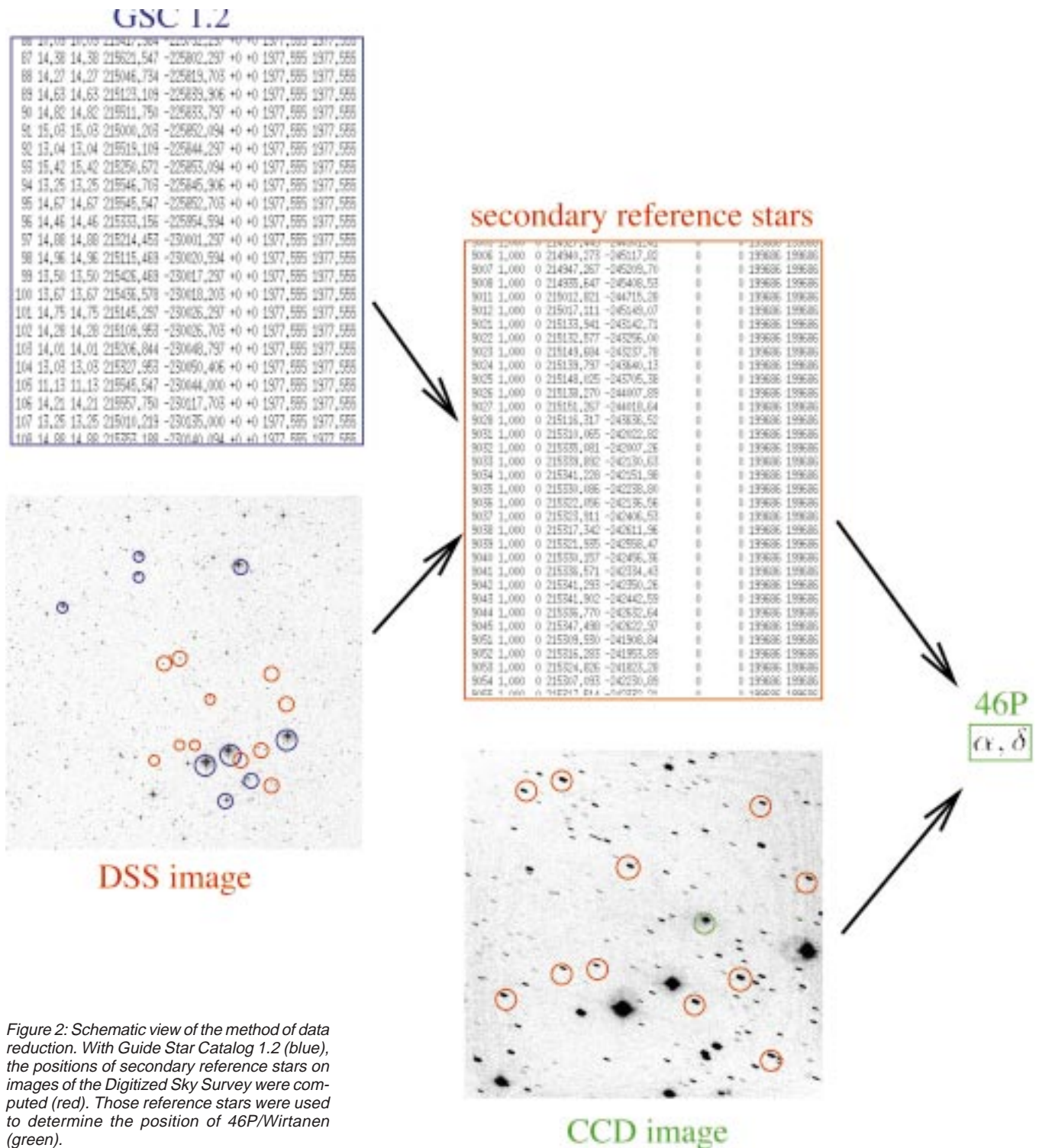


Figure 2: Schematic view of the method of data reduction. With Guide Star Catalog 1.2 (blue), the positions of secondary reference stars on images of the Digitized Sky Survey were computed (red). Those reference stars were used to determine the position of 46P/Wirtanen (green).

2. Astrometry Support for the Cometary Mission

For mission-planning purposes, in particular for an economic planning of the use of manoeuvre propellant during the cruise phase to the comet, it is important to know the object's orbit with a very high accuracy. The orbit characterisation becomes particularly difficult because of the non-gravitational forces. These perturbations of the orbit are caused by the outgassing of the cometary nucleus. Therefore, astrometric positions all along the orbit and over several orbital revolutions

are required for an accurate orbit determination which then can be used for proper mission planning of ROSETTA. In the case of 46P/Wirtanen, it is a difficult task to obtain such measurements because the object is very faint due to its large distance from the Earth and the Sun during most of its orbit.

The only possibility to observe distant and faint moving objects and to measure their positions accurately and in a suitable time (the exposure times must not be arbitrarily long because of the orbital motion of the target object!) is given by the use of CCD imaging. However, this

leads to the problem that due to the small field sizes of CCDs, the number of reference stars within the field is too small for a good transformation from the CCD positions to the celestial coordinates.

In the following, we present a recently developed technique which is tailored for the determination of very accurate astrometric positions of faint solar-system objects on small-sized CCD frames. The positions of 46P/Wirtanen, which we obtained from La Silla observations in 1996, were used to improve the orbit parameters of the comet in support of ESA's ROSETTA mission.

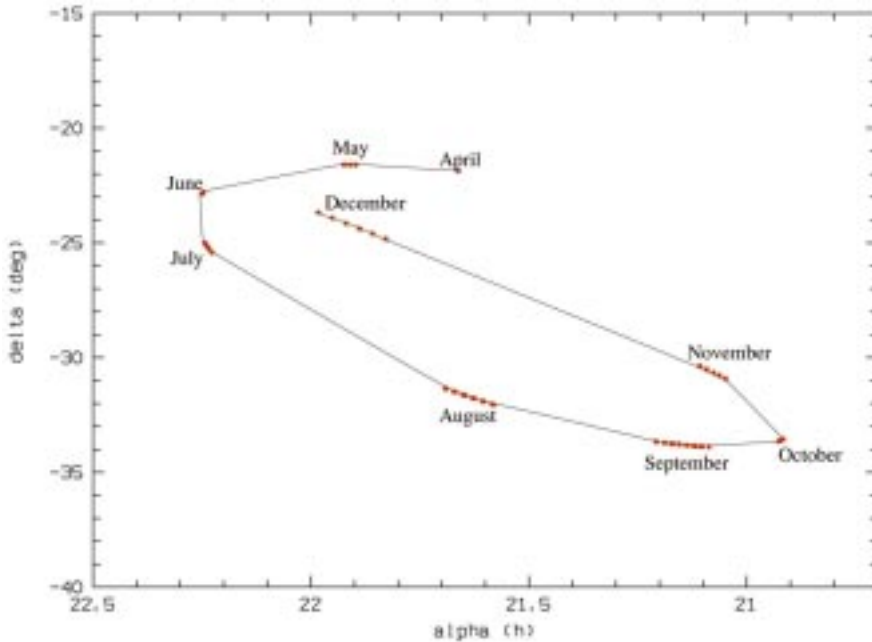


Figure 3: Trajectory of comet 46P/Wirtanen during April to December 1996. Note that the coordinates given are topocentric and therefore superimposed by the Earth's parallax.

3. The ESO Observations of the Comet in 1996

The observations used in our analysis were collected at the ESO La Silla observatory in Chile in the context of a coordinated campaign for the assessment of the nucleus properties and the coma activity of 46P/Wirtanen in preparation of the ROSETTA mission. The CCD images were taken in 1996 by various observers (see Table 2) at two different telescopes, the 1.54-m Danish telescope equipped with DFOSC ($2k \times 2k$ CCD with a pixel size of $0.4''$) and the ESO/MPG 2.2-m telescope equipped with EFOSC2 (until July 1996 $1k \times 1k$ CCD of pixel size $0.32''$, thereafter $2k \times 2k$ CCD of pixel size $0.27''$). With these telescope-instrument combinations, one obtains images with a field of view of $13.7'$ (DFOSC) and $5.5'$ or $9'$ (EFOSC2), respectively. Due to CCD artefacts in DFOSC, only the inner 1500×1500 pixels were useful for our measurements. The images of the comet were exposed

through broadband BVR filters with different durations ranging from 30s to 600s (depending on the comet's brightness and motion rate). As the telescope was guided on the target object, the stellar images were more or less elongated, depending on the exposure times and apparent velocity of the comet.

The main goal of the astrometry part of the programme was to measure the positions of the comet over the whole orbit arc from a distance close to the point where ROSETTA will start its science mission until almost to perihelion. The early observation phase when the comet was fainter than 20 mag imposed the challenge to measure the position of a very faint, hardly detectable object on a scary star background. Towards the end of our observing period, its brightness had increased to ~ 14 mag which made it a more comfortable object, but now also with a much higher motion rate since it was closer to the Earth and the Sun.

From the several hundred frames of the comet obtained in 1996 we selected

a total of 79 images (all taken through Bessell R filter) for the astrometric measurements. An example image from the first run in April 1996 is shown in Figure 1.

4. The Astrometric Data Reduction

Before the astrometric measurements were performed, all images were bias subtracted and flat-fielded. Due to the small fields of the images, classical reference stars from catalogues like the Guide Star Catalog (GSC) [6], PPM Star Catalogue [10, 11], etc. do not cover the sky sufficiently dense to be used directly for the astrometric processing of the frames. In addition, most of them were saturated on the CCD images due to the relatively long exposure times used for depicting the comet. Therefore, we developed a concept for the determination of the positions of the comet by the use of *secondary* reference stars determined from rectangular positions of stars on the Digitized Sky Survey (DSS) [9]: for each CCD frame, we derived positions of 10 to 15 secondary reference stars (covered both by the CCD image and DSS) with respect to about 30 nearby GSC stars.

For the determination of the rectangular pixel coordinates of the objects on the CCD frames and the DSS we used the `imexamine` routine of the IRAF software package. Earlier tests of this routine had shown that a positional accuracy of about 0.1 to 0.2 pixel can be achieved [4]. This value corresponds to a positional uncertainty of less than $0.1''$ (corresponding to about 300 km at a distance of 5 AU which is approximately Wirtanen's distance during the first measurements), which provides a sufficient accuracy for the astrometry of comets. This uncertainty does not play any role for the 2011 rendez-vous with ROSETTA, because the non-gravitational forces do not allow to make an orbit prediction of the comet to this level of accuracy over several revolutions (and the comet will pass perihelion twice before ROSETTA will arrive).

The improved version 1.2 of the GSC [15] was taken for the reduction. Since the GSC does not contain proper motions and the epochs of the DSS and GSC differ, we omitted all stars showing deviations larger than 3σ from the root mean square (rms) between measurements and catalogue.

In a first step, the coordinates of the secondary reference stars on the DSS images were determined with respect to the GSC stars with a third order polynomial approximation (i.e. 10 plate constants). Secondly, the comet's position was computed using the images of the secondary reference stars on the CCD frames. Figure 2 sketches this method.

5. The Results and Discussion

Figure 3 shows the apparent motion of comet Wirtanen on the sky during the time of our 1996 observations.

TABLE 2: The ESO imaging campaign of comet 46P/Wirtanen. Besides the information on the observing runs themselves, Wirtanen's motion rate v , distances r and Δ from Sun and Earth, respectively, are given. The values are averaged over the monthly observing periods.

Date	Δ [AU]	r [AU]	v ["/h]	telescope	observer
25.04.96	3.4	3.3	33	1.5-m DK	Bönnhardt, Rauer
11.-13.05.96	3.1	3.2	28	2.2-m	West
18.-19.06.96	2.3	3.0	14	1.5-m DK	Jorda, Schwehm
09.-12.07.96	1.9	2.8	23	2.2-m	Peschke
18.-23.08.96	1.2	2.5	46	1.5-m DK	Thomas, Rauer, Bönnhardt
10.-17.09.96	1.5	2.3	33	2.2-m	Schulz, Tozzi
02.-04.10.96	1.5	2.2	12	1.5-m DK	Rauer
01.-05.11.96	1.6	1.9	29	1.5-m DK	Bönnhardt
06.-08.12.96	1.7	1.6	71	1.5-m DK	Cremonese, Rembor
08.-11.12.96	1.7	1.6	73	2.2-m	Rembor, Cremonese

The positions obtained [12] revealed a larger than expected offset from the previously predicted positions. This indicates that the data gathered during earlier apparitions may be too inaccurate and/or badly sampled to compute a sufficiently precise long-term orbit of the comet.

The rms of the deviations between DSS measurements and the catalogue positions was less than $0.2''$ corresponding to an uncertainty of $0.1''$ for the secondary reference stars. We obtained a rms of the deviations between catalogue and rectangular coordinates on the CCD frames of better than $0.2''$.

For the accuracy of the final positions, we have to consider contributions from different sources. First of all, the comet appeared as a diffuse object (and not as a point-like star), which leads to problems in finding the “centre” of the comet. Another possible error source is the influence of higher-order image distortions due to imperfect optics of the telescope/instrument system. However, since in our images the comet was located essentially in the central region of the frames and since the secondary reference stars were distributed evenly over the frame, we think that in our data this effect will be small. A third problem lies in the motion of the comet with respect to the star background and the possible trailing of the comet images due to imperfect telescope guiding, which lead to elongated images – especially for the long exposures (up to 600s). Moreover, epoch differences of observations and catalogues in combination with the proper motions of the stars could cause systematic deviations of these positions. All these effects are difficult to evaluate. However, the orbit calculation of the comet based on our and other positions can give an estimation of the accuracy of our astrometry of the comet.

The data were compared with an orbit calculated by T. Morley (ESA) [8]. He used all data available from November 1985 until December 1996, i.e. three apparitions of Wirtanen, including our own data. He also took into account the non-gravitational forces which he extrapolated from the previous apparitions (Non-gravitational forces can only be determined *a posteriori*, i.e. long after the corresponding perihelion passage).

From a comparison of our results with this orbit we obtained “O–C” (observed – calculated) deviations of $+0.27'' \pm 0.85''$ in α and $+0.22'' \pm 0.32''$ in δ . The larger deviations in right ascension are mainly seen in the observations in August and September 1996. During this period the comet had a large motion in right ascension, which caused elongated images and possibly the larger uncertainty of the positions. The deviations in right ascension and declination are shown in Figures 4 and 5.

6. Outlook and Summary

46P/Wirtanen will be monitored over the following years by many observato-

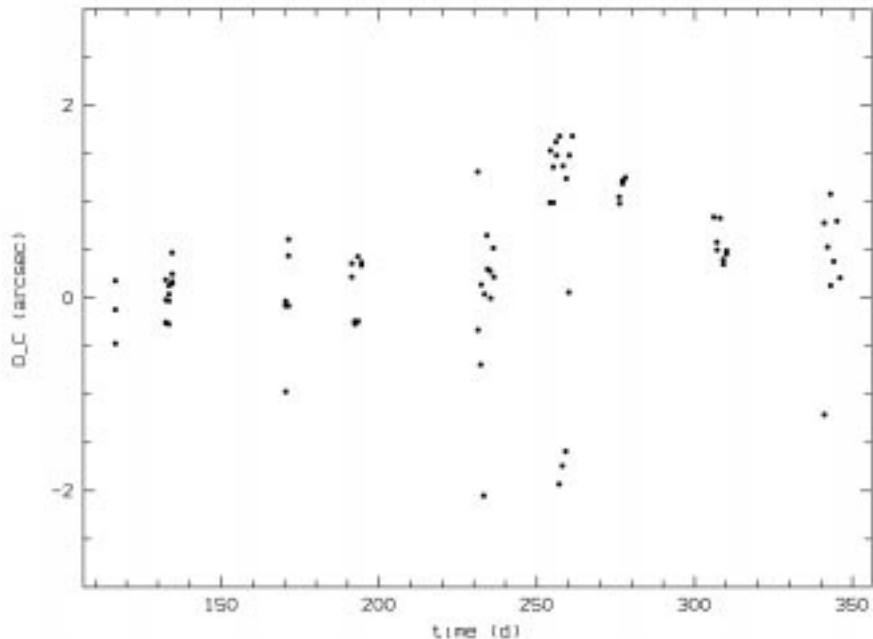


Figure 4: Plot of the O–C values in right ascension. The errors are plotted with respect to the time of observation, given in days of the year 1996. Note the high scatter of the values especially around 250 d (August/September).

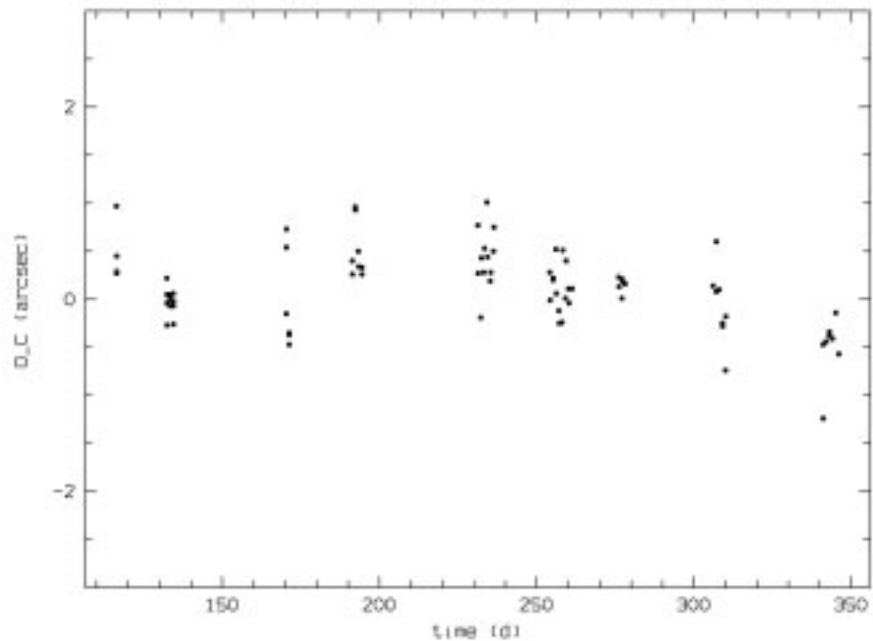


Figure 5: Plot of the O–C values in declination. It seems that there is a systematic trend of the O–C values with time. Such effects can be due to an imperfect modelling of the perturbing non-gravitational forces.

ries. This includes ESO, but it can be expected that this will be on a smaller level than during the 1996 campaign. The orbit will be continuously improved with new data as well as the model for the non-gravitational forces. As the ROSETTA probe will follow a flight path which lets it catch up slowly with the comet, the ground-based observations should already lead to an ephemeris which is sufficiently precise to reach the target with very slight in-flight corrections of the trajectory. By that time, also the ESO support can be expected to be on a much higher level again. And in the final phase

of the approach, an on-board camera will take additional images of the comet for a fine-tuning of the manoeuvres.

Our work plays a significant role for the project for two reasons: Firstly, CCD imaging gave the chance to observe Wirtanen in the remote part of the orbit which increased the understanding of the orbit itself and the non-gravitational forces, and on the other hand, our method to use the DSS as a coupler between the coarse reference catalogues and the CCD fields allows astrometric work on small fields of any part of the sky. Of course, the method is not sufficient for high-precision

astrometry (e.g. proper-motion studies), but it can be very well used for CCD astrometry of faint solar-system bodies.

References

- [1] Bönhardt H., West R.M., Babion J., Rauer H., Mottola S., Nathues A., 1996, *IAUC* **6392**, 3.
- [2] Bönhardt H., Babion J., West R.M., 1997, *A&A* **320**, 642.
- [3] Bönhardt H., Fiedler A., Geffert M., Sanner J., 1997, The ROSETTA/ISO Target Comets Imaging Campaign, Final Report of an ESA Study Project.
- [4] Geffert M., Reif K., Domgörgen H., Braun J.M., 1994, *AG Abstr. Ser.* **10**, 125.
- [5] Lamy P., 1996, *IAUC* **6478**.
- [6] Lasker, B.M., Jenkner, H., Russell, J.L., 1987, The guide star catalog, Space Telescope Science Institute.
- [7] Marsden B.G., 1996, *The Minor Planet Circulars* **27080**, eds. B. Marsden, G.V. Williams, S. Nakano.
- [8] Morley T., 1997, private communication.
- [9] Postman M., 1996, Technical Report, Space Telescope Science Institute, Baltimore.
- [10] Röser S., Bastian U., 1991, PPM Star Catalogue North, Akademischer Verlag.
- [11] Röser S., Bastian U., 1993, PPM Star Catalogue South, Akademischer Verlag.
- [12] Sanner J., Hainaut O.R., Bönhardt H., Rauer H., West R.M., Jorda L., Schwehm G., Thomas N., Schulz R., Tozzi G.-P., Cremonese G., Rembor K., 1997, *The Minor Planet Circulars* **30125**, eds. B. Marsden, G.V. Williams, S. Nakano; also available on-line at <http://www.astro.uni-bonn.de/~jsanner/mpc30125.html>
- [13] <http://www.british-museum.ac.uk/highligh.html>
- [14] <http://nssdc.gsfc.nasa.gov/planetary/factsheet/cometfact.html>
- [15] <http://www-gsss.stsci.edu/gsc/gsc12/description.html>
- [16] <http://www.estec.esa.nl/spdwww/rosetta/html2/toc.html>

J. Sanner
jsanner@astro.uni-bonn.de

NTT Archives: the Lyman α Profile of the Radio Galaxy 1243+036 Revisited

L. BINETTE ¹, B. JOGUET ², J.C.L. WANG ³ and G. MAGRIS C. ⁴

¹Instituto de Astronomía, UNAM, México, DF, México

²European Southern Observatory, Santiago, Chile

³Astronomy Department, University of Maryland, USA

⁴Centro de Investigaciones de Astronomía, Mérida, Venezuela

Abstract

All observations of very high redshift radio galaxies attest to a highly complex interaction between large-scale astro-

physical processes as violent and diverse as that of nuclear activity and of cosmogonic star formation. Ly α is seen in emission over scales exceeding galactic sizes and its resonant nature leads by itself

to a wide range of phenomena such as absorption lines due to intervening HI gas layers of very small columns, or enhanced dust extinction due to the manifold increase in path length traversed before escape. The resonant nature of Ly α can also manifest itself in emission through the process of Fermi acceleration across a shock discontinuity which leads to a large blueshift of the line photons. We propose that such a process is at work in the radio galaxy 1243+036 ($z = 3.6$) and can account for the three narrow emission peaks present on the blue side of the profile. The ultimate source of the photons present in those peaks likely consists of a jet-induced starburst of $\geq 5 \cdot 10^7 M_{\odot}$ situated at the position of the radio jet bend. Our investigations illustrate one possible use of the user friendly archival database developed by ESO.

1. General Context

Lyman α is the strongest emission line observed in High-Redshift Radio Galaxies (HZRG). Although the brightness of the line reaches a maximum towards the nucleus, most of the emission is spatial-

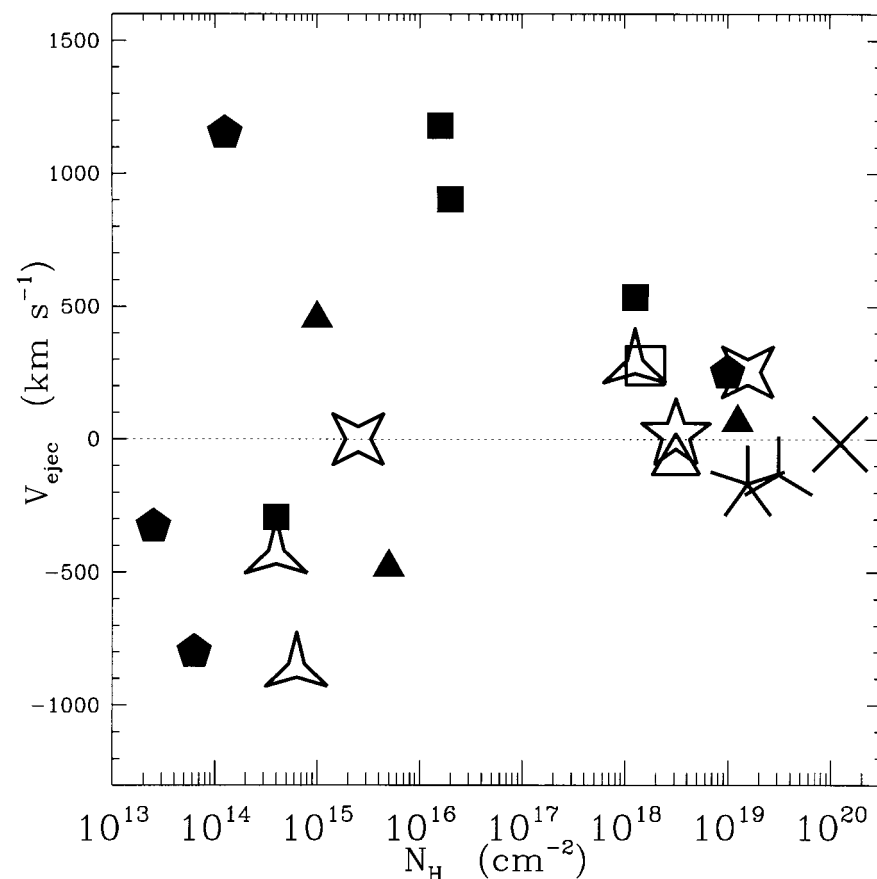


Figure 1: Velocity shifts of the absorbers relative to line centre as measured by van Ojik et al. (1997). Distinct symbols are used to distinguish different objects. For instance, all the four absorbers of 0828+193 are represented by solid squares. Negative and positive ejection velocities are of comparable likelihood. The figure does not contain the absorption dips reported in 1243+036.

ly resolved with the fainter emission extending up to radii 40–130 kpc. The work of van Ojik et al. (1997) shows that the full width at half-maximum of the integrated Ly α profile is in the range of 700–1600 km/s. One striking feature discovered by van Ojik et al. is that out of 18 intermediate-resolution ($\approx 3 \text{ \AA}$) spectra of HZRG, fully 60% of the objects showed deep absorption troughs superposed to the Ly α emission profile. The HI absorption column density of the dominant absorber is in the range of 10^{18} – 10^{20} cm^{-2} . In some cases, more than one absorber is present but with much smaller columns (10^{14} – 10^{16} cm^{-2}). An important conclusion reached was that the absorbers were part of the local environment of the parent radio galaxy. The fate and nature of the absorbers are still a matter of debate. If one converts into ejection velocities the absorption trough positions relative to the emission line centre, the smaller columns show some tendency towards higher velocity shifts as shown in Figure 1. Globally, the sign of the velocity shifts is randomly distributed without any strong preference towards either ejection (blueshift) or infall (redshift).

2. The Asymmetric Ly α Profile of 1243+036

The study of van Ojik et al. (1997) reveals that the underlying Ly α emission profiles within their 18 objects sample are remarkably gaussian and symmetric once allowance is made for the presence of the absorption troughs (fitted with Voigt profiles). In this respect, 1243+036 stands as a noteworthy exception with an asymmetric profile due to a significant excess of flux on the blue side. Superposed on this blue excess are narrow features which van Ojik et al. (1996) interpreted as four *absorption dips*. Interestingly, these all arise on the blue side, which is uncommon. The Ly α profile of 1243+036 is displayed in the top panel of Figure 2. Our proposed and variant interpretation is that the blue asymmetry consists merely of three narrow *emission peaks* with little if any absorption at all. This possibility is best illustrated by the dotted blue line of Figure 2 which is the *difference* between the blue half and the smoothed and folded red half of the Ly α profile. It thus becomes apparent that the narrow features which stand out most significantly above noise consist of net emission.

3. Fermi Acceleration and the Equidistant Peaks

A study by Neufeld and McKee (1988) of the transfer of resonant Ly α across a shock discontinuity has shown how the repeated scattering of resonant Ly α photons across the shock front can lead to a systematic blueshift of the line. The blueshift can greatly exceed the shock velocity V_s if the HI column density on

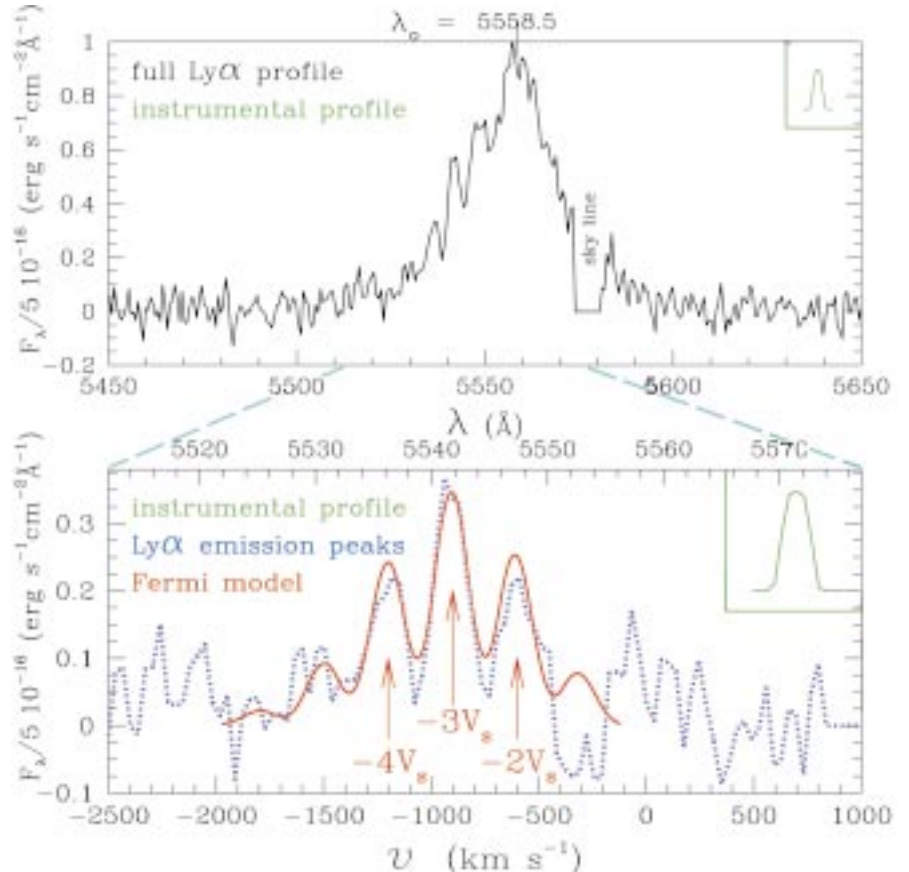


Figure 2: The top panel shows the Ly α profile of 1243+036. Originally taken by van Ojik et al. (1996), the spectrum was retrieved from the ESO archives (<http://arch-http.hq.eso.org>) and re-reduced by one of us (BJ). Extraction along the long slit was performed using a 7" window centred on the radio bend rather than on the nucleus (2" away). The narrow blueshifted features shown in the bottom panel (blue dotted line) were isolated by subtracting the smoothed and folded red side of the profile. The top abscissa is the observed wavelength scale while the bottom abscissa represents velocity shifts with respect to λ_0 , the wavelength we attribute to systemic velocity. The red line is a model based on Fermi acceleration across a shock discontinuity moving at 300 km/s. The model was convolved by the instrumental profile which is depicted in green.

either side of the shock is very large, thus providing a new and interesting explanation for the blue asymmetric profiles observed in a few radio galaxies.

We have further developed the Neufeld and McKee (1988) model by extending its validity to the regime of smaller columns in which individual emission peaks become identifiable (see Binette, Joguet and Wang, 1998). The close correspondence between the model as represented by the red line in Figure 2 and the emission features is certainly encouraging. Unlike absorption features which appear at random velocities, the three emission peaks occur only in the blue wing, as the Fermi acceleration process would predict. In fact, each successive emission peak corresponds to the incremental blueshift resulting from two scatters – back and forth – across the shock discontinuity, with each across-shock scattering giving a blueshift of $V_s/2$. Multiple scatters and some diffusion in frequency still takes place within the HI columns on either side of the shock front after each shock crossing. However, the velocity shift incurred by this frequency diffusion is very small

compared to the huge blueshift obtained in just a single shock front crossing. Thus, the gas velocity discontinuity across the shock front provides the most efficient escape route for resonant Ly α photons, cutting down the millions of 'local' scatterings otherwise necessary in static media for escape far in the damping wings to a comparatively small number of scatters (across the shock front and within the HI columns after each shock crossing).

In our model, the separation between successive peaks gives the shock velocity V_s and must therefore be equal, as is observed. Our fit gives directly a $V_s \approx 300 \text{ km/s}$. The bulk (or the maximum) of the Ly α flux emerges at a velocity position proportional to $(N_{HI} V_s)^{1/2}$. Larger columns necessitate more across-shock scatters before escape and so result in Ly α emerging in peaks of higher order, farther to the blue. The model shown here implies an HI column for each of the two scattering layers of $N_{HI} = 1.3 \cdot 10^{21} \text{ cm}^{-2}$. One layer is associated with the preshock gas ahead of the shock and the other is associated with the recombined gas shell in the trailing postshock gas.

4. A Powerful Jet Induced Starburst in 1243+036?

Using a different slit orientation, Van Ojik et al. (1996) report that the blue excess Ly α flux is displaced spatially from the nucleus and coincides with the radio jet bend seen in their radio maps 2" south-east of the nucleus. Such a radio bend confirms the existence of a shock while its spatial association with Ly α only adds to the plausibility of the Fermi acceleration model. But what is the ultimate source of the Ly α photons which are blueshifted across the shock front? It cannot be the shock itself as this would imply absurdly high densities to account for the observed Ly α luminosity ($\sim 10^{43.4}$ erg/s). It cannot be nuclear photoionisation since the existence of two neutral gas mirrors bracketing the accelerated Ly α photons is essential to the Fermi accel-

eration process; nuclear photoionisation would prevent the trailing H I mirror from existing. The most plausible explanation remaining is that of a colossal jet-induced starburst, similar in nature to that envisaged by Rees (1989). Moreover, the non-detection of C IV emission in 1243+036 argues against nuclear photoionisation or shock excitation and favours the starburst picture. Interestingly, the ubiquitous C IV line has also been reported missing in 3C326.1, another radio galaxy with asymmetric Ly α to which Neufeld and McKee (1988) applied their novel Fermi acceleration model. It may be that blue asymmetric Ly α profiles are a sign of extranuclear starbursts. Adopting a Salpeter initial mass function of slope 1.35 which extends from 0.1 to 125 M_{\odot} , we derive a luminosity for the hot stars of $1.3 \cdot 10^{54}$ ionising photons/s from the observed Ly α luminosity. Assuming

an instantaneous burst of star formation with this initial mass function gives a mass of newly formed stars of $\geq 5 \cdot 10^7 M_{\odot}$ (Bruzual and Charlot, 1996).

References

- Binette, L., Joguet, B., Wang, J.C.L., 1998, *ApJ* in press.
Bruzual A., G. and Charlot, S., 1996, in *A Data Base for Galaxy Evolution Modeling*, eds. C. Leitherer et al., *PASP*, **108**, 996.
Neufeld, D.A., McKee, C.F., 1988, *ApJ* **331**, L87.
Rees, M.J., 1989, *MNRAS* **239**, 1P.
van Ojik, R., Röttgering, H.J.A., Carilli, C.L., Miley, G.K., Bremer, M.N., Macchetto, F., 1996, *A&A* **313**, 25.
van Ojik, R., Röttgering, H.J.A., Miley, G.K., Hunstead, R. W., 1997, *A&A* **317**, 358.

L. Binette
binette@astroscu.unam.mx

Photos from Science Writers' Symposium

On the occasion of the VLT UT1 First-Light Event, a Science Writers' Symposium took place on Monday, April 27, and Tuesday, April 28, 1998, at the ESO Headquarters (Garching, Germany) with a complete briefing for media representatives about the VLT Project (technology, science) and its continuation after the UT1 First Light. The presentations were mostly made by ESO technical and scientific staff. About 40 media representatives participated, from all ESO member countries and beyond.

The ESO Director General, Prof. Riccardo Giacconi, introduces the VLT and its many scientific and organisational aspects. ►



The participants enjoy the teleconference with Paranal.



Massimo Tarenghi during the teleconference with Paranal. On the other side, at Paranal, Jason Spyromilio and Peter Gray.

Joint Committee Between ESO and the Government of Chile for the Development of Astronomy in Chile

In accordance with Article Nine of the interpretative, supplementary and amending agreement to the "Convention between the Government of Chile and the European Organisation for Astronomical Research in the Southern Hemisphere for the Establishment of an Astronomical Observatory in Chile", a Joint Committee has been constituted, on 13 March 1998, to co-operate directly in programmes for training young scientists, for engineers and technologists, and for equipment in general. The founding document was officially signed by the Minister of Foreign Affairs, His Excellency Mr. José Miguel Insulza S., and the ESO Director General, Prof. R. Giacconi.

The membership of this Committee consists of three representatives of the Government of Chile, the Director of "Política Especial", Ambassador R. González, the Chairman of the Presidential Commission for scientific matters, Dr. C. Teitelboim, and the Australian Astronomer Dr. K. Freeman, and three representatives of ESO, the Associate Director for Science, Dr. J. Bergeron, the Director of the Paranal Observatory, Dr. M. Tarenghi, and the ESO Representative in Chile, D. Hofstadt.

To foster scientific and technical co-operation between ESO and Chile, ESO will provide and administrate funds allocated for the development of astronomy and related technologies in Chile. The Joint Committee has the responsibility to define the framework of the co-operation, and to evaluate and select the programmes which will be financed by these funds.

Prior to the first meeting of the Joint Committee, extensive consultation took place between the Chilean astronomers and Dr. K. Freeman. The discussions during the meeting were very positive, and unanimous decisions were easily reached. On 13 March 1998, the Joint Committee agreed to make an announcement of opportunities for the six programmes summarised below:



- **Creation of new astronomical research groups.** To help Chilean Academic Institutions in the creation of an astronomical group, ESO will share with the selected Academic Institution the costs of hiring a full professor for a two-year period and two associate professors for a one-year period. After those terms have expired, the Academic Institution will take over the established programme.

- **Complementary funding for post-doctoral Astronomy programmes.** The goal of this programme is to make post-doctoral positions at Chilean Academic Institutions competitive at the international level.

- **Strengthening of already established astronomical research groups.** To this end, ESO will finance two new posts for full or associate professors for a three-year period. This term may be extended to a five-year period. After those terms have expired, the hosting Aca-

demical Institutions will commit themselves to maintain these new positions.

- **Training of professors for the teaching of astronomy in high schools.** Special attention will be given to programmes which are already sponsored, and ESO will share their funding.

- **Research infrastructure.** The goal of this programme is to strengthen the research capacities of academic institutions.

- **Development of systems and instruments.** Chilean engineers and technicians will be invited to participate, through public tenders, in the development of systems and instruments for the VLT telescope units.

The total level of funding available in 1998 for this ESO-Chile co-operation programme is DM 660,000. Additional programmes by ESO (for DM 340,000 in 1998) include social help to local communities, education programmes in high schools and university scholarships.

ESO Imaging Survey: Update on EIS-deep and the Hubble Deep Field South

L. DA COSTA and A. RENZINI, ESO

The second part of EIS (deep), as originally recommended by the EIS Working Group, envisioned the observation of a 15×15 arcmin region centred on the HST

Hubble Deep Field South (HDF-S), in six passbands (the EIS proposals for Periods 59, 60, and 61 can be found at http://www.eso.org/research/sci-prog/eis/eis_

[obs.html](http://www.eso.org/research/sci-prog/eis/eis_obs.html)). The programme was split between Periods 61 and 62, and 7 SUSI2 and 6 SOFI nights in Period 61 have already been allocated. However, with the

final selection of the HDF-S by ST Scl ($\alpha = 22^{\text{h}}32^{\text{m}}56^{\text{s}}$, $\delta = 60^{\circ}33'02''$) it became clear that the selected field is not ideal for deep imaging as it contains several relatively bright stars. Taking this into account, the EIS Working Group in its meeting of January 21–22, 1998 decided to recommend a different field coverage for EIS-deep. The WG now proposes EIS-deep to cover the minimum area required to include all HDF-S fields (WFPC2, NICMOS, STIS) and use the remaining observing time to cover a new field at high galactic latitude. In accordance to the reviewed strategy, the following observations are now planned, pending the endorsement of the OPC for those in Period 62:

1. The observations of the HDF-S will cover three adjacent SOFI/SUSI2 fields (5×5 arcmin each) which will include the WFPC2, NICMOS and STIS fields. In this way adequate target selection can be

secured for spectroscopic studies with FORS1 and ISAAC, for which teams in the community may wish to apply to the OPC. Note that HDF-S may also be observed with the VLT first Unit Telescope as part of the VLT Science Verification (see article by Leibundgut, de Marchi and Renzini in this issue).

2. The remaining deep imaging observations will be conducted in the direction of the region with the lowest H I column density in the Southern Hemisphere ($\alpha = 03^{\text{h}}32^{\text{m}}28^{\text{s}} = -27^{\circ}48'30''$), equivalent to the well-known Lockman hole in the North. The field contains very few stars, hence it is ideally suited for very deep optical imaging. It has also been chosen for a very deep AXAF exposure (field size 15×15 arcmin). The field will be covered by four contiguous tiles (10×10 arcmin) with both SUSI2 and SOFI, with the same filters and depth as for the HDF-S field. Besides J and

Ks imaging, H-band observations are also proposed for this field. This will make the data coverage of this field equivalent to that of the HDF-S field where the H-band observations will be carried out and made public by CTIO.

The recommended limiting magnitudes at 5σ remain the same as in the proposal for Period 61, while the 'g'-band imaging has been replaced by *B* and *V* observations since an optimal 'g'-band filter is not yet available. For the optical passbands the targeted limiting magnitude is ~ 26 mag in all filters. In the infrared the observations are expected to reach $J \sim 23.5$, $H \sim 22.5$ and $Ks \sim 21.5$, except in the WFPC2 field where the WG has recommended that the SOFI observations should reach ~ 0.5 magnitude deeper than in the other fields.

More information on EIS-deep can be found at "<http://www.eso.org/eis>"

ESO Fellowship Programme 1999

The European Southern Observatory (ESO) awards up to six postdoctoral fellowships tenable at the ESO Headquarters, located in Garching near Munich, and up to six postdoctoral fellowships tenable at ESO's Astronomy Centre in Santiago, Chile. The ESO fellowship programme offers a unique opportunity to learn and to participate in the process of observational astronomy while pursuing a research programme with state-of-the-art facilities.

ESO facilities include the Very Large Telescope (VLT) Observatory on Cerro Paranal, the La Silla Observatory and the astronomical centres in Garching and Santiago. At La Silla, ESO operates eight optical telescopes with apertures in the range from 0.9 m to 3.6 m, the 15-m SEST millimetre radio telescope, and smaller instruments. The VLT consists of four 8-m diameter telescopes. First light for the first telescope is expected late May 1998. Both the ESO Headquarters and the Astronomy Centre in Santiago offer extensive computing facilities, libraries and other infrastructure for research support. The Space Telescope European Coordinating Facility (ST-ECF), located in the ESO Headquarters building, offers the opportunity for collaborations. In the Munich area, several Max-Planck Institutes and the University Observatory have major programmes in astronomy and astrophysics and provide further opportunities for joint programmes. In Chile, astronomers from the rapidly expanding Chilean astronomical community collaborate with ESO colleagues in a growing partnership between ESO and the host country's academic community. The main areas of activity at the Headquarters and in Chile are:

- research in observational and theoretical astrophysics;
- constructing and managing the VLT;
- developing the interferometer and adaptive optics for the VLT;
- operating the Paranal and La Silla observatories;
- development of instruments for the VLT and La Silla telescopes;
- calibration, analysis, management and archiving of data from ESO telescopes;
- fostering co-operation in astronomy and astrophysics within Europe and Chile.

In addition to personal research, fellows spend a fraction of their time on the support or development activities mentioned above:

In Garching, fellows are assigned for 25% of their time to an instrumentation group, a user support group or a telescope-operation team in Chile. The fellowships are granted for one year with the expectation of a renewal for a second year and exceptionally a third year.

In Chile, the fellowships are granted for one year with the expectation of a renewal for a second and third year. During the first two years, the fellows are assigned to a Paranal operations group or a La Silla telescope team. They support the astronomers at a level of 50% of their time, with 80 nights per year at either the Paranal or La Silla observatory and 35 days per year at the Santiago Office. During the third year, two options are provided. The fellows may be hosted by a Chilean institution and will thus be eligible to propose for Chilean observing time on all telescopes in Chile; they will not have any functional activity. The second option is to spend the third year in Garching where the fellows will then spend 25% of their time on the support of functional activities.

The basic monthly salary will be not less than DM 4853 to which is added an expatriation allowance of 9–12% in Garching, if applicable, and up to 40% in Chile. The remuneration in Chile will be adjusted according to the cost of living differential between Santiago de Chile and the lead town Munich. The fellow will also have an annual travel budget, for scientific meetings, collaborations and observing trips, of approximately DM 12,000.

Fellowships begin between April and October of the year in which they are awarded. Selected fellows can join ESO only after having completed their doctorate.

Applications must be made on the ESO Fellowship Application Form. The form is available either at URL <http://www.hq.eso.org/gen-fac/adm/pers/vacant/fellow.html> or from the address below. The applicant should arrange for three letters of recommendation from persons familiar with his/her scientific work to be sent directly to ESO. Applications and the three letters must reach ESO by October 15, 1998 (but not earlier than June 1998).

Completed applications should be addressed to:

European Southern Observatory
Fellowship Programme
Karl-Schwarzschild-Str. 2
D-85748 Garching bei München, Germany

Tel.: 0049-89-32006-438 or -219 — Fax: 0049-89-32006-497
e-mail: ksteiner@eso.org

FIRST ANNOUNCEMENT

ESO Conference on Chemical Evolution from Zero to High Redshift

ESO Headquarters, Garching, Germany

October 14–16, 1998

The topic of the conference is the determination and interpretation of chemical abundances and evolution from stars, interstellar medium and local group galaxies at zero redshift to distant galaxies, clusters of galaxies and inter-galactic medium at high redshift. Whilst problems undoubtedly remain in the determination of stellar and nebular abundances in the nearby Milky Way, results are beginning to converge.

The observational and interpretative tools are starting to be mature enough that they can be applied with some confidence to extra-galactic systems and integrated populations at increasingly high redshift.

Ultimately the tools should be applicable to determination of the chemistry and enrichment of young galaxies at large look-back times.

The broad aim of the conference is to assess the interplay between methods of measuring chemical abundances with the astrophysical models of galaxy evolution. About half of the conference will be devoted to consideration of abundances and the factors that regulate them in nearby well-studied systems of the Milky Way and Local Group Galaxies. The remainder will concentrate on more distant systems where the abundance data is more slender and the tools under refinement. In addition there will be sessions on forthcoming and future instrumentation applicable to abundance determinations across the whole electromagnetic spectrum. The format for the meeting is invited talks, with contributed papers as talks or posters and some discussion sessions.

There will be five main facets to the conference. The invited speakers are indicated.

- Milky Way stellar and ISM abundance patterns and their models (Gustafsson, Lennon, Peimbert, McWilliam, Meyer and Matteucci)
- Abundances in nearby galaxies and clusters: observations (Pagel, Skillman, Garnett, Worthey and Renzini)
- Evolution of abundances (e.g. effect of dynamics, mergers, supernovae) (Thielemann, Edmunds, Haehnelt and Kauffmann)
- Abundances in the distant Universe (QSO absorption lines and starburst galaxies) and primordial abundances (Pettini, Songaila, Combes, Leitherer and Tytler)
- New windows on abundance determinations in the UV, optical-IR, X-ray and radio (Jenkins, D'Odorico, Kahn and Thatte)

Conference summary by S. White

Scientific Organising Committee:

F. Combes, D. Garnett, G. Kauffmann, C. Leitherer, D. Lennon, J. Mathis [Chair], M. Pettini, M. Rosa, P. Shaver, E. Terlevich

Local Organising Committee:

G. Contardo, J. Walsh, C. Stoffer

Registration has already begun and the deadline for registration is 1 August 1998.

More details and a registration form can be found at:

<http://www.eso.org/gen-fac/meetings/chemev98/>
or contact: chemev98@eso.org for further information.

The Astronomical Almanac to Be Revised

The U.S. Naval Observatory and the Royal Greenwich Observatory are currently conducting a thorough review of the content and format of the Astronomical Almanac.

In order to assess the needs of the users, a survey is being conducted by the two offices and users can make their needs known in detail by accessing the site <http://www.ast.cam.ac.uk/nao/survey.html> or writing to Dr. Alan D. Fiala adf@newcomb.usno.navy.mil.

The survey will close on 1 August 1998.

List of Scientific Preprints

(March–May 1998)

1263. Contributions of the ESO Data Management and Operations Division to the SPIE Workshop "Observatory Operations to Optimize Scientific Return". 20–21 March 1998.
1264. P.A. Mazzali et al.: Nebular Velocities in Type Ia Supernovae and their Relationship to Light Curves.
1265. O.R. Hainaut et al.: Early Recovery of Comet 55P/Temple-Tuttle. *A&A*.
1266. J.C. Vega Beltrán et al.: Mixed Early- and Late-Type Properties in the Bar of NGC 6221: Evidence for Evolution Along the Hubble Sequence. *A&A*.
1267. M. Turatto et al.: The Peculiar Type II Supernova 1997 D: A Case for a Very Low ^{56}Ni Mass.
1268. F. Bresolin et al.: An HST Study of Extragalactic OB Associations. *The Astronomical Journal*.
1269. F. Comerón et al.: ISO Observations of Candidate Young Brown Dwarfs. *A&A*.
1270. D.R. Silva and G.D. Bothun: The Ages of Disturbed Field Elliptical Galaxies: I. Global Properties. *The Astronomical Journal*.

PRELIMINARY ANNOUNCEMENT

ESO Workshop on Minor Bodies in the Outer Solar System

ESO Headquarters, Garching, Germany

November 2–5, 1998

A four-day ESO Workshop on Minor Bodies in the Outer Solar System (ESO MBOSS-98), their orbital and physical characteristics, as well as their origins and inter-relationships will be held at a time when several new observational facilities, including the ESO Very Large Telescope (VLT), are about to enter into operation. With larger collecting areas and equipped with a host of advanced instruments, they have the potential of revolutionising observational studies of these faint objects. An overview of this active research field at this time will therefore provide an important contribution to the efficient planning of these investigations.

This is a hot subject in current solar-system studies. There is an image emerging of interconnections between Jovian Trojans, the Centaurs, the newly found classes of TNO's, comet nuclei, interplanetary dust and the icy moons of outer planets, including Pluto itself. The ESO Workshop will allow observers and theoreticians to get together and to discuss plans for future studies in this rapidly evolving field. The emphasis will be on establishing a comprehensive, overall picture which attempts to describe the formation, evolution and interaction of these components.

The meeting will be held in the ESO main auditorium, and the number of participants is therefore limited to a maximum of approximately 120.

The main topics of the Workshop will be the following:

- Inventory of Minor Bodies in Outer Solar System (overview)
- Outer Solar System reservoirs (Outer Main Belt and Trojans; Centaurs and Interplanetary Rings; TNO's and Edgeworth-Kuiper Belt; Trans-Neptunian Disk and Oort Cloud)
- Orbital dynamics and evolution (High-precision orbital determinations; Resonance trapping; Similarity and diversity of orbital types; Pathways between the reservoirs)
- Physical properties (Size, shape and rotation; Composition and atmospheres)
- Physical interrelationships (Transitional asteroid/comet cases; Interplanetary dust)
- Origin and physical evolution (Theories of planetary formation; Collisional history; Growth and physical evolution)
- Future lines of research (Research possibilities with new generation of very large telescopes; Spacecraft missions; Innovative techniques; Collaboration/coordination)

Scientific Organising Committee:

Rudi Albrecht (ST/ECF, Garching, Germany); Mark Bailey (Armagh Observatory, N. Ireland, UK); Hermann Boehnhardt (ESO, Santiago, Chile); Martin Duncan (Queen's University, Kingston, Ontario, Canada); Julio A. Fernandez (Universidad de la Republica, Montevideo, Uruguay); Alan Fitzsimmons (Queen's University, Belfast, N. Ireland, UK; SOC Chair); David Jewitt (Institute of Astronomy, Honolulu, Hawaii, USA); Hans Rickman (Astronomiska Observatoriet, Uppsala, Sweden); Alan Stern (South-West Research Institute, Austin, Texas, USA); Jun-ichi Watanabe (National Observatory, Tokyo, Japan); Richard West (ESO, Garching, Germany; LOC Chair)

More details and a registration form can be found at: <http://www.eso.org/gen-fac/meetings/mboss98/> or contact: rwest@eso.org for more information or one of the SOC members.

1271. P.A. Woudt et al.: Multiwavelength Observations of a Seyfert 1 Galaxy Detected in ACO 3627. *A&A*.
1272. E. Tolstoy et al.: WFPC2 Observations of Leo A: A Predominantly Young Galaxy within the Local Group. *The Astronomical Journal*.
1273. Th. Rivinius et al.: Stellar and Circumstellar Activity of the Be Star μ Cen. II. Multiperiodic Low-Order Line-Profile Variability. *A&A*.

DICHIRICO, Canio (I), Temporary transfer to Paranal
GIORDANO, Paul (F), Temporary transfer to Paranal
DOUBLIER, Vanessa (F), Fellow La Silla
PATAT, Ferdinando (I), Fellow La Silla
MARCO, Olivier (F), Fellow La Silla
VANZI, Leonardo (I), Fellow La Silla
SELMAN, Fernando (RCH), Associate

PERSONNEL MOVEMENTS

International Staff (1 April – 30 June 1998)

ARRIVALS

EUROPE

MØLLER, Palle (DK), User Support Astronomer
TOLSTOY, Eline (NL), Fellow Garching

CHILE

FRANÇOIS, Patrick (F), Astronomer
STERZIK, Michael (D), Astronomer

DEPARTURES

EUROPE

HERLIN, Thomas (DK), Software Engineer
HESS, Matthias (D), Mechanical Engineer
VAN DIJSELDONK, Anton (NL), Opt. Lab. Technician
KAPER, Lex (NL), Senior Fellow Garching
BÜTTINGHAUS, Ralf (D), Mechanic
CRANE, Philippe (USA), Astronomer/Physicist

CHILE

GREDEL, Roland (D), Astronomer
KRETSCHMER, Gerhard (D), Mechanical Engineer

ESO, the European Southern Observatory, was created in 1962 to . . . establish and operate an astronomical observatory in the southern hemisphere, equipped with powerful instruments, with the aim of furthering and organising collaboration in astronomy . . . It is supported by eight countries: Belgium, Denmark, France, Germany, Italy, the Netherlands, Sweden and Switzerland. It operates the La Silla observatory in the Atacama desert, 600 km north of Santiago de Chile, at 2,400 m altitude, where fourteen optical telescopes with diameters up to 3.6 m and a 15-m submillimetre radio telescope (SEST) are now in operation. The 3.5-m New Technology Telescope (NTT) became operational in 1990, and a giant telescope (VLT = Very Large Telescope), consisting of four 8-m telescopes (equivalent aperture = 16 m) is under construction. It is being erected on Paranal, a 2,600 m high mountain in northern Chile, approximately 130 km south of Antofagasta. Eight hundred scientists make proposals each year for the use of the telescopes at La Silla. The ESO Headquarters are located in Garching, near Munich, Germany. It is the scientific, technical and administrative centre of ESO where technical development programmes are carried out to provide the La Silla observatory with the most advanced instruments. There are also extensive facilities which enable the scientists to analyse their data. In Europe ESO employs about 200 international Staff members, Fellows and Associates; at La Silla about 50 and, in addition, 150 local Staff members.

The ESO MESSENGER is published four times a year: normally in March, June, September and December. ESO also publishes Conference Proceedings, Preprints, Technical Notes and other material connected to its activities. Press Releases inform the media about particular events. For further information, contact the ESO Information Service at the following address:

EUROPEAN
SOUTHERN OBSERVATORY
Karl-Schwarzschild-Str. 2
D-85748 Garching bei München
Germany
Tel. (089) 320 06-0
Telex 5-28282-0 eo d
Telefax (089) 3202362
ips@eso.org (internet)
ESO::IPS (decnet)

The ESO Messenger:
Editor: Marie-Hélène Demoulin
Technical editor: Kurt Kjær

Printed by
Druckbetriebe Lettner KG
Georgenstr. 84
D-80799 München
Germany

ISSN 0722-6691

Local Staff (1 April – 30 June 1998)

ARRIVALS

RICHARDSON, Felipe (RCH), Software Engineer Developer
RODRIGO, Manuel (RCH), Scientific Instruments Operator/ Night Assistant
MONTEZ, Lucia (RCH), Bilingual Secretary

DEPARTURES:

WENDEROTH, Erich (RCH), Scientific Instruments Operator
TIMMERMANN, Gero (RCH), Electronic

Contents

First Light	1
R. Giacconi: First Light of the VLT Unit Telescope 1	2
The Final Steps Before "First Light"	3
R.M. West: VLT First Light and the Public	4
OBSERVING WITH THE VLT	
B. Leibundgut, G. de Marchi, A. Renzini: Science Verification of the VLT Unit Telescope 1	5
Scientific Evaluation of VLT-UT1 Proposals. Observing Period 63 (April 1 – October 1, 1999)	9
P. Quinn, J. Breysacher, D. Silva: First Call for Proposals	9
TELESCOPES AND INSTRUMENTATION	
R.G. Petrov, F. Malbet, A. Richichi, K.-H. Hofmann: AMBER, the Near-Infrared/ Red VLTI Focal Instrument	11
NEWS FROM THE NTT: G. Mathys	14
Ph. Gitton and L. Noethe: Tuning of the NTT Alignment	15
THE LA SILLA NEWS PAGE	
M. Kürster: CES Very Long Camera Installed	18
J. Brewer and J. Andersen: Improving Image Quality at the Danish 1.54-m Telescope	18
VLT DATA FLOW OPERATIONS NEWS: D. Silva: The NTT Service Observing Programme: Period 60. Summary and Lessons Learned	20
A. Moorwood: SOFI Infrared Images of the "NTT Deep Field"	25
OBSERVATIONS WITH THE UPGRADED NTT	
P. Bonifacio and P. Molaro: Upgraded NTT Provides Insights Into Cosmic Big Bang	26
R. Neuhauser, H.-C. Thomas, F.M. Walter: Ground-Based Detection of the Isolated Neutron Star RXJ185635-3754 at V = 25.7 Mag with the Upgraded NTT	27
I. Burud, F. Courbin, C. Lidman, G. Meylan, P. Magain, A.O. Jaunsen, J. Hjorth, R. Østensen, M.I. Andersen, J.W. Clasen, R. Stabell, S. Refsdal: RX J0911.4+0551: A Complex Quadruply Imaged Gravitationally Lensed QSO	29
OTHER REPORTS FROM OBSERVERS	
J. Sanner, M. Geffert, H. Böhnhardt, A. Fiedler: Astrometry of Comet 46P/Wirtanen at ESO: Preparation of ESA's ROSETTA Mission	33
L. Binette, B. Joguet, J.C.L. Wang, G. Magris C.: NTT Archives: the Lyman α Profile of the Radio Galaxy 1243+036 Revisited	37
Photos from Science Writers' Symposium	39
ANNOUNCEMENTS	
Joint Committee Between ESO and the Government of Chile for the Develop- ment of Astronomy in Chile	40
L. da Costa and A. Renzini: ESO Imaging Survey: Update on EIS-deep and the Hubble Deep Field South	40
ESO Fellowship Programme 1999	41
First Announcement of an "ESO Conference on Chemical Evolution from Zero to High Redshift"	42
The Astronomical Almanac to Be Revised	42
List of Scientific Preprints (March–May 1998)	42
Preliminary Announcement of an "ESO Workshop on Minor Bodies in the Outer Solar System"	43
Personnel Movements (1 April – 30 June 1998)	43